Molecular Recognition of Chlorine-Doped Polypyrrole

by

Kiley Preston-Halfmann Miller

M. A. Chemistry
The University of Texas at Austin, 2002

SUBMITTED TO THE DEPARTMENT OF BIOLOGICAL ENGINEERING IN PARTIAL FULFILMENT OF THE REQUIREMENTS FOR THE DEGREE OF

DOCTOR OF PHILOSOPHY IN BIOENGINEERING
AT THE
MASSACHUSETTS INSTITUTE OF TECHNOLOGY

April 2005
[June 2005]

Signature of Author_____
Department of Biological Engineering
April 8, 2005

Certified by_____
Angela Belcher
Professor of Biological Engineering
Thesis Supervisor

Accepted by_____

Molecular Recognition of Chlorine-Doped Polypyrrole

by

Kiley Preston-Halfmann Miller

Submitted to the Department of Biological Engineering
on April 8th, 2005 in Partial Fulfillment of the Requirements
for the Degree of Doctor of Philosophy in
Bioengineering

ABSTRACT

The objective of this work is to functionalize an existing polymer such that it better mimics natural tissue for tissue growth and regeneration. Numerous other processes have tried and accomplished this by non-specific protein adsorption, covalent attachment, biomolecule entanglement, and synthesis of new polymers with the desired functionality. The focus of this work is to modify the polymer's binding capability to cells while not altering the bulk properties. Through the use of both phage display of peptide libraries and yeast surface display of scFv libraries the surface of chlorine-doped polypyrrole (PPyCl) has been modified to facilitate binding of neuronal phenotype cells. The selection of peptides using phage display found a surface specific recognition peptide (T59) that was made bivalent by altering the C-terminus with an integrin binding epitope. The bivalency of the modified T59 peptide was exploited to tether phenochromocytoma (PC12) cells to the surface of PPyCl. Furthermore the tethering of the cells to PPyCl through the peptide does not decrease the cells neuronal function and maintains the bulk conductive polymers characteristics. Using the peptide as a bivalent linker, the addition of other types of cells, drugs, growth factors, and enzymes could be incorporated for various biomedical applications. An antibody (Y2) specific to PPyCl was found using yeast surface display. This antibody was utilized to mediate cellular binding to PPyCl by expression of the antibody on the surface of PC12 cells. Complimenting the peptide studies of having an exterior bivalent linker the antibody recognition provides the means for any cell type to adhere to PPyCl, through expression of the antibody on the surface of the cell. This type of system could be used for various types of tissue growth supports.

Thesis Supervisor: Angela Belcher
Title: Professor of Biological Engineering

Dedication

To My Family-

I would like to dedicate this thesis to my family. I would also like to thank them all for their unending support and patience of both the research and the writing of this thesis. I would especially like to thank my wife Tish. You are always interested in the work that I am conducting, although the complexity of it may be vast, you always lend an ear. Tish, Phoenix, and Bhodey are what I work for and every moment I am thinking about you. I love you all with my entire mind, heart, and soul.

Tish-

You are my soul mate.

...two hearts that beat as one

... two souls with but a single thought.

Acknowledgements

This thesis could not have been written without the help of many people. I would like to thank Angela Belcher her guidance concerning the research. Special thanks goes to Archit Sanghvi for the long discussions we had about research. I would also like to thank everyone at the Biopolymers Lab at MIT for obtaining the numerous sequences contained in this thesis. I have thoroughly enjoyed working in the Belcher Lab, with Christine, Ioana, Erin, Esther, Roz, Dan, Brian, Steve, Kwan, Lee, Jifa, Harshal, Chaunbin, Sreeker, Chung, Yan, Yu, Saeeda, Eric, Andrew, Davide, Glenn, Charlene, Ki-Tae, Julie, Beau, Kate, Asher, Mo, and Yun. Most importantly, I am very grateful for my family, wife Tish, daughter Phoenix, son to be Bhodey, mother Peggie Ann Stacy, father Max Arnold Miller, and sister Whitney Leigh Miller.

Table of Contents

List of Tables and Equations

List of Figures

CHAPTER 1: Introduction

1.1 Objectives of this Study

The objective of this project is to functionalize an existing polymer such that it better mimics natural tissue for tissue growth and regeneration. By using a random bacteriophage library that displays a peptide insert on the gPIII of a bacteriophage protein capsid, $1x10^9$ random peptide inserts were rapidly screened against a polymer of interest. As an alternative to the peptide selection, a yeast surface display library was used to screen human derived single chain fragment antibodies (scFv) against the surface of the polymer to reverse engineer cell-binding to the polymer surface. Specifically, peptides were selected using bacteriophage display and scFv using yeast surface display that bind directly to the polymer, oxidized polypyrrole doped with chlorine (PPyCl).

By selecting and identifying individual peptides that bind specifically to polymers, one can quickly and easily synthesize the peptides with the polymer binding domain on one terminus, and a domain that binds to cells, drugs, or growth factors on the other. These selected peptides could be used as bi-functional linkers to attach a wide variety of biologically active molecules to a biomaterial surface. Since this approach can be used for existing materials, no changes to the biomaterial's physical properties or re-characterization of the biomaterial would be necessary. The versatility of this technique is demonstrated by the ability to modify many different types of existing biomaterials. This represents a clear advantage over present approaches to modify synthetic polymers, which include non-specific protein adsorption, covalent attachment methods, and the synthesis of entirely new polymers with desired functionality.

Using yeast surface display to screen scFv against the PPyCl surface as an alternative to bacteriophage display presents two major advantages. First, the bacteriophage length scale is extremely small (6 nm X 880 nm) and there is difficulty in visualizing an individual bacteriophage particle. Although the scFv is on the same order of magnitude as the phage, the use of the yeast cellular surface to display the scFv provides a much larger particle to image with a yeast cell being 3-5 μm. Second, knowing the scFv sequence one can manufacture a biological label for PPyCl, as can the peptide from the bacteriophage. But the major advantage of knowing the scFv sequence is that it provides a large enough surface area on a foreign cell for that cell to bind to PPyCl, through the scFv linkage.

As described above, the goal of this work is to understand the binding of the selected peptides while creating a novel bi-functional linker between a polymeric surface and cells or biomolecules. Additionally, a secondary aim for this work is to evaluate the ability to screen scFv against polymers and then incorporate them into different species to evaluate relative binding affinity. Figures 1.1 and 1.2 illustrate the microscopic type of interactions that will be created between biomolecules, the polymer, and cells.

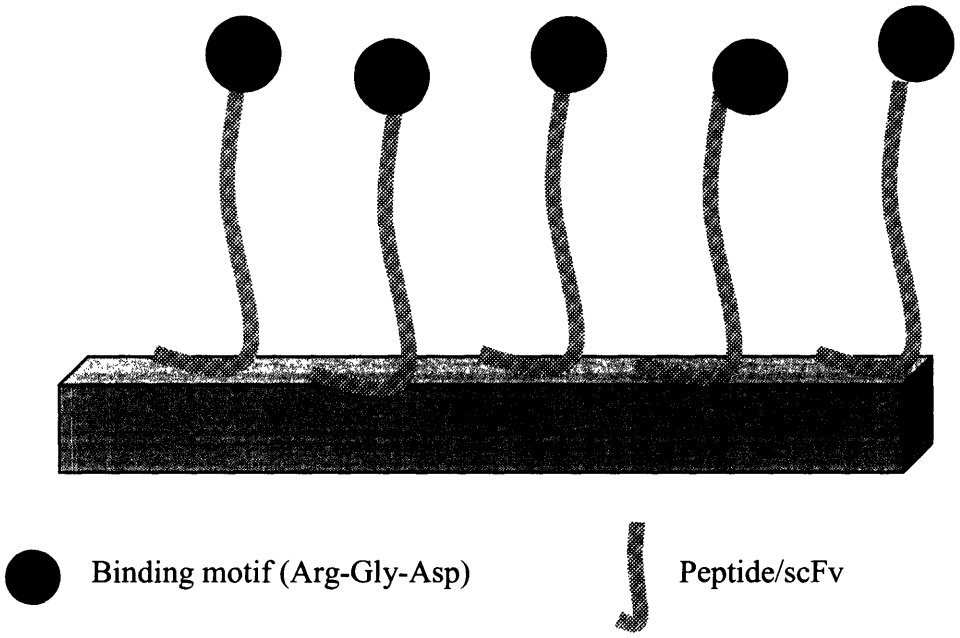

Figure 1.1: Microscopic illustration of bi-functional linker.

Once determined, the peptide sequence that binds to the surface of the biomaterial will be used incorporated with binding motifs for nerve-like cells, such as arginine-glycine-aspartic acid (RGD), thus creating a bi-functional linker between materials and cells. A brief diagram of the cellular attachment through motif modification and nerve regeneration capabilities is shown in Figure 1.2.

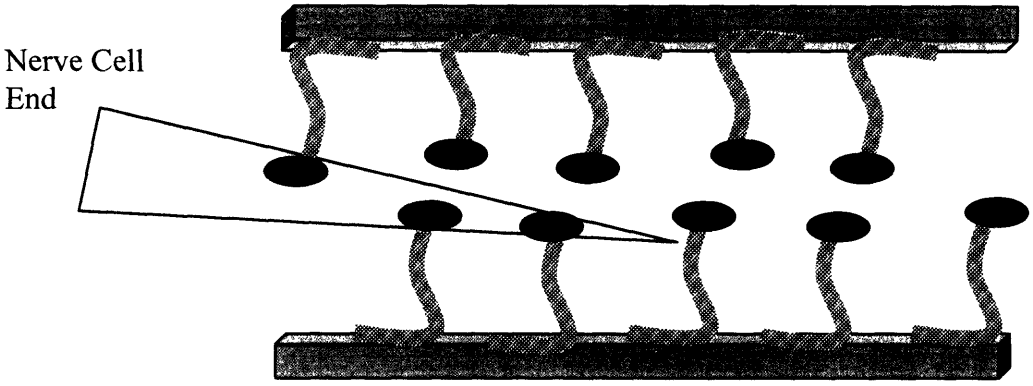

Figure 1.2: Microscopic illustration of the bi-functional system used inside a host.

By using these types of connections between materials and cells the effectiveness of a nerve guidance channel created from these pieces will increase compared to that of the nerve autograft. The nerve autograft has the largest average recovery of function rate for nerve damage (~50%), but it requires multiple surgeries which incorporate increased possibility of infection [1]. By providing a surface modified biomaterial and a concentration gradient of cells and biomolecules the limitations of the nerve autograft hope to be surpassed, thus far these ideas can not be accomplished with the current use of autografts.

1.2 Previous Techniques Used for Biomaterial Surface Modification

This research centers on new ways to generate hybrid-biomaterials that better resemble natural tissue. These materials will be useful for a wide range of tissue engineering applications in which materials and cells are combined to reconstruct living tissue, or in which materials on their own are used to stimulate the regeneration of damaged tissue directly in the body. Applications may include therapies for nerve

regeneration [2-5], bioreactors [6], biosensors [7], and organ-specific tissue regeneration [8-12].

There are various approaches that researchers have taken to make non-biological materials resemble natural biological tissue. Through protein adsorption [13], synthesis of graft-copolymers [14], non-covalent surface modification [15], and entanglement [16-18] attempts have been made to create a biomaterial that is flexible to changes in molecular design, is easy to synthesize, and is adaptable for a broad range of applications.

Researchers have investigated methods for the microfabrication of biological surfaces by attaching proteins and other biomolecules for specific molecular recognition and cell attachment [13]. For example, microcontact printing using a PDMS stamp has often been used to create micropatterns, followed by the adsorption of proteins and cells to the solid surface. Since protein adsorption is largely dependent upon non-specific interactions between the protein and the surface, the stamping method using proteins does not consistently orient the adsorbed proteins to expose the desired functionalities [13].

Other investigators have engineered polymer surfaces to create materials that control cellular adhesion and maintain differentiated phenotypic expression [14]. Because of the absence of suitable functional groups on the surface of many polymers to covalently attach peptides, many groups have investigated methods for modifying the chemistry of these polymer surfaces. Common approaches involve introducing reactive groups, such as poly(L-lysine), at existing polymer surfaces by incorporating monomer units with appropriate functionality into the polymer backbone to create new polymer materials [19]. However, such approaches often require complicated synthetic pathways, and lack consistent surface coverage of the grafted biomolecules [14].

An alternative method to functionalize materials uses a silanization technique to immobilize peptides. This method was demonstrated by utilizing silane films deposited on titanium oxide surfaces with terminal functional groups that can be further modified with different bi-functional linkers, eventually leading to the covalent attachment of a cell adhesive RGD containing peptide motif [20]. A variety of routes using aminosilanes for further modification have been utilized. Examples are: 1.) an aminosilane reaction with glutaraldehyde, which yields an aldehyde that can form an imine linkage with primary amines on the peptides [21], or 2.) the reaction of aminosilanes with a mixture of peptides and carbodiimides, which yields an amide linkage with carboxyl groups on the peptides [15]. These two methods used primary amino groups and carboxyl groups that occur with high frequency in peptides and proteins. However, specific peptide attachment at a defined site was difficult to achieve due to the limited ability of the surface modification technique to incorporate these functional linkages. Consequently, these approaches produce unordered surfaces.

The surface modification of materials with peptides designed to mimic the extracellular matrix of a nerve cell, have been used to couple peptides to polymeric surfaces [22]. Poly(tetrafluroethylene-*co*-hexafluoropropylene) was first reduced with sodium naphthalide to introduce surface carbon-carbon double bonds at two reaction conditions: 20 min at -78°C, and 3 h at 25°C. Reduced poly(tetrafluroethylene-*co*-hexafluoropropylene) film surfaces were further modified to introduce hydroxyl groups via hydroboration/oxidation or carboxylic acid groups via oxidation. The hydroxyl (-OH) and carboxylic acid (-COOH) functionalized surfaces provided reactive handles for peptide coupling using tresyl chloride, eventually leading to the covalent attachment of 5-

and 6-mers that promoted neurite extension [23]. Material scientists have designed and synthesized surfaces that first resist protein adsorption and fouling, and then build back in the chemistry to promote specific cellular interactions. This technology works for polymers, like poly(ethylene glycol) (PEG), that resist protein binding. For example, peptides containing the extracellular matrix binding domain RGD were incorporated into mixtures of PEG diacrylate and acrylamidoyl peptides. The PEG diacrylate and acrylamidoyl peptides were polymerized via photoinitiation [24]. Even though this technique successfully linked peptides to PEG, it could not adequately control spatial orientation of peptides on the material's surface, and it lacked the flexibility for functionalizing the PEG surface with multiple biomolecules.

An additional method for cellular attachment involves the use of a combination of Panacryl®, a poly(L-lactide-*co*-glycolide) resorbable material, and Pluronic®, a tri-block copolymer consisting of a poly(propylene oxide) block sandwiched between two poly(ethylene oxide) blocks 3DP™ patterned or solvent-cast to create a material that supported cellular attachment. The polymer matrix materials were interacted with cells to monitor adhesion. The findings of this research state that the 3DP™ patterned material provided good cellular adhesion, through multiple entanglement processes, but state that the cellular adhesion does not differ from that of solvent cast surfaces [18]. These technique's, though novel, approach to patterning cells on surfaces provides non-specific attachment of the cells to the poly(ethylene oxide). Although the poly(ethylene oxide) layer is easily modified, it lacks the functional ability to prevent cellular aggregation which would represent specific interaction with the surface.

The approaches outlined above do not meet the ideal criteria to create a surface functionalized with a variety of biomolecule linkages. The strategy presented in the current research is a different approach to functionalize a material's surface. The novel methods of bacteriophage display of peptides and yeast surface display of scFv provides the basic strategy to screen for peptide binding motifs that bind specifically to materials with high affinity.

CHAPTER 2: The Substrate: Chlorine-Doped Polypyrrole

2.1 Purpose

PPyCl is an electrically conductive material that can be consistently deposited onto a microscope slide. In addition, PPyCl has been used as a substrate for nerve regeneration in previous studies [2, 3]. This makes PPyCl an ideal substrate for nerve regeneration by modifying the surface of the polymer with peptides that can attach biomolecules, or glial cells. As described previously, the focus of this work is to create a surface that resembles a natural biological surface for the eventual incorporation into a nerve guidance channel. PPyCl peptides and/or antibodies attached to it's surface would create a hybrid-biomaterial that could provide a specific link between a conductive polymer and a biological surface, and thus surpass the effectiveness of the nerve autograft for nerve regeneration.

2.2 Experimental Methods and Results

PPyCl is a polycation with delocalized positive charges along its highly conjugated backbone. The chloride ions provided charge neutrality when they were incorporated as radical anions or "dopants". The PPyCl film was electrochemically deposited on indium tin oxide (ITO)-conductive borosilicate glass (Delta Technologies) [25]. ITO glass slides were cleaned before use by sonication in hexane, methanol, and dichloromethane for 5 min each. A three-electrode setup consisting of a saturated calomel reference electrode, platinum gauze counter electrode, and an ITO slide as the working electrode, was used for the electrochemical deposition of the PPyCl. The polymer was deposited at a constant potential of 720 mV versus the saturated calomel reference from

an aqueous solution of 0.1 M pyrrole monomer (Fisher Scientific) containing 0.1 M NaCl (Fisher Scientific) providing the chloride ion as dopant. A Pine Instruments AFRDE5 bipotentiostat was used as the DC voltage source. Film thickness ranged from 150 nm-200 μm which was determined by integrating current over time, and was controlled by the passage of charge based on the standard value of 50 mC/cm^2 [25]. The charge allowed to pass through the working electrode was measured with a current integrator (IT001, Cypress Systems, Inc.) that was coupled to a multimeter (Sperry, DM-8A) for digital display. The films were rinsed with Millipore water and stored in a desiccator for two days before surface sterilization and sample interaction with either the bacteriophage library or the yeast library.

The surface morphology of PPyCl was investigated using a scanning electron microscope and an optical microscope for visualization of the microscopic surface that individual bacteriophage and yeast would be screened against, Figure 2.1. The surface has a characteristic "wrinkle" effect that is an effect of polymer thickness. Thus, with a thinner sample thickness (< 10 μm) the "wrinkle" is less apparent.

The formation of the polymer is controlled by a radical cation polymerization process and can be initiated and terminated by the introduction of charge into the system [25]. From the chemical structure, Figure 2.2A, one can observe that the polymerization process can proceed either at the α-carbon or the β-carbon. These two polymerization points can form three different monomer linkages: α–α, α–β, or β–β. PPyCl monomer linkages are usually constrained to the α–α attachment and the α–β attachment because of the lack of reactive polymerization sites. The α–α linkage is a linear attachment and the α–β linkage provides for some degree of branching to occur in the polymer. The

linear polymer is formed by α–α linkages with two α-carbons bound, Figure 2.2B. The branched polymer is formed by both α–α linkages, as described previously, and α–β linkages with an α-carbon and a β-carbon bound, Figure 2.2C. The α–α polymer is a much more conductive material because of its fully conjugated double bonds, which provides an essential property for the electrical stimulation of cells for proliferation and differentiation [26]. X-ray photoelectron spectroscopy (XPS) was used to chemically characterize the surface of the polymer. High resolution XPS was able to resolve the C1s peak area from 292-282 eV, which can determine whether the monomers are linked either by α–α linkages or α–β linkages. The C1s peak area represents the accumulation of photoelectrons, produced by excitation of PPyCl by X-rays, which correlate in binding energy to the carbon 1s electron shell. In the spectrum Figure 2.3, the α–α linkage is centered on 284.5 eV and the α–β linkage is centered on 283.6 eV [27]. Based on this data the linkages in PPyCl are mainly α–α linkages, which increases conductivity and are consistent with previous studies [27, 28]. The XPS instrument used was a Physical Electronics Phi ESCA 5700 equipped with an Al X-ray source (1,487 eV X-rays).

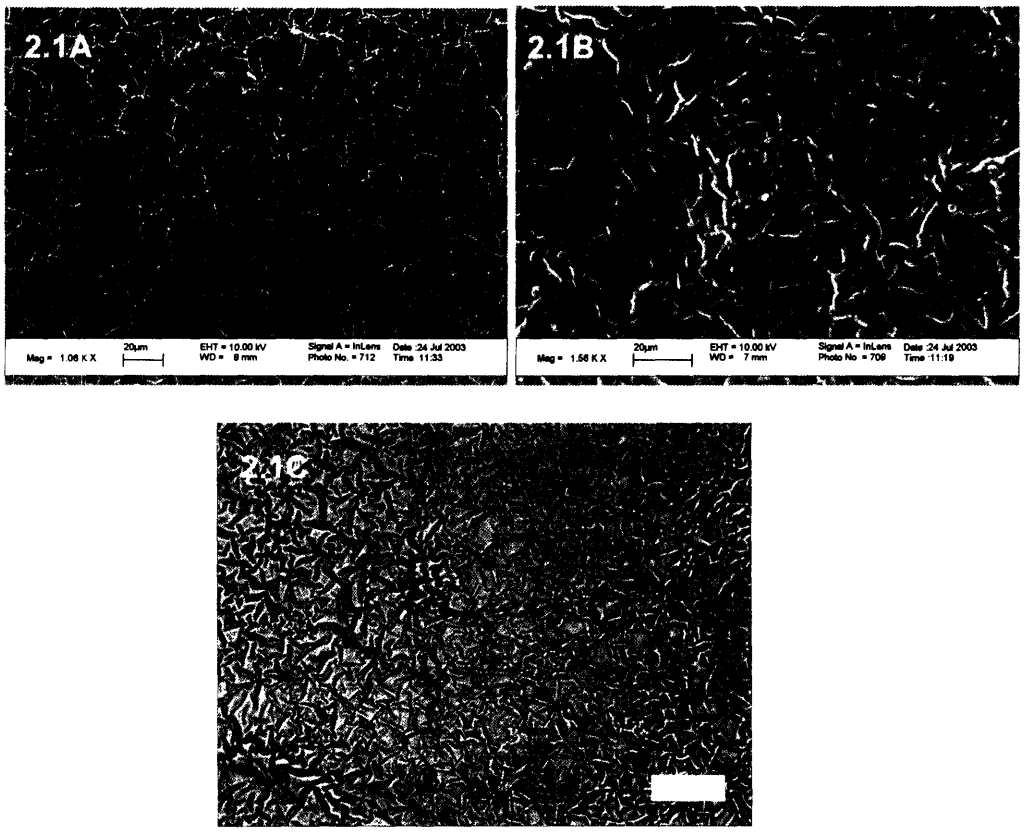

Figure 2.1: Micrographs showing the surface topology of PPyCl . 2.1A-B) Scanning electron micrographs with film thicknesses being 150-250 nm and 150-200 μm, respectively, 2.1C) Optical micrographs film thickness: 5-10 μm, Scale bar = 50 μm.

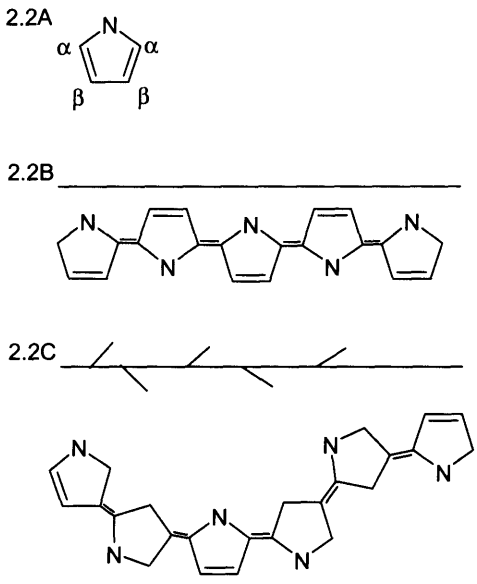

Figure 2.2: 2.2A) Chemical structure of the pyrrole monomer, with α and β-carbons labeled, 2.2B) Linear formation of polypyrrole, with α – α linkages, 2.2C) Branched formation of polypyrrole, with α – α, α – β, and β – β linkages.

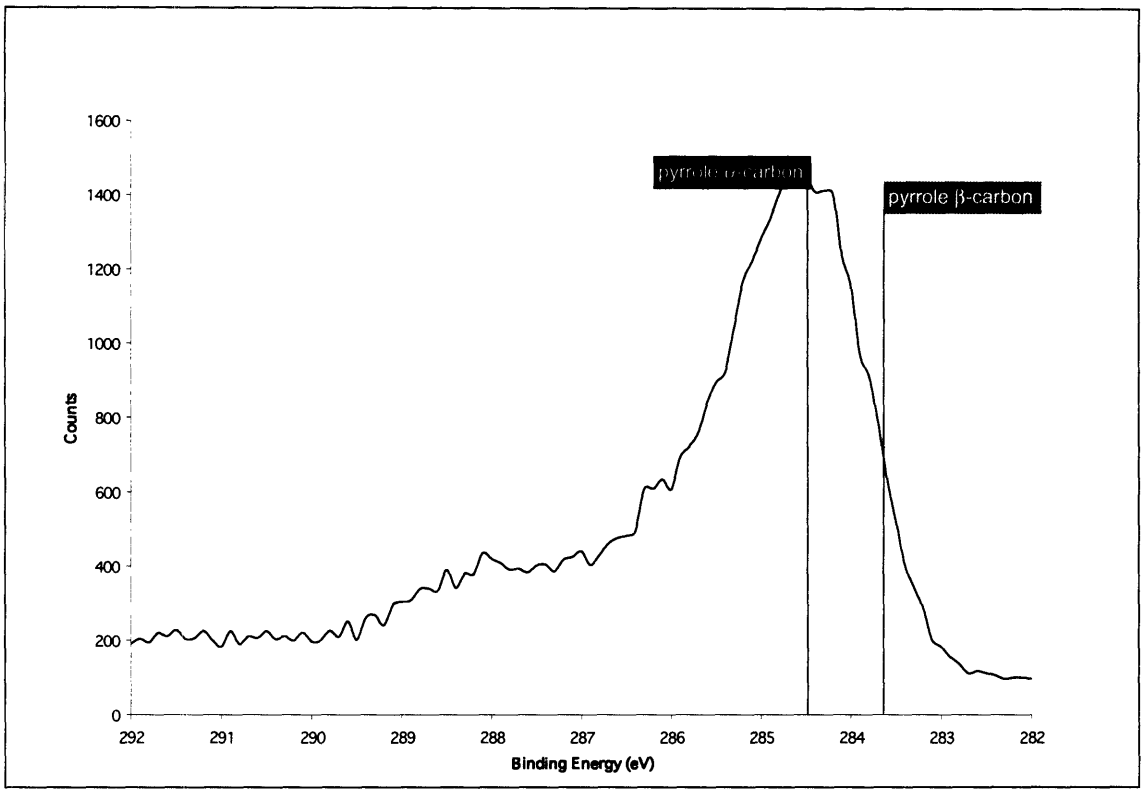

Figure 2.3: C1s core-line spectra for the 5-10 μm thick PPyCl film with characteristic α-α carbon binding energy at 284.5 eV and α-β carbon binding energy at 283.6 eV.

To initiate the screening process, experiments analyzing the chemical makeup of the substrate were needed. These experiments were used to determine if the screening of such a material would be possible in aqueous solutions and give information regarding if any deterioration would occur over the timescales used in either peptide or antibody screens, which are on the order of 1.5 hour time span, and for *in vitro* cellular studies, lasting up to 1 week.

The experiments consisted of placing recently electrically deposited, with in 24 hours, 0.5 cm^2 samples of PPyCl in various solutions for varying time periods. Table 2.1 represents the solutions and time periods used for PPyCl degradation studies.

Sample Identification	Solution	Time Period (hr)
PPyCl	none	0
PPyCl-TBS	1X Tris Buffered Saline (TBS)	1.5
PPyCl-SG	SG-CAA	1.5
PPyCl	Serum-free media (F12)	168

Table 2.1: Experimental parameters tested for substrate degradation. Select-Galactose Casoamino Acids (SG-CAA).

From Table 2.1, the solutions used for interaction with PPyCl are the same as those used for screening of peptides (TBS), antibodies (SG-CAA), and interaction with mammalian cells (serum-free media, F-12, Invitrogen). The above experiments were carried out in triplicate using the same larger sample of PPyCl cut to experimental dimensions. Analysis of the above experiment was conducted using a Kratos AXIS Ultra Imaging X-ray Photoelectron Spectrometer equipped with a monochromatic Al X-ray source (1,487 eV) to determine the concentration of major and minor atomic components of the substrate and using the various time periods to determine if there is degradation over time in various solutions. Figure 2.4 represents this data with atomic concentration ratios of C1s, N1s, O1s, and Cl2p. Macroscopically; there was no apparent degradation of PPyCl in any of the solutions, which would have consisted of flaking and or dissolving.

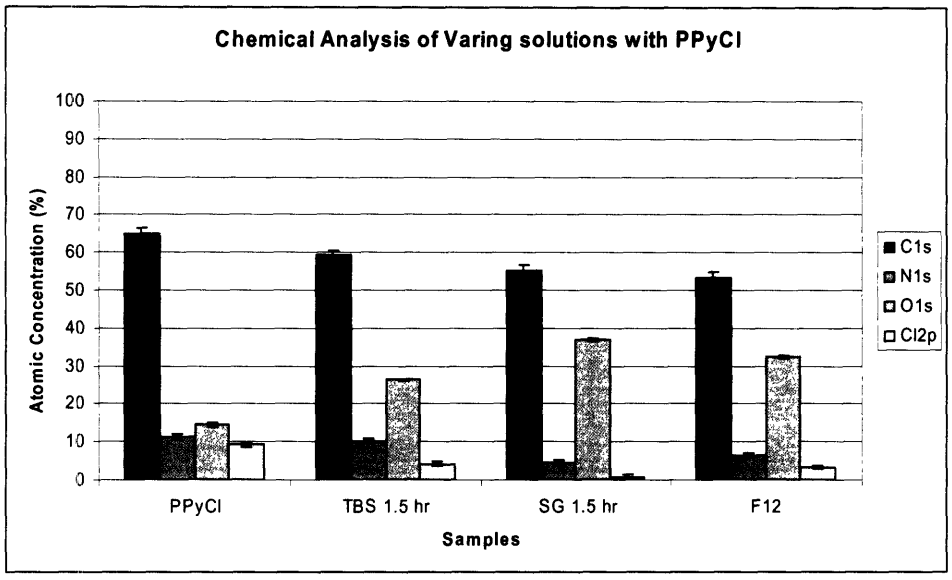

Figure 2.4: XPS chemical analysis of varying PPyCl samples. Error bars = ±1.38% (C1s), ±0.70% (N1s), ±0.38% (O1s), ±0.5% (Cl2p).

From the XPS atomic concentration ratio data there seems to be a general trend of increased exposure to solution decreases the atomic concentration ratio of carbon, this is evident by the gradual decline of the atomic concentration ratio of C1s from a zero time point to 1 week. Granted there is still approximately 80% of the original concentration maintained after 1 week of interaction in solution. A possible reason for this decrease in carbon's atomic ratio is the gradual increase in the oxygen atomic ratio over time, but this increase is also media dependent. The oxygen atomic ration for the TBS sample is almost doubled compared to PPyCl, but the use of SG-CAA for media interaction almost triples the oxygen atomic ratio. The reason for these increases in oxygen atomic ratio can be explained because PPyCl is an easily oxidized material and tends to do so when not maintained with desiccant. Also of interest to note is the reduction in chlorine atomic ratio in the films over a period of time, which is reduced from 9% to less than 1% in SG-CAA containing media for 1.5 hrs. Understanding that the ratios are a percent composition of the film explains this decrease in chlorine because of the increase in

oxygen atomic ratio. From this data one can state that there is little loss of bulk material with an increase in oxygen over a period of 1.5 hrs in all media types. Therefore the increase in oxygen does not reduce the capabilities of screening the PPyCl film with either peptides in TBS, antibodies in SG-CAA, or cells in F12 over the time period needed for interactions.

2.3 Conclusions

Numerous polymeric materials have been used for tissue engineering applications. PPyCl, being one of the many, was used for nerve regeneration studies and this work's intention is to improve on the previous techniques used to modify polymeric materials by biological selection of the polymer's surface. This provides experimental control on how binding occurs. By electrochemical polymerization of the pyrrole monomer with a chlorine ion as dopant, a chemical equivalent of the previously reported PPyCl was produced [26]. Topographical characterization consisted of both scanning electron and optical microscopy, with surface chemical characterization using XPS. Additional information was extracted from the XPS data with the determination of the majority of bonds between pyrrole monomers being α–α linkages. These α–α linkages create fully conjugated double bonds along the backbone of polymer, which increases the polymers conductivity compared to the α–β linkages. The lack of degradation of the polymer was also confirmed in TBS for peptides and in SG-CAA for antibodies to be insufficient to deter continued experiments using the electrochemically deposited PPyCl. The data shows that the polymeric material is consistent with previous work and will be used to screen both peptides by bacteriophage display and antibodies by yeast surface display.

CHAPTER 3: Peptide Selection of Chlorine-Doped Polypyrrole

3.1 Purpose

As previously described, the methods used for the surface modification of tissue engineering applicable polymers have progressed significantly except in the area of specific recognition towards the polymer's surface. By using a viral based combinatorial display of peptides, one can selectively identify biological entities that specifically bind the surface of the polymer of interest. This combinatorial selection process provides two major advantages over the previous work performed: 1, the large number of experiments that can be conducted simultaneously, up to one billion within the time frame of an hour. This is advantageous to that of previous techniques which were limited to the monitoring of only two or three different types of polymer modifications; 2, by controlling time and pH of the interaction, one is able to selectively bind peptides that preferentially adhered under these types of reaction conditions. Thus, one is able to identify specific peptides that specifically bind peptides to the surface of a polymer, which can be further modified with cellular binding domains such as RGD to create a bi-functional linking moiety.

3.2 Background of Bacteriophage Display of Peptides

Bacteriophage display of peptides, or phage display, is composed of viruses that are genetically engineered to display 5-2700 copies random peptides per virion of a specified length, on a portion of the virus' protein coat. This technique provides a very flexible combinatorial approach and has traditionally been utilized for many applications including antibody-antigen binding studies, mapping of protein-protein contacts, and

identification of non-peptide ligands [29, 30]. Numerous researchers have taken advantage of the versatility of the random peptide libraries displayed on phage to identify bioactive peptides for immobilization of purified thrombin receptors and intact cells [31, 32]. Smith used the phage display technique to identify protease substrates by attaching an affinity insert prior to the randomized region in order to separate cleaved from the uncleaved phage [33]. Conversely, other investigators have used phage display to isolate antibodies, hormones, and DNA binding proteins from their variants, using altered affinity or specificity from libraries created from random mutant analogs [34]. A more novel use of the phage display of peptides technique is used to determine a peptide binding motif for a material to which nature has not had a chance to evolve such an interaction. These types of attachments are being investigated for numerous materials including semiconductors and metals such as gallium arsenide, cadmium sulfide, zinc sulfide, and gold [35-40].

The phage display process has been applied to many substrates, ranging from proteins to semiconductors, with successful identification of specific binding motifs. This system is beneficial and unique for application purposes and the research in this project addresses the ability to analyze numerous variants for a polymeric material, with the eventual goal of specific surface engineering. Once material-specific peptides are identified, any biomolecule, or cell, can potentially be immobilized and spatially controlled for functionalizing biomaterials for tissue engineering applications.

The phage display of peptides uses genetic engineering to incorporate a random amino acid sequence on the minor coat protein (pIII) of a filamentous virus, or bacteriophage. Commercially-available libraries that have differing peptide lengths

(twelve amino acid linear, seven amino acid linear, or seven amino acid constrained, where cysteins are at the 1st and 9th position on the peptide to create a loop structure through a disulfide bridge) on the pIII of the M13 phage can be adapted for the screening of numerous materials [36, 38]. The twelve amino acid linear peptide on the phage was chosen because it was the longest of the peptide inserts, thereby providing the highest variability of the commercially available libraries. After determining the polymer specific peptide, the size of the peptide can be reduced to determine which amino acids are significant to the binding of the peptide to the surface of the biomaterial.

3.2 Experimental Methods

The phage library was interacted after the PPyCl was synthesized (Chapter 2.2) and samples cut into 0.5 cm^2 segments and sterilized by submersion in 100% ethanol and then dried in a laminar flow hood. The samples were then interacted with the phage display library (Ph.D.-12™ Phage Display Peptide Library Kit, New England Biolabs) for 1 hr at 25°C with medium rocking. The screening processing can be seen in Figure 3.1.

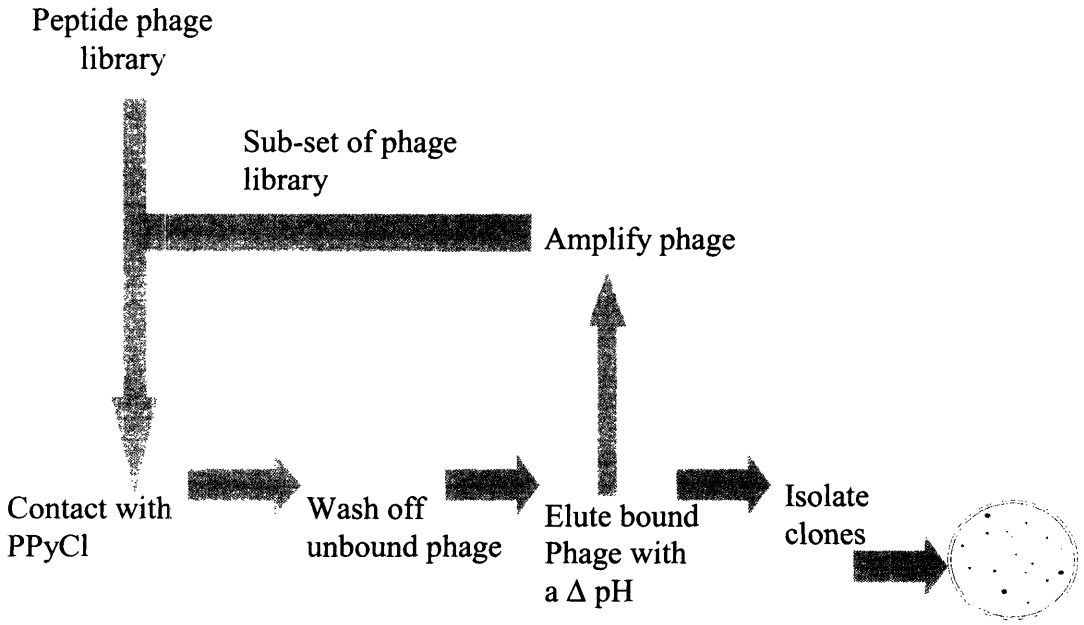

Figure 3.1: Illustration of the selection process of peptides that recognize the surface of PPyCl. On the right, *E. coli* was infected with phage to isolate individual phage clones for sequencing.

An initial volume of 10 µl of phage-display library solution, corresponding to a $1x10^{12}$ phage/µl, was interacted with the PPyCl in 1ml of 0.1 M Tris-buffered saline containing 0.1% vol:vol Tween-20 (0.1% TBS-T) pH 7.4. The library was incubated with the PPyCl for 1 hr at room temperature. The PPyCl was then washed multiple times with 1 ml of 0.1% TBS-T to discard non-specific phage. To disrupt binding of the phage that successfully bound to the surface of the material, 500 µl of 0.2 M glycine-HCl pH 2.2 was added to the substrate (see pH elution Figure 3.1) for 10 min at room temperature. The solution was collected and neutralized with Tris-HCl pH 9.13. Half of the volume of the elution was then added to a 1:100 dilution of overnight culture of *E. coli* ER2837 bacteria (New England Biolabs) in LB media and was allowed to amplify in its bacterial host to amplify for 4.5 to 5 hrs at 37°C. The bacteria were removed from phage by centrifugation at 14,000 rpm for 10 min at 4°C. The phage were then precipitated with poly(ethylene glycol) (PEG) for 15 min at 4°C. The PEG-precipitated phage were

pelleted by centrifugation at 10,000 rpm for 15 min. The phage were resuspended in 200 µl of TBS and saved as the amplification product.

The elution and amplification product were quantified by titering (infection into bacterial host) serial dilutions on LB media plates. To achieve this ten fold serial dilutions of the amplification product and the elution were prepared, 10 µl of a serial dilution was added to 185 µl of a mid log bacterial culture (Optical Density $_{600\ nm}$ = 0.5 OD/ml). The genetically engineered phage and infected bacteria, which posseses the lac*Z* gene, were plated on LB plates with isopropylthio-β-D-galactoside (IPTG) and 5-Bromo-4-chloro-3-hydroxyindolyl-β-D-galactose (X-gal), producing β-D-galactosidase that hydrolyses X-gal forming an indigo-type blue-green precipitate. Thus, bacteria which express the lac*Z* gene due to a phage infection event produce blue colonies when grown in the presence of IPTG/X-gal were counted and used to determine phage concentration (see plate Figure 3.1).

The phage concentration from the titer of the amplification was used to determine the input of the next round of biopanning against the material. A fresh piece of PPyCl was used for the next sub-set of library screening with input of phage ~10^9 virons. Interaction, washing, isolation, and amplification were repeated as described above. The process was continued until five rounds of selection were completed. After 3rd to the 5th round of biopanning, blue colonies plated during titering were picked with a tooth pick and amplified individually for 5 hr in 1:100 an overnight culture of *E. coli* in LB media (1 ml) to produce DNA to send for sequencing. The bacteria were separated from phage by centrifugation for 30 sec at 14,000 rpm. 500 µl of the phage solution were PEG-precipitated for 10 min at room temperature and then pelleted by centrifugation for 10

min at 14,000 rpm. The phage pellet was suspended in a 100 µl solution of 4 M sodium iodide to rupture the phage protein coat. DNA from the phage was precipitated with 250 µl of 100% ethanol. The precipitated DNA was then suspended in 30 µl sterile Millipore water. Nucleotide sequences from the phage DNA were obtained from The Institute for Cellular and Molecular Biology DNA Core Facility (The University of Texas, Austin, TX) and then translated into N-terminus to C-terminus peptide sequences.

After PPyCl was screened, the peptide sequences deciphered from nucleic acid sequences were analyzed for a predominant or consensus sequence, in order to determine a preferential binding motif for the polymer. Subsequent studies are centered on this selected peptide that was specifically chosen for PPyCl under controlled conditions.

An amplification of individual clones was performed to verify that the clones did not preferentially amplify better than other clones due to the screening process. This experiment consisted of re-amplifying the corresponding phage containing the selected peptides, as described previously. The titer counts of the T59 were compared to the amplification of the other phage selected from the screening process (T36, T45) and WT, to verify that the peptides were not selected because of their amplification ability. Results are shown in Figure 3.3.

The quantification of phage clones bound to the surface of PPyCl consisted of both titering and immunolableing. The titering of the binding clones consisted of interacting $1x10^8$ virons per clone (T59, T36, T45, WT) with ethanol sterilized 0.5 cm^2 samples of PPyCl in 1 ml TBS for 1 hr at room temperature with medium rocking. The samples were then washed three times with 1 ml of 0.1% TBS-T to remove any unbound phage. Elution of bound phage with 500 µl 0.2 M glycine-HCl pH 2.2 for 10 min was

used to isolate phage bound to the surface. This suspension was then neutralized with 150 ml Tris-HCl pH 9.1 and stored as elution. The elution's of the phage clones was then titered to determine the concentration of the recovered phage and these clones were sequenced again to determine the abundance of clones from the interaction. The experiment was conducted in triplicate with 34 clones selected from the first sample and 33 clones from the second and third samples to total 100 clones. Results are shown in Figure 3.4.

The immunolableing of phage clones bound to PPyCl consisted of interacting a phage concentration of $1x10^4$ virons/µl with 0.5 cm^2 sample of PPyCl for 1 hr, to allow the phage to bind to the surface. The samples of PPyCl were then washed three times with 1 ml of 0.1% TBS-T, to remove any unbound phage from the surface of PPyCl. The samples were then interacted with the biotinylated primary anti-body (Sigma-Aldrich), at a dilution of 1:400 antibody to 4% Bovine Serum Albumin (BSA) in TBS pH 7.5, for 1 hr at room temperature. The samples were washed twice with 1 ml of TBS pH 7.5. Samples were interacted with the fluorescein-labeled-streptavidin (Exaplha), at a dilution of 1:200 fluorescein-streptavidin to 4% BSA in TBS pH 7.5, for 30 min at room temperature in the dark. Samples were washed twice with 1 ml of TBS pH 7.5. The samples were mounted on microscope slides (Fisher Scientific) and imaged. The samples were imaged using a Leica TCS 4D confocal microscope equipped with differential interference contrast optics and a Kr/Ar mixed gas laser with a selected excitation wavelength of 488 nm for fluorescein and emission at 520 nm was collected through a 40X oil immersion objective (Microscopy Laboratory of the Institute for Cellular and Molecular Biology, University of Texas, Austin, TX). Results are shown in Figure 3.5.

3.3 Results

Sequences were obtained from the clones selected after each subsequent screen following the 3rd round. Results from the study for screening PPyCl rounds three through five are illustrated in Figure 3.2.

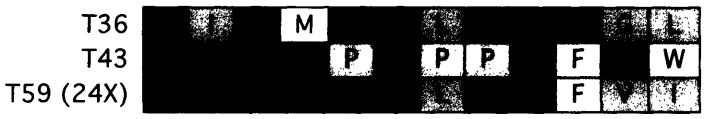

Figure 3.2: Peptide sequences from selection rounds three through five obtained from PPyCl-specific phage. The single letter code for the 20 amino acids was used in depicting the peptide sequence. The color coding corresponds to the amino acid group: Basic-blue (lysine, histidine, arginine); Acidic-red (aspartic acid, glutamic acid); Hydrophobic-orange (glycine, alanine, valine, leucine, isoleucine); Hydroxyl-green (serine, tyrosine, threonine); Aromatic-brown (phenylalanine, tryptophan); Amines-purple (asparagine, glutamine), Methionine-white, Proline-yellow

From Figure 3.2 it is apparent that the predominant sequence is that of T59 by an overwhelming margin of 92% to both the other clones. It is interesting to note that the increase in hydroxyls and lack of prolines amino acid groups were significantly different in comparison to the combinatorial peptide library reported values for these groups (Selected Peptides: hydroxyl = 41.0% and proline = 1.0%; Library: hydroxyl = 24.7% and proline = 12.2%). Note that the polymer backbone of PPyCl has alternating secondary amines on adjacent pyrrole monomers making the overall polymeric charge somewhat positive (Figure 3.2). One possible scenario for the increase in hydroxyl groups in the peptide is an amide interaction that could occur between these two functional groups at the surface of the material. The rigid structure that is created from the influence of proline may increase the probability of conformational alterations to the twelve-mer peptide which could increase the peptide's binding capability. These types of interactions, electrostatic and secondary structure presentations, which commonly occur

between proteins, may play an integral role in the binding of the predominant sequence to conductive PPyCl.

3.3.1 Amplification of Phage Selected for Chlorine-Doped Polypyrrole

A good understanding of how the phage amplify in their bacterial host is needed to confirm that the predominant sequence selected for the PPyCl surface was specific for the material and not chosen for the phage's ability to amplify in its bacterial host. This can be a concern because of the multiple rounds of selection/bacteriological infection that the phage undergoes in the selection process. If predominant phage multiply better than naturally occurring wild type (WT) phage, which has no engineered peptide insert, then there is a possibility that the phage containing the predominant sequence peptide was selected because of its ability to amplify and not because of its specific binding ability to the surface of PPyCl.

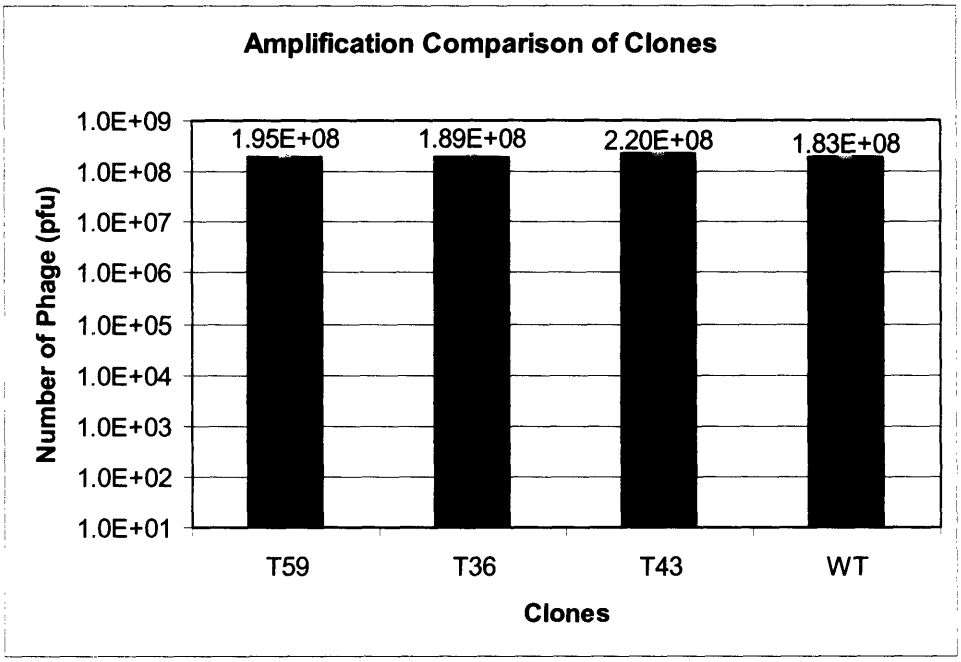

Figure 3.3: Amplification study of phage selected for PPyCl, Error bars = ±5%.
T59: THRTSTLDYFVI; T36: TIKMHTLSYTGL; T43: SHKYPKPPYFHW; WT: NA

The similarities between the phage concentrations after amplification are sufficient to determine that they are within 5% of each other. From Figure 3.3 T59, T36, T43 and WT amplify to the same order of magnitude under the conditions described. The similarities in the amplification of the different phage demonstrate that T59 was not selected because of its increased ability to amplify.

3.3.2 Binding Ability of Phage Selected for Chlorine-Doped Polypyrrole

To investigate whether the predominant viral-bound peptide binds specifically to the PPyCl surface, the binding ability of the peptide was investigated using two methods: phage concentration (titering) and immunolabeling of phage. The concentration of phage bound to PPyCl was determined using a titer count which is semi-quantitative and provides a relative binding comparison of phage counts for each of the clones selected from the screen and WT.

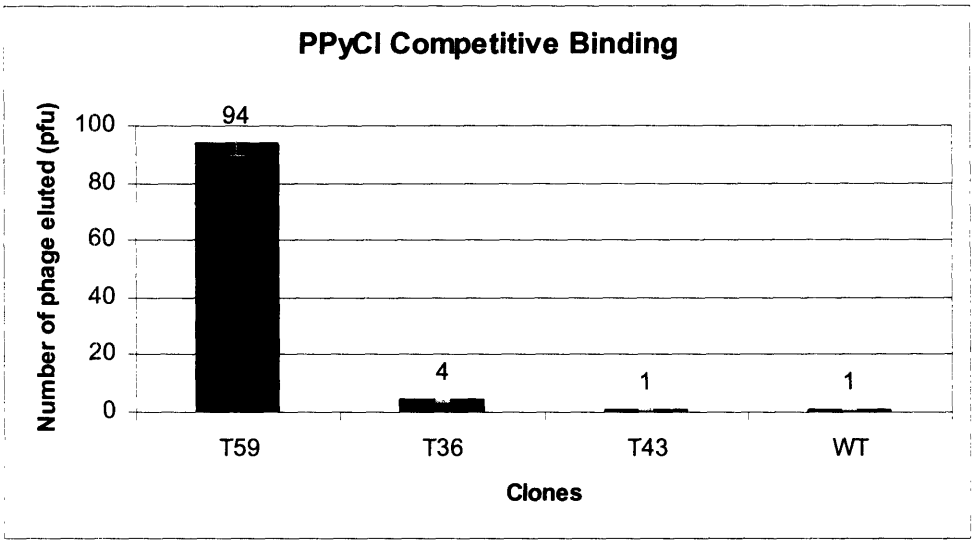

Figure 3.4: Competitive binding study of phage selected for PPyCl, Error bars = ±5%. T59: THRTSTLDYFVI; T36: TIKMHTLSYTGL; T43: SHKYPKPPYFHW; WT: NA.

This study was performed to compare the competitive binding ability of T59, T36, T43, and WT by comparing the amount of phage that could be recovered from the surface of PPyCl. The titer count method of binding ability of PPyCl shows that T59 binds more successfully than other types of phage tested. T36, T43, and WT had minimal recovery most likely due to non-specific interactions with the surface of PPyCl as can be seen by the recovery of a single WT clone. T59 has the greatest recovery rate of phage bound to the surface with 94 clones out of 100. This result verifies the ability of T59 phage clone to bind to PPyCl through its unique minor coat protein, pIII, since all of the other clones have identical major coat proteins, pVIII. This is initial encouraging data showing that T59 is specific to the polymer surface.

Immunolableing of phage particles was used to fluorescently label the phage bound to the surface of the PPyCl, permitting quantification of phage bound to the PPyCl. A biotinylated antibody was used to bind to the M13 bacteriophage, specifically on the pVIII protein of the virus (Sigma-Aldrich Corp.). The biotin end of the antibody afforded attachment of a streptavidin labeled fluorescein (Exaplha) to visualize the phage on the polymer using fluorescence microscopy.

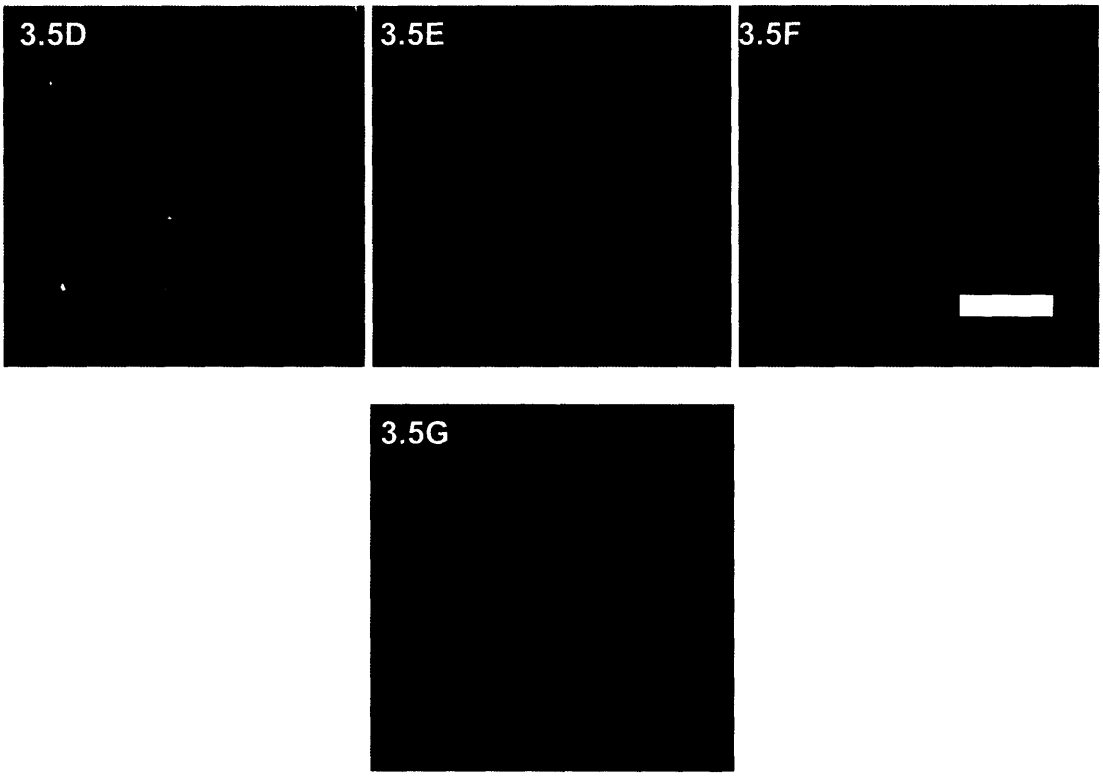

Figure 3.5: 3.5A) Reflectance image of PPyCl-with phage, 3.5B) T59-1°-2°, 3.5C) random phage-1°-2°, 3.5D) WT-1°-2°, 3.5E) 1°-2°, 3.5F) 2°, 3.5G) mounting media. Scale bar = 50 μm. 1° = primary antibody (anti-M13-biotin), 2° = secondary antibody (streptavidin-fluoroscein). T59: THRTSTLDYFVI; Random sequence: IEHPKTPDSHSR

From Figure 3.5B due to high fluorescent signals T59 was shown to have specific interaction with the PPyCl surface. The intensity of the fluorescein emission at 520 nm is monitored on all samples for comparative purposes. Through Figures 3.5B-G the greatest intensity is that of T59, further confirming T59's specificity for PPyCl. Random phage and WT were used as controls to verify T59's binding specificity. The viral bound peptides on the random clone and WT were different than that of the peptide sequence displayed on T59 and also have lower fluorescence intensity, suggesting that the T59 phage bind specifically to PPyCl. When Figure 3.5B (T59) and 3.5D (WT) are compared the PPyCl specific phage showed a difference in both coverage and intensity in favor of the T59 clone. This intensity difference may represent WT non-specific phage interaction

occurring at the PPyCl surface. The WT phage is the naturally occurring phage and the pIII coat protein of the WT phage has not undergone genetic engineering. Therefore the only difference between T59 and WT phage is the pIII peptide insert on T59. The increased intensity for the T59 compared to WT is therefore likely due to the interaction that occurs between the engineered peptide on T59 and the surface of PPyCl. From Figures 3.5E-G, that the amount of fluorescence from the antibody, streptavidin labeled fluorescein, and mounting media is minimal compared to the intensity of labeled phage. All samples were imaged using the same intensity of laser light and exposure times, except for the reflectance image (Fig. 3.5A) which was not imaged with the laser but with a 100 W Hg lamp.

3.4 Conclusions

Extensive screening processes have been performed to obtain the best binding peptide under controlled conditions. After selecting the phage that displays the peptide that binds specifically to PPyCl, the phage containing the engineered peptide of interest was confirmed to not be selected as a result of amplification bias in its bacterial host. A better understanding of how well the T59 phage binds to the surface was further investigated. In the competitive binding comparison, T59 had a much higher population compared to that of other clones selected from the screen as well as WT which verifies that T59 is best binding peptide for PPyCl under controlled conditions analyzed so far. To confirm that we had found the best binding peptide, a second comparative binding assay was performed investigating actual phage bound to the surface of the conductive polymer. Through the use of immunolabeling, the phage were visualized by fluorescence microscopy bound specifically to the surface of the conductive polymer. The

immunolabeling experiments further reconfirmed what was observed from competitive binding comparison. Thus, the T59 peptide sequence of THRTSTLDYFVI has the best binding ability to the conductive polymer PPyCl while in neutral pH buffer at room temperature, binding that can be disrupted with an acid elution.

Eventually peptide connections that are being made between the surface of a material and a peptide will play an integral role in the modification of surface binding. Ultimately one will be able to spatially control peptide incorporation onto a hybrid-biomaterial providing a bi-functional linker for attachment to cells, such as Schwaan cells, and biomolecules (nerve growth factor) along with the ~50% increase in nerve regeneration associated with electrical stimulation, all of which have been shown to regenerate nerve cells on their own [3, 11, 41, 42]. This type of integration of peptides and materials will further expand the possibilities of the tissue engineering industry. This interface of materials science with biology, will allow the tailoring of properties that are needed in biomedical materials such as degradation rate, surface area, and immunogenic response, and the exploitation of natural biological processes leading to new and exciting research. Starting with a material such as PPyCl that has already undergone extensive investigation for the regeneration of nerve tissue one can modify the surface of this material, by using phage display to isolate and identify specific peptides that recognize the surface of PPyCl, and presumably construct a "hybrid-biomaterial."

Chapter 4: T59 Binding Mechanism Using Peptide Analogs

4.1 Purpose

The T59 peptide expressed on the PPyCl-specific phage has been shown to bind specifically to the surface of PPyCl. From the T59 peptide amino acid composition, there are several reasons to explain the interaction with the polymeric surface. For instance, from looking at the sequences and comparing the experimental values of amino acids in the peptide to the literature values of expected populations, as reported in the previous chapter it was determined that there was an increase in the presence of hydroxyl groups by 16.3% compared to the literature value. This increase could possibly be because of potential hydroxyl-amide interaction at the surface of the material. Here, to elucidate how T59 binds to PPyCl, substitutions in the T59 peptide sequence were made to create peptide variants. By studying the interactions of these variants, aspects of the peptide can be verified for the importance in binding to the polymer.

Protein concentration assays were used to evaluate the proposed peptide variants binding to the surface of PPyCl. Most protein assays are simply colorimetric and are comprised of a signal molecule for detection. A list of colorimetric protein concentration assays used in the literature are shown for comparison in Table 4.1.

Assay	Dynamic range	Time	Advantages	Disadvantages
UV	10 ug/ml-50 μg/ml or 50 μg/ml-2 mg/ml	none	Low cost, nondestructive, well established procedure	Sensitivity depends on the number of tyrosine and tryptophan residues present
Lowry	1 μg/ml-1.5 mg/ml	1.5 hrs	Well established procedure, little protein to protein differences	Lengthy procedure, not compaitble with surfactants or reducing agents
Bradford	1 μg/ml-1.5 mg/ml	30 minutes	Well established procedure, useful when accuracy is not crucial	Not compatible with surfactants, high protein to protein variations
OPA	200 ng/ml-25 μg/ml	5 minutes	Compatible with aqueous solutions	Not comaptible with Tris or glycine buffers
BCA	500 ng/ml-1.2 mg/ml	1-1.5 hr	Compatible with surfactants	Certain amino acids can interfere
NanoOrange	10 ng/ml-10 μg/ml	1 hr	Little protein to protein differences	Not a well established assay
Fluorescamine	100 ng/ml-200 μg/ml	1 minute	Well established procedure, unbound dye is nonfluorescent	Not compatible with aqueous solutions

Table 4.1: Table of protein assays there dynamic range, assay time, advantages and disadvantages.

For the work that was performed, the assay to be used needs to be an established method that has a dynamic range of nM to μM concentration regimes and has a limited amount of incubation time for high throughput. Therefore, the technique that was selected was the fluorescamine assay, because it has been well established, lacks the incubation time required from the others and the dynamic range is with the limits necessary for detection of peptides on PPyCl. An additional benefit from the use of this technique is that it is a fluorescence technique; therefore the opaque surface of PPyCl should not give significant background fluorescence.

Most protein assays are based on the conversion of reagents to products with characteristic absorption spectra which correlate to relative protein concentrations. Fluorescamine, spiro(furan-2(3H),1'(3'H)-isobenzofuran)-3,3'-dione, 4-phenyl, is an intrinsically nonfluorescent molecule but it reacts in milliseconds with primary aliphatic amines, including peptides and proteins, to yield a fluorescent derivative, Figure 4.1 [43].

The amine-reactive reagent has been shown to be useful for determining protein concentrations of aqueous solutions and is well suited for a fluorescence microplate reader [44-47]. Additionally, the reaction with fluorescamine proceeds efficiently at room temperature in aqueous solution, with the half-time of the reaction of 200-500 msec at pH 9.0, for most amino acids, with excess reagent concomitantly hydrolyzed allowing the assay of submicromolar concentrations of amines.

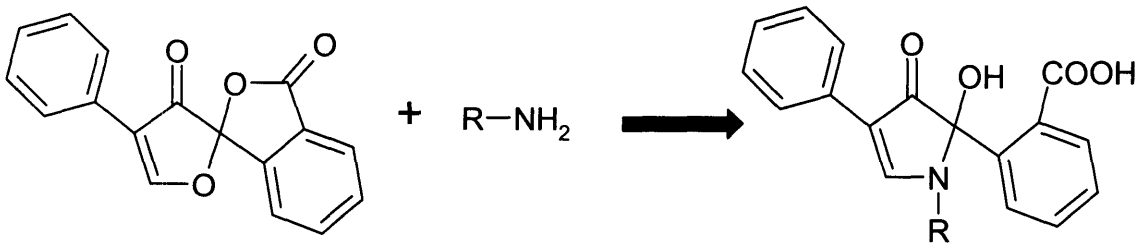

Figure 4.1: Fluorescamine reacts with primary aliphatic amines to form a pyrrolinone that fluoresces at 475-490 nm with excitation at 390 nm.

4.2 Experimental Methods

Substitutions in the T59 peptide were made strategically to remove/replace reactive groups that could be responsible for the peptide binding to PPyCl. Specific substitutions were as follow: the amino acid composition of T59 was reversed to determine if amino acid order plays a role in binding; reduced to half to negate half of the amino acids in the peptide on both the N-terminus and C-terminus; halves reversed to reduce amino acid content and determine if order plays a role in binding; reduced to half with glycine spacer to determine if the reduced amino acids played a role in binding but require a better secondary structure supplied by an extended peptide; histidine (H) and arginine (R) replaced with serine to determine if HR plays a role in binding and how serines influence binding; HR replaced with glycine to determine if HR plays a role in binding and how glycines influence binding; HR replaced with aspartic acid (D) to

determine if HR plays a role in binding and how aspartic acids influence binding; D replaced with R to determine what role D plays in binding and how R influences binding in this area of the peptide; D replaced with glycine to determine what role D plays in binding and how glycine influences binding; HRD replaced with glycine to determine if a complete substitution of the charged reactive groups in the peptide has an influence on binding to the polymeric surface; front half of T59 with HR replaced with glycine to determine if the lack of charged groups in the front half is sufficient for binding; front half of T59 reversed with HR replaced with glycine and a glycine spacer to complete the 12-mer to determine if structure, order, and lack of charge play a role in binding; in the front half replace HR with tyrosine (Y) and phenalanine (F); and in the back half replace YF with HR to determine if order of the amino acids play a role in binding the surface of PPyCl. All variants are shown in Table 4.2.

T59	THRTSTLDYFVI
T59R	IVFYDLTSTRHT
F6	THRTST
B6	LDYFVI
F6R	TSTRHT
B6R	IVFYDL
F6G	THRTSTGGGGGG
B6G	LDYFVIGGGGGG
F6RG	TSTRHTGGGGGG
B6RG	IVFYDLGGGGGG
HR/S	TSSTSTLDYFVI
HR/G	TGGTSTLDYFVI
HR/D	TDDTSTLDYFVI
D/R	THRTSTLRYFVI
D/G	THRTSTLGYFVI
HRD/G	TGGTSTLGYFVI
F6HR/G	TGGTST
F6RHR/GG	TSTGGTGGGGGG
HR-YF	TYFTSTLDHRVI

Table 4.2: Strategic amino acid substitutions in the T59 peptide. Right column: variant label, Left column: single letter amino acid peptide sequence.

The above sequences were fabricated on an ABIMED peptide arrayer system consisting of a computer controlled Gilson diluter and XYZ liquid handling robot (Biopolymers Lab, MIT) and purified to 95% by HPLC. The peptide variants were interacted with a sterilized 0.5 cm^2 sample of PPyCl at concentrations ranging from 0-15 μM in 1X PBS for 1 hr at room temperature. Standard curve concentrations of T59 peptide ranged from 0-15 μM to determine actual peptide concentrations on the surface of PPyCl. The above samples were washed three times with 1X PBS and rehydrated with 300 μl of 1X PBS. One minute before reading the samples emission at 480 nm (excitation at 390 nm), 100 μl of 1.79 mM fluorescamine in acetone was added to label peptides bound to PPyCl. All experiments were repeated in triplicate. Emission readings were taken on a Gemini XPS system controlled by SoftMax Pro® software.

4.3 Results

Sub-sets of the above modifications to T59 were screened against the surface to better understand the potential of a 12-mer peptide and a 6-mer peptide. The first of the interactions consisted of the following modifications to the T59 peptide: T59, T59R, F6G, B6G, B6RG, B6RD/GG, and HR/G.

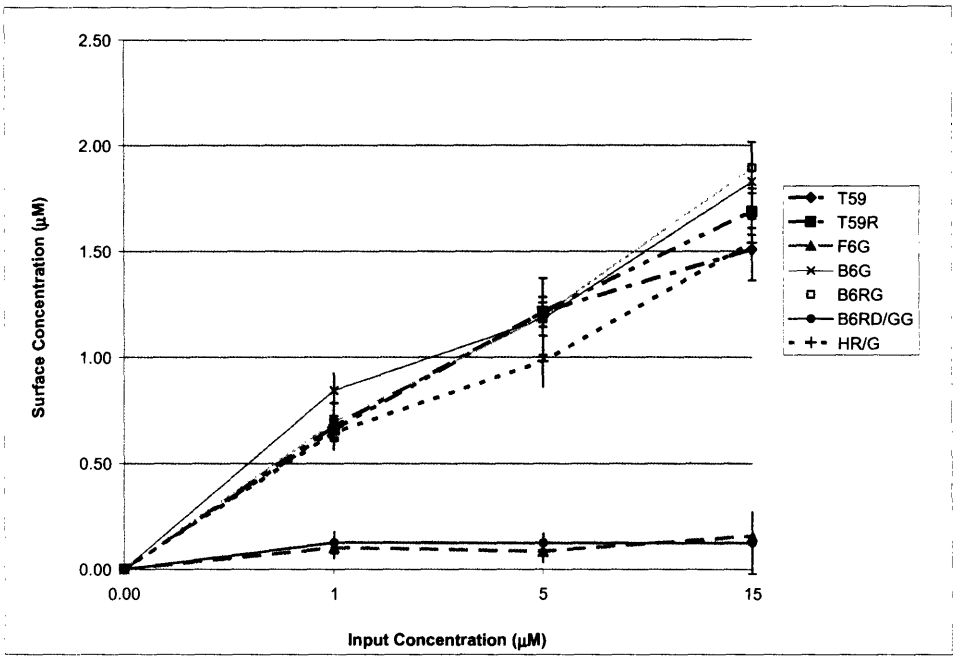

Figure 4.2: Surface concentration of peptides interacted with PPyCl. Error bars = ±1 SD.

From Figure 4.2, the data shows that peptides that do not contain the aspartic acid (D) residue have little binding capability to PPyCl. Additionally, all other peptides containing D bind within a standard deviation of each other.

To determine if peptide variants bind with higher affinity to PPyCl than the T59 peptide, the same procedure was used as before by interacting peptide variants with PPyCl samples, then washing and labeling bound peptides with fluorescamine. The D/G variant was used along with T59, F6G, B6G, and B6R.

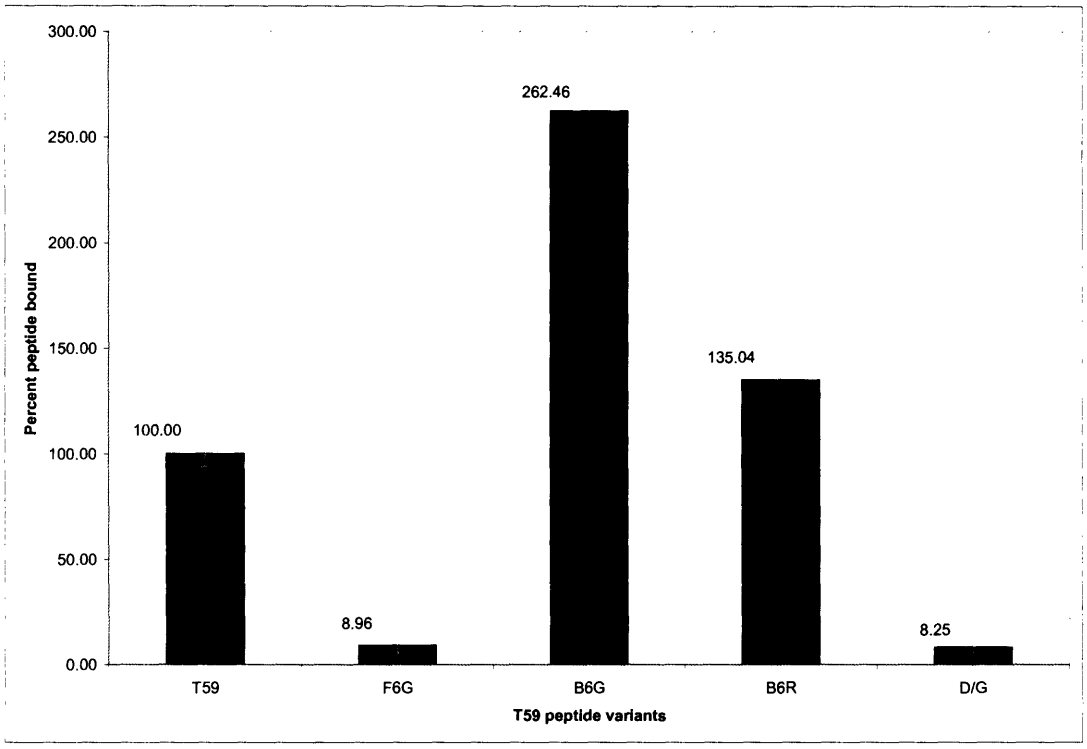

Figure 4.3: Peptide variants binding compared to T59 peptide at 15 μM.
Error bars = percent deviation.

For data analysis of this study, peptide variant surface concentrations were compared to the T59 surface concentration and converted to a percent of T59 surface concentration. From the above data it is shown that both F6G and D/G, which lack D in their amino acid composition, bind significantly less than that of T59. B6G and B6R, which contain D, have increases in binding compared to T59, with B6G having a significant increase of almost 1.5 times more surface concentration compared to that of T59. Ultimately, Figure 4.3 reiterates the conclusion that was drawn about the data from Figure 4.2, that the role of aspartic acid is playing an essential role in binding T59 to PPyCl.

The initial phage screening was performed at pH 7.4 with elution or release of the binding phage at pH 2.2. The pK_a of the reactive groups in T59 (H, R, D, Y), are 6.04, 12.48, 3.90, and 10.46, respectively [48]. From the pK_a values it is apparent that the only

species that would protonate at the release pH would be that of the β-COO- of the aspartic acid. The previous experiments concerning the use of T59 peptide variants have hinted that aspartic acid plays a significant role in binding T59 to PPyCl. To test this hypothesis, a binding assay was conducted where a change of pH is involved. The experiment was performed by interacting the same concentration range of 0-15 μM of T59 peptide with samples of PPyCl in 1X PBS adjusted to a pH of 2, 4, 6, 7.4, and 8. The data is shown in Figure 4.4 with input concentrations on the ordinate and peptide surface concentration on the abscissa. From the data represented by the change in pH over the scale of 2-8 that is used for screening, it was observed that the binding of the T59 peptide above that of a pH 2 all follow the same trend of increased binding with increased input concentration. As for T59 binding in pH 2 PBS it is significantly less than that of all other pH ranges.

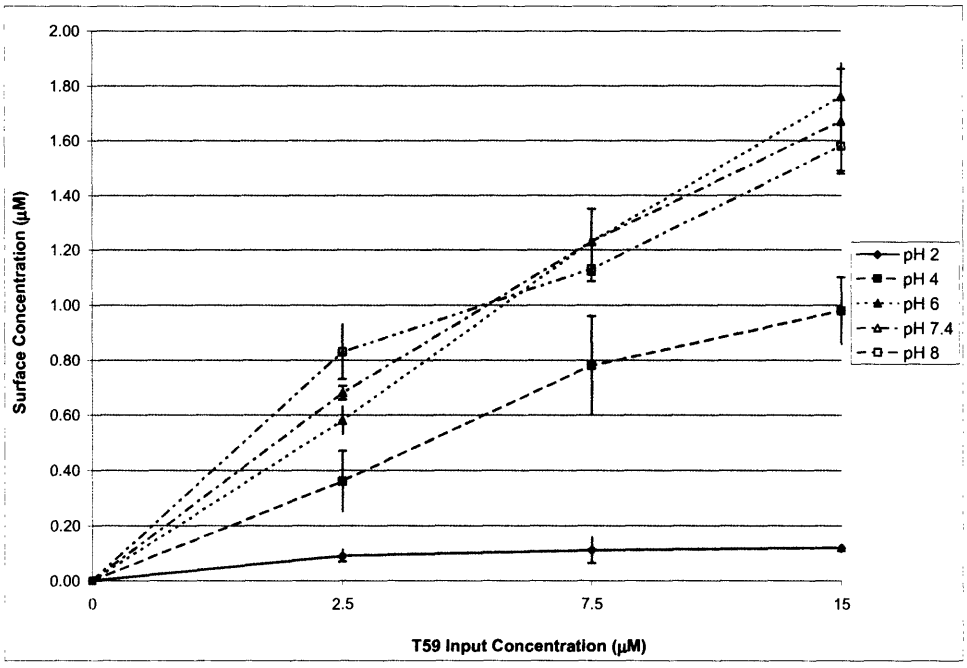

Figure 4.4: T59 peptide binding comparison in differing pHs. Error bars = ±1 SD.

If one evaluates this scenario on a molecular scale, the aspartic acid reactive group β-COO- is being protonated at a pH below 3.86 to β-COOH, thus thereby disrupting the binding between the negatively charged residue and the positively charged surface of PPyCl.

To better understand what it takes to bind to PPyCl, an additional set of clones was created that only represented the last six amino acids of the T59 peptide. This grouping was selected because of its ability to bind to PPyCl, as seen in Table 4.3 clones (B6G and B6R). This additional set of clones focused in on the ability of aspartic acid to mediate peptide binding to PPyCl with strategic replacements of aspartic acid with glutamic acid and asparagine. To determine if any of the adjacent residues have a minor role in binding to PPyCl, they were replaced sequentially from N-terminus to C-terminus and vice-versa with alanine. An alternative clone with two aspartic acids centrally located in the peptide with two flanking alanines on both sides was also synthesized to determine if there is an increase in binding to PPyCl with an increase in aspartic acid residues. The above mentioned clones are represented graphically by their single letter amino acid code in Table 4.3.

B6	LDYFVI
B6E	LDYFVI
B6N	LDYFVI
A8-12	ADYFVI
A10-12	ADAFVI
A11-12	ADAAVI
A12	ADAAAI
A7-11	LDYFVA
A7-10	LDYFAA
A7-9	LDYAAA
A7-8	LDAAAA
AD	ADAAAA
DD	AADDAA

Table 4.3: Amino acid substitutions of the last six residues of the T59 peptide.

As shown previously with the fluorescamine assay of the T59 clone binding to PPyCl, these peptide variants were assayed and their results are as follows in the Figure 4.5.

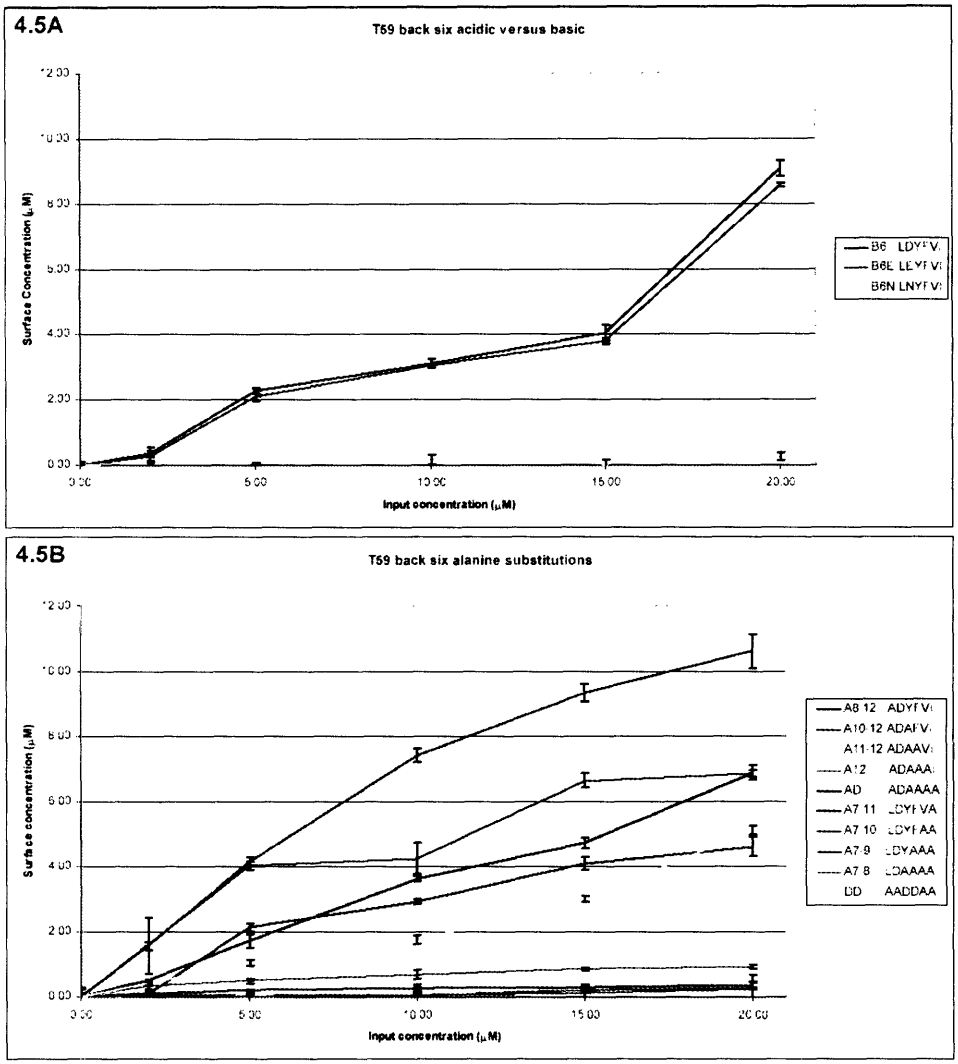

Figure 4.5: T59 back six amino acid variant clone fluorescamine binding assay. 4.5A) Acidic/Basic comparison, 4.5B) Alanine substitutions. Error bars = ±1 SD.

The comparison of acidic and basic residue alterations to the back six of the T59 peptide shows that when the aspartic acid residue was replaced with glutamic acid (B6E) there was very little change in binding capacity of the peptide variant, but when the aspartic acid was replaced with asparagine (B6N) there was a significant decrease in the

binding capability of the peptide to PPyCl. This suggests that the acidic residues, aspartic acid and glutamic acid, are interchangeable when incorporated into this peptide and that the lack of a carboxylate reactive group significantly reduces the binding of the peptide to PPyCl supporting the hypothesis that when protonation occurs with aspartic acid and glutamic acid around a pH of 4 the peptide releases from the surface of PPyCl.

Figure 4.5B represents the evaluation of the binding of various alanine substitutions made in the back six amino acids of the T59 peptide. From this data some surprising conclusions can be drawn. When alanine replaces leucine (A8-12), which is directly adjacent to the aspartic acid residue, there is slight reduction in binding compared to the full back six (B6). When alanine replaces leucine and tyrosine (A10-12) there is a significant decrease in binding and secondarily (A11-12, A12, AD), suggesting there is some secondary importance to both leucine and tyrosine being adjacent to aspartic acid within the peptide. This is reconfirmed when the alanine replaces the last three residues of the peptide leaving only leucine, aspartic acid, and tyrosine (A7-9). As can be seen in the graphical analysis the A7-9 clone is the only clone of all 13 back six clones to bind at least half of the input concentration, reaching 10.61±0.53 μM. Other alanine substituted clones A7-11, A7-10, and A7-8 lead to the same conclusion of the secondary importance of adjacent leucine and tyrosine to aspartic acid. The DD clone provided some very interesting binding data suggesting that without either leucine or tyrosine adjacent to aspartic acid there can still be some binding to PPyCl by increasing the number of aspartic acid residues in the peptide.

4.4 Conclusions

T59 peptide and its variants were evaluated using a fluorescamine assay by interacting known concentrations of the peptide variant with 0.5 cm^2 samples of PPyCl, washing the samples, and labeling the remaining peptide bound to PPyCl. Initial experiments alluded to the premise that the charged species, aspartic acid, could play a significant role in peptide binding to PPyCl. Further variants reinforced this idea, cued from the initial work that residues with higher aspartic acid occurrence, bound to PPyCl more significantly than the T59 peptide. This data revealed the possibility that the complete T59 peptide need not be present for binding to PPyCl, specifically the front six amino acids. However, without aspartic acid binding was drastically reduced revealing its necessity. The variant B6G had the best relative binding to PPyCl which when compared to B6R; this confirms secondary structure is also important for good binding, because these two variants differ only by a glycine spacer. The validity of this statement is represented by the increase in binding with B6G at 1.5 more and with B6R at 1/3 more than the full T59 peptide.

To determine the pH sensitivity of the T59 peptide, differing pHs, ranging from 2-8 were evaluated. These results revealed that, at pH 2, T59 binds significantly less than all other pH values attempted. This data confirms the function of aspartic acid in T59 binding of PPyCl, by protonating the reactive carboxylate group at pH 2 the binding is greatly reduced. Thus, the data from these experiments suggests that the binding of the T59 peptide is dependent on the interaction of negatively charged residue, aspartic acid, with the surface of positively charged surface of PPyCl and not the hydroxyl groups making amide bounds with the surface as previously hypothesized. This interaction

suggests that the mechanism for binding is a shared hydrogen between that of aspartic acid and certain areas of the polymer.

Working off of the hypothesis that the last six amino acids contain the residues responsible for binding T59 to PPyCl, other peptide variants were made with strategic sequential alanine substitutions. This permitted the evaluation of binding of an individual or groups of amino acids in the peptide. From this data it was determined that aspartic acid can be replaced with glutamic acid with little decrease in binding capability. This lack of difference in binding is most likely due to glutamic acid's similar pK_a of 4.07 compared to aspartic acid's pK_a of 3.86. When a basic residue replaced aspartic acid there was a significant decrease in binding, suggesting that an acidic residue is necessary for the peptide to bind to PPyCl. The sequential alanine substitutions provided insight in to possible secondary residues necessary for binding. From the findings it appears that having leucine and tyrosine adjacent to aspartic acid is essential to binding PPyCl represented by an increase in binding capability. Finally, using multiple aspartic acids in the peptide showed a similar binding capability as the full back six at 15 μM input concentration.

Chapter 5: Peptide Functionalization of the Chlorine-Doped Polypyrrole

5.1 Purpose

To show proof of concept for a nerve guidance scaffold, where by nerve cells are specifically attached to the surface of the scaffold through a biological tether, one needs to group together the necessary components. These components consist of the scaffold material, the biological bi-functional linker, and nerve cells that have been used as a model system for *in vitro* system evaluation. The components for the system described here are comprised of 5-10 μm thick PPyCl, a T59 peptide that has been modified on the C-terminus with a spacer GGSK, a cell adhesion promoting heptmer peptide GRGDS, and model neuronal cells from rat. These components will be used to create a single unit bi-functional linker between a neuronal scaffold and cells that in the presence of nerve growth factor will differentiate, producing axon processes.

5.2 Experimental Methods and Results

The T59 peptide was modified with a spacer GGSK at the C-terminus and a cell adhesion promoting sequence GRGDS linked to the spacer producing a single letter amino acid sequence of THRTSTLDYFVIGGSKGRGDS (T59-GRGDS) (Institute of Cellular and Molecular Biology Core Facilities, University of Texas at Austin). The peptide was purified to >99% by HPLC by the manufacturer.

Initial studies focused on the optimizing the input concentration of T59-GRGDS. As previously described, these studies were conducted using the fluorescamine assay with T59-GRGDS peptide as the standard curve peptide. The studies were carried out by

interacting knows concentrations of T59-GRGDS (0-60 μM) in 1X PBS with ethanol sterilized PPyCl 0.5 cm^2 samples for 1 hr with medium rocking. The samples were then washed three times with 1 ml for 5 min with subsequent labeling of bound peptide using fluorescamine and then assayed as described previously in Chapter 4. The experiment was conducted in triplicate and the data is represented in Figure 5.1.

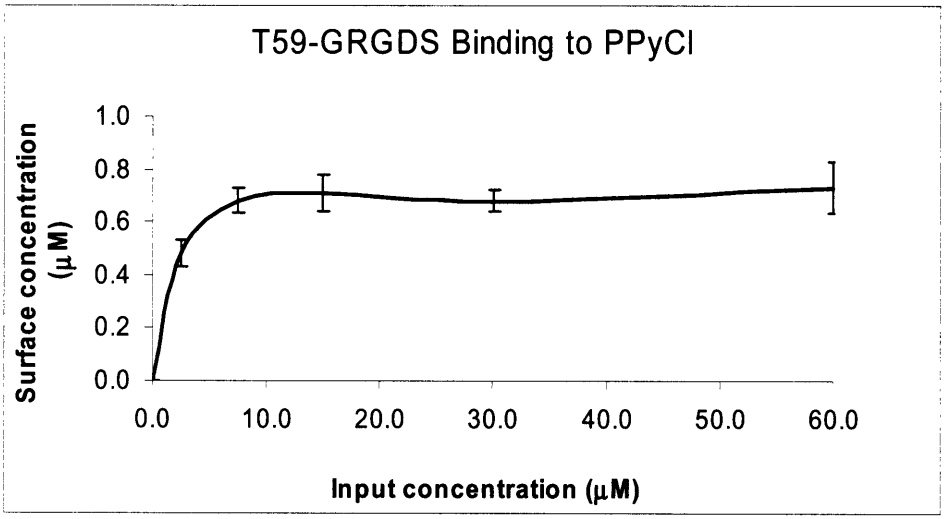

Figure 5.1: T59-GRGDS input optimization. Error bars = ±1 SD.

From the above data one can observe that there is a gradual rise in surface concentration as the input concentration is increased up until the input concentration of 15 μM. At 15 μM it seems that the PPyCl surface has been saturated with T59-GRGDS. This is evident because as the input concentration is increased further to 30 μM and 60 μM the actual surface concentration remains within 1 SD of the 15 μM surface concentration. This suggests that at an input concentration of 15 μM or higher all of the binding sites on a 0.5 cm^2 sample of PPyCl are occupied by peptides. Therefore, for further studies an input concentration of 15 μM will be used to saturate the PPyCl surface with the bi-functional peptide T59-GRGDS.

As well as determining the optimal input concentration of bi-functional peptide, it would also be of interest to note for what period of time is T59-GRGDS bound to the surface of PPyCl in the presence of cellular media. This would give an idea as to what is influencing the binding of cells from one hour to one month. To perform such an experiment, an input concentration of 15 μM of T59-GRGDS peptide was used per the previous experiment, to saturate the surface of PPyCl. The time points for the experiment were taken at 1 hour, 3 hours, 1 week, and 1 month, and were conducted in triplicate in both serum-free and serum-containing media. In the serum containing experiment, controls of serum only samples were used to obtain quantity of bound T59-GRGDS. The PPyCl samples were sterilized as previously described prior to interaction with the respective media. Figure 5.2 represents these set of experiments.

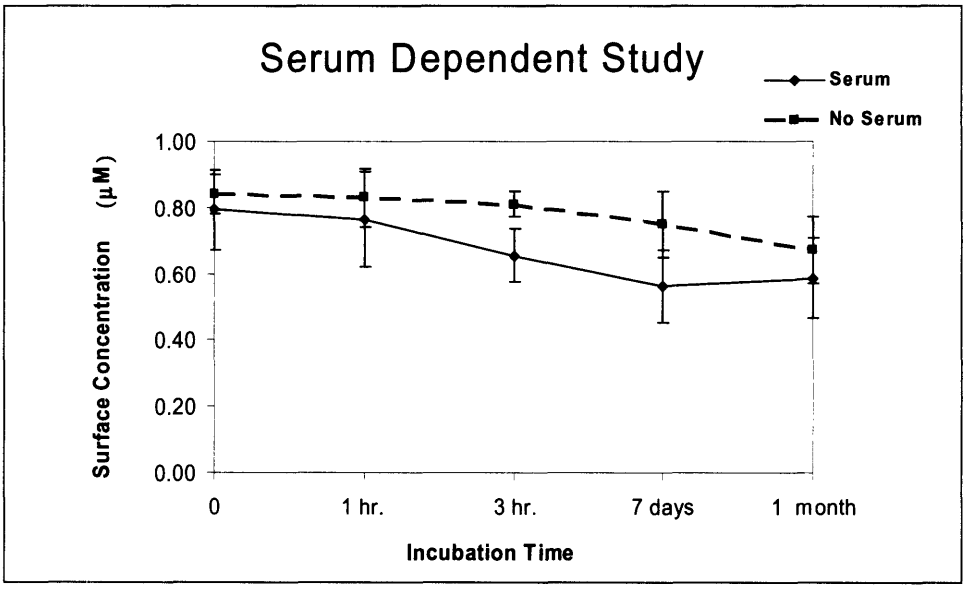

Figure 5.2: Serum dependent study of T59-GRGDS peptide bound to PPyCl over varying time points. Error bars = ±1 SD.

As the above data suggests there was little change in surface concentration of T59-GRGDS in both serum and serum-free media. Quantitatively, over a period of 1 hr, there was a decrease in peptide concentration by 3.7% and 1.2% for serum and serum-

free media, respectively. A significant deviation between serum and serum-free peptide concentration becomes evident at a period of 7 days, when the difference between them is 18.5%. This most likely occurs because the serum is displacing the peptide on the surface of PPyCl. This displacement is even more apparent after a period of 1 month when the percent decrease of T59-GRGDS bound to the surface of PPyCl is 26.0% and 20.2% in serum and serum free media. But more importantly from the experiments conducted, it was determined that the overall reduction in T59-GRGDS concentration on the surface of PPyCl is at most reduced to 74.0% and at least to 79.8% of the original bound peptide in serum-containing and serum-free media over a period of 1 month, respectively. When these values are compared to that of varying surface concentrations in Figure 5.1, we see that most of these values could represent, when bound to the surface of PPyCl, an input concentration of 4.4 μM which represents 1.32×10^{15} peptides/mm^2 which is still a significant number of peptides to have available for adhesion to cells.

For the cellular studies, PPyCl samples were prepared by sealing plexi-glass wells (1.5 cm x 1.0 cm x 1.0 cm) using silicone rubber sealant (DAP, Inc.) onto PPyCl thin films prepared on ITO-coated glass slides which was allowed to cure overnight. The samples were washed three times with 1X PBS and ethanol sterilized for 30 min. The samples were rinsed three times with 1X PBS prior to peptide incubation and maintained in sterile environment continuously. Incubation of 15 μM T59-GRGDS peptide on 0.5 cm^2 PPyCl samples for 1 hr in 1X PBS at room temperature was followed by thorough rinsing three times with 1X PBS to remove any unbound peptide.

The cells used were a neuronal, PC12, rat phenochromocytoma cell line that responds to nerve growth factor (NGF) by expressing 'neurite-like' processes, which

were purchased from the American Type Culture Collection. PC12 cells were cultured in 85% F-12 media supplemented with 10 mM 4-(2-hydroxyethyl) piperazine-1-ethanesulfonic acid, 25 mM glucose, 1 mM sodium pyruvate, 10% horse serum, and 5% fetal bovine serum and plated onto collagen coated flasks. Cells were maintained at 37°C in a humidified 5% CO_2 incubator. Media was replaced every 2-3 days, and cells were passed with 2.5 mM trypsin/1 mM ethylene-diaminetetraacetic acid.

PC12 cells were seeded onto PPyCl or PPyCl with T59-GRGDS peptide in serum-free and serum-containing media at a density of 10^4 cells/cm^2 and were allowed to attach at 37°C in 5% CO_2, overnight. Cell growth media was removed from the samples each day and then replaced with fresh media after rinsing the substrates once with 1X PBS for a total of 3 days. At the end of the third day (72 hrs), an inverted phase contrast microscope (IX-70, 20X or 40X objective, Olympus) and a high resolution CCD video camera (CCD-72, Dage-MTI, Inc.) were used to visualize cell adhesion.

To determine whether the modified peptide had bi-functional capabilities, the peptide was interacted with PPyCl samples, then subsequently with neuronal PC12 cells. The T59-GRGDS peptide will confirm its bi-functional capabilities if there is monodisperse cellular attachment to PPyCl. Images were taken to evaluate these experimental results and are represented in Figure 5.3 and 5.4.

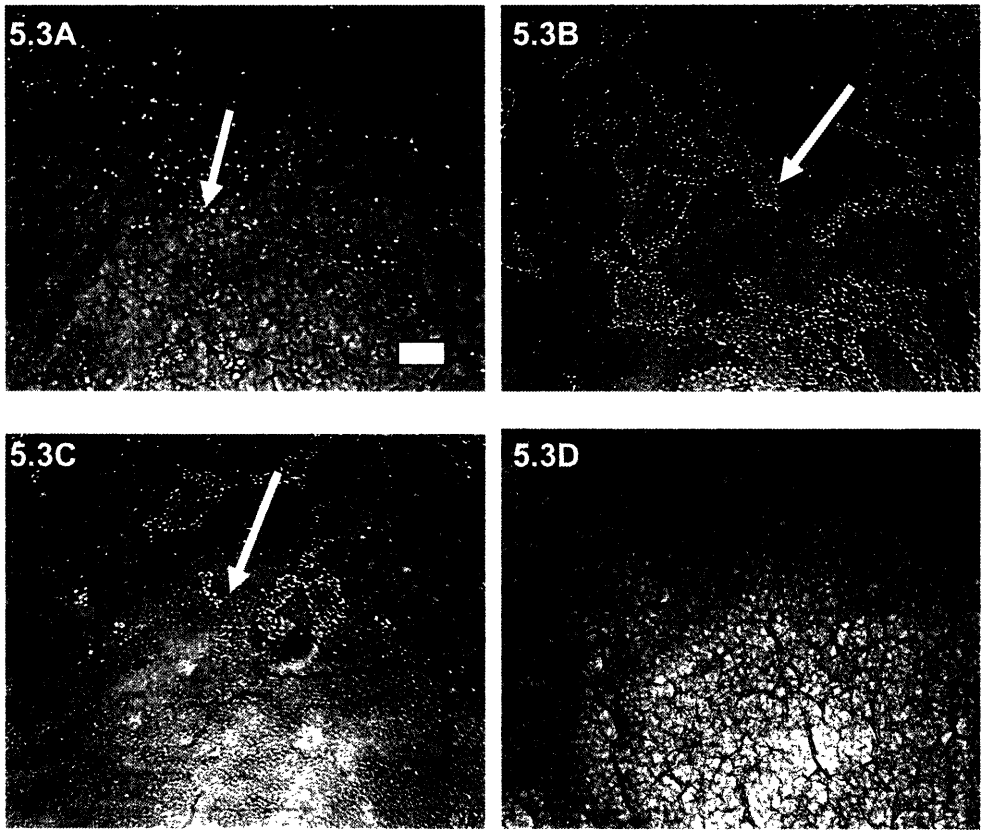

Figure 5.3: PC12 cells interacted with PPyCl. 5.3A) T59-GRGDS interacted with PPyCl and PC12 cells. 5.3B) No peptide interacted with PPyCl with PC12 cells. 5.3C) T59-GRGDS peptide interacted with PPyCl and PC12 cells in serum containing media. 5.3D) No peptide interacted and no PC12 cells. All samples interacted in serum free media unless otherwise noted. Bar =50 μm.

As can be seen from the above optical micrographs, when T59-GRGDS was interacted with PPyCl and PC12 cells in serum-free media (Figure 5.3A) the cells are distributed evenly across the surface of the sample. But when no peptide was present to attach the cells to PPyCl (Figure 5.3B), the cells create cellular clumps or aggregates. This phenomenon typically represents nonspecific attachment to the surface. Additionally experiments were performed to determine if T59-GRGDS binds sufficiently to PC12 cells to deter cellular clumping in serum containing media. As seen previously from Figure 5.2, there should be approximately 1.32×10^{15} peptides/mm^2 to promote adhesion. The micrograph representing this data shows clumpy cells, Figure 5.3C. This data

suggests that, although T59-GRGDS has the ability to bind PPyCl and PC12 cells in serum-free media, there are most likely protein interactions that are much stronger in serum-containing media which prevent the interaction of the GRGDS portion of the modified peptide with the PC12 cellular surface.

To analyze the binding of PC12 cells to PPyCl more thoroughly, rotational agitation was used. If the above figures (Figure 5.3A-C) are compared in actual numbers of cells on the surface of PPyCl, then it is obvious that the serum containing interaction binds more PC12 cells to PPyCl. It is assumed that the serum containing media binds the cells to PPyCl non-specifically and the binding of the cells to PPyCl through T59-GRGDS is a specific recognition event. To test this hypothesis the same conditions were used for peptide adhesion to PPyCl and either serum-free or serum containing media was used to interact PC12 cells with the functionalized PPyCl except after the cellular interaction 5 min of medium rotational agitation was used to disrupt the PC12 cells tethering to PPyCl.

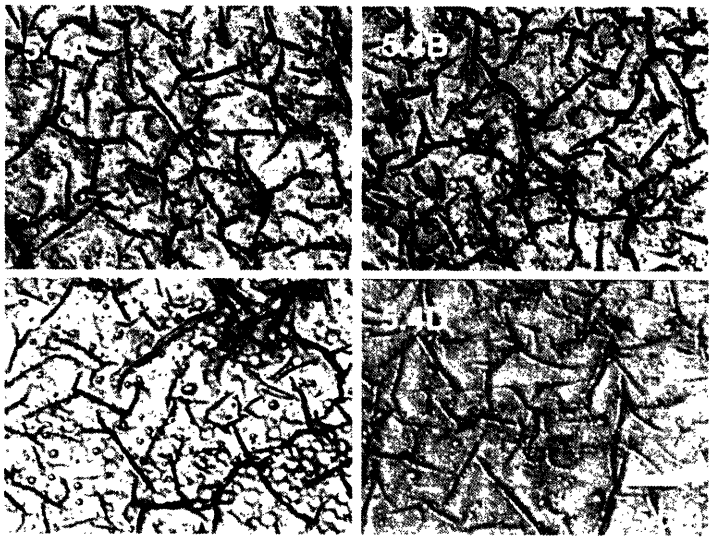

Figure 5.4: 5.4A) PPyCl/T59-GRGDS/PC12 cells in serum free media, 5.4B) PPyCl/T59-GRGDS/PC12 cells in serum free media after 5 min agitation, 5.4C) PPyCl/PC12 cells in serum containing media, 5.4D) PPyCl/PC12 cells in serum containing media after 5 min agitation.

The optical micrographs comparing the specific tethering of PC12 cells to PPyCl through the T59-GRGDS peptide (Figure 5.4A) and the non-specific attachment of the cells to PPyCl by serum proteins (Figure 5.4C) before and after 5 min of rotational agitation show that the non-specific attachment can be physically disrupted (Figure 5.4D) while there are no significant lose of cells on the T59-GRGDS tethering, as shown in Figure 5.4B.

Neurite extension was also studied by inducing differentiation of PC12 cells. After the cells were seeded, as described previously, soluble 100 ng/ml β-Nerve growth factor (Invitrogen) was incorporated in serum-free media for 7 days and imaged using an inverted phase contrast microscope.

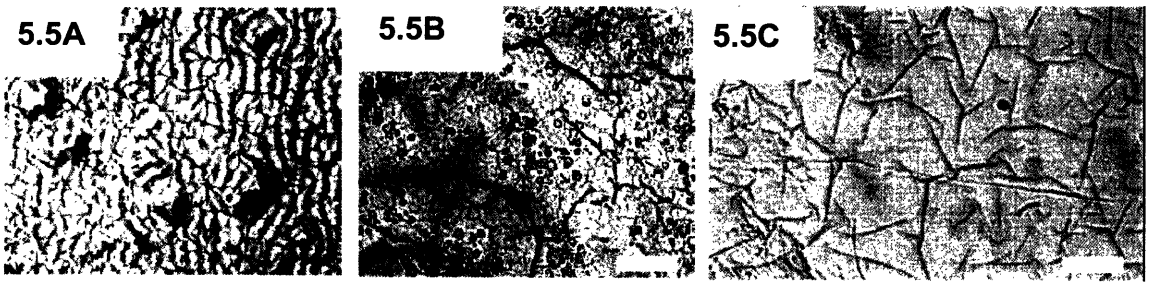

Figure 5.5: T59-GRGDS promotes PC12 cell adhesion in serum-free environment. 5.5A) PPyCl sample without T59-GRGDS or PC12 cells interacted, 5.5B) with 15 μM of T59-GRGDS peptide interacted prior to cellular incubation, 5.4C.) Extension of neuronal processes was induced with 100 ng/ml β-NGF for 7 days in serum-free media. Scale bar = 50 and 5 μm.

As was shown in Figure 5.3B, samples without T59-GRGDS did not permit cellular adhesion, whereas the sample with T59-GRGDS did support cell adhesion with monodisperse cells (Figure 5.5B). In addition to cell adhesion, the PPyCl-T59-GRGDS modified surface also supported neurite outgrowth (Figure 5.5C). This represents a significant step forward in the possible use of this system for *in vivo* cell studies.

5.3 Conclusions

After selection of T59 from the peptide-phage library, the peptide was modified with a cellular binding domain of GRGDS. This hepta-peptide binds to the integrin binding domain, which is present on most cells. This modification to the C-terminus of the T59 peptide facilitates a bi-functionality that can bind both the PPyCl surface and the cellular surface. Initial studies were performed to optimize the input concentration of peptide. This value was determined to be 15 μM for a PPyCl sample size of 0.5 cm^2. Additionally, studies were performed to confirm the presence of bound T59-GRGDS in both serum and serum-free media after periods of up to 1 month. This data resulted in the presence of 74.0% and 79.8% of original surface concentration of peptide bound. These experiments were essential in determining the quantity of peptide available for bi-functional adhesion to PC12 cells. From the bi-functional binding experiments, it is seen that the modified peptide does mediate cellular attachment of the PC12 cells to the surface of PPyCl. To determine if the PC12 cells attached to PPyCl non-specifically by serum proteins were more adherent than T59-GRGDS tethered cells, rotational agitation created a physical disruption with the serum containing attached cells significantly reducing the cells on the surface of PPyCl. While the T59-GRGDS tethered cells quantity remained unchanged. Additionally, not only does the bi-functional peptide promote cellular attachment to PPyCl, it also provides a substrate where neurite extension can occur through the differentiation of the PC12 cells with β-NGF.

These above results provide a proof of concept that the use of T59-GRGDS as a bi-functional linker is a viable option for the use in a nerve guidance channel. By being able to specifically link nerve cells and the nerve guidance channel substrate one is able

to control the cellular attachment within the conduit, which has been one of the major limitations thus far in nerve guidance channel device fabrication. This modified peptide would provide a proportional increase in regeneration capabilities when coupled with electrical stimulation of the conduit.

Chapter 6: Yeast Surface Display of ScFv against Chlorine-Doped Polypyrrole

6.1 Purpose

Single-chain antibody fragments (scFv), as opposed to full length antibodies, are used to decrease immunogenic response within the body. Numerous studies have been performed using yeast surface display of scFv to screen biological relevant targets, such as T-cell receptors and epidermal growth factor fragments [49-51]. Alternatively, the Belcher lab has performed many phage based selections against semiconductors and metals [35-38, 40, 52]. Learning from these screening studies, it seems that the antigen binding tool created by biological selection of materials is a superior technique compared to that of direct surface chemical modification. Unfortunately, there is also a size dilemma of using phage to screen materials. Phage with a length scale of 6 nm x 880 nm require secondary markers to visualize optically. Yeast as an alternative are easily visualized optically with their 4-5 μm size and a doubling time that is comparable to phage in the selection process. Another advantage of using antibodies is there high specificity for biological antigens [53]. In this work the biological antigen would be

replaced with non-biological PPyCl, with the hope of obtaining the same high affinity binding to the surface. The use of the scFv's provides an order of magnitude advantage of overall binding compared to peptides used for the same purpose [54]. To utilize all of the yeast display system's advantages and the continued staple of biological selection of inanimate materials, this study focuses on yeast display selection of a single human derived scFv that binds to a tissue engineering applicable polymer, PPyCl.

6.2 Experimental Methods

A human derived scFv antibody library extra-cellularly linked to *Saccharomyces cerevisiae*, described previously by Boder and Wittrup [35-38, 40, 52, 55, 56], consisting of $1x10^8$ different clones was used to screen PPyCl. Screening consisted of inducing $2x10^9$ clones for 48 hrs in select-galactose containing media supplement with 100 μg/ml Pennicillin/Streptomyocin (SG-CAA P/S) and interacting these clones with a pre-sterilized 0.5 cm^2 sample of PPyCl in SG-CAA P/S for 24 hrs. The resultant interaction was rinsed twice with blocking buffer (0.1 M TBS, 5 mg/ml BSA, 100 μg/ml P/S). A wash step proceeded in SG-CAA for 2 hrs at 25°C. The PPyCl sample was removed from the wash solution and transferred to a new tube to enrich the population of bound clones in select-dextrose containing media (SD-CAA) incubating overnight at 30°C. This screening continued for five rounds under the same conditions with 62 sample clones acquired from rounds three through five. A thorough diagram of the yeast selection process is represented in Figure 6.1.

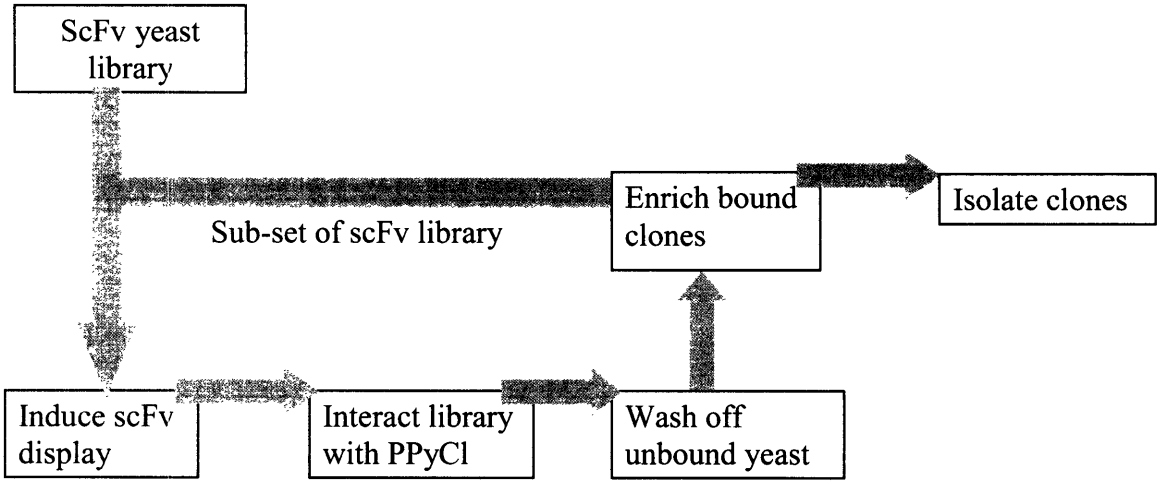

Figure 6.1: Illustration of the process for selection of antibodies that recognize the surface of PPyCl.

Isolation and sequencing of these clones consisted of selecting a single yeast colony with a sterile pipette tip from a select-dextrose plate grown for 48 hrs at 30°C and growing this colony overnight in SD-CAA supplemented with P/S at 30°C, yeast plasmid isolation using RPM® Yeast Plasmid Isolation Kit (Q-Biogene), transformation of the clone's DNA into Top 10 One Shot® Electrocompetent Cells (Invitrogen). The corresponding bacterial clone's DNA were isolated using QIAprep Spin Miniprep Kit (Qiagen). The DNA was prepared with a forward and a backward primer, for sequence conformation, and sequenced at MIT Biopolymers Lab. Acquired sequences were compiled and analyzed using Sequencher™ (Gene Codes Corp.) and NIH IgBlast was used to determine sequence homology, Appendix 1 [57].

From the selection process nine unique clones were identified. These clones were induced from individual yeast colonies in SG-CAA supplemented with P/S. The cultures were grown until approximately 0.25 OD_{600nm}/ml (approx. $2.5x10^6$ yeast/ml). Yeast were interacted with the substrate for 18 hrs at 25°C with medium rocking in SD-CAA or SG-CAA 5 mg/ml BSA and P/S in triplicate. The samples were then rinsed twice with SD-

CAA or SG-CAA 5 mg/ml BSA P/S containing 0.1% (v/v) Tween-20. The samples were then washed for 2.5 hrs with the same solution. The wash solution was then removed and replaced with fresh SD-CAA 5 mg/ml BSA and P/S. The samples were imaged immediately and subsequently enriched for 43 hrs with optical density (OD_{600nm}/ml) readings taken immediately. Images and OD readings are represented in Figure 6.3 and 6.4, respectively.

6.2 Results

After 5 rounds of screening, clone sequences were compiled and are represented in Figure 6.2.

The 9 clones named Y1-Y9 were tested for binding affinity to PPyCl by interacting ~$2x10^6$ cells with the surface in both galactose and dextrose containing media (galactose induces the expression of the cellular surface antibody) as described in the Experimental Methods. Images were taken after clone interaction with PPyCl samples and washing, but before growth, Figure 6.3.

Y1 (x16)
QVQLVQSGAEVKKPGASVKVSCKASG[redacted]TFT**SYG**[redacted]SWVRQAPGQGLEW[redacted]**GW**I[redacted]**YNGNTNYA**[redacted]**K**
[redacted]**Q**GRVT[redacted]TTD[redacted]ST[redacted]TAYMELR[redacted]LRSDDTAVY[redacted]CAR**DSHPMGIPFDH**WGQGTLVTVSSGILGSGGG
GSGGGGSGGGGLQEF*

Y2 (x15)
QVQLQQSGPGLVKPSQTLSLTCAISGDSVS**SNSAAWN**WIRQSPSRGLEWLG**RT**[redacted]**YRSKWYNDYA**
VSVKSRITINPDTSKNQFSLQLNSVTPEDTAVYYCAR**VGCGTYCNNWFES**WGQGTLVTVSSGSAS
APTGILRSGGGGSGGGGSGGGGSDIQ[redacted]TQSPSSLSASVGDRVTITC**RASQSIS**[redacted]**YLN**WYQQK[redacted]GKA
PK[redacted]LIY[redacted]**ASSLQS**GVPSRFSGSGSGTDFTLTISSLQPEDFATY[redacted]C**QQGDS**TPYTFGQGTKLEIKSGILE
QKLISEEDL*

Y3 (x2)
QVQLQQSGPGLV[redacted]PSQTLSLTCAISGD[redacted]VS**SNSAAWN**WIRQSPSRGLEWLG**RTY**[redacted]**RSKWYN**[redacted]**YA**[redacted]
SVKSRITINPDTSKNQFSLQLNSVTPEDTAVYYCAR**RTGTGIDY**WGQGTLVTVSSGILGSGGGGSG
GGGSGGGGLQEF*

Y4 (x2)
QGTAAAVRSRPGEALADPLTHLCHLRGQCLYQQCCLELDQAVPIERP*

Y5 (x1)
[redacted]VQLVES[redacted]GGLVKPGGSLRLSCAASGFTFSN[redacted]**WMS**WVRQAPGKGLEWVG**R**[redacted]**SK**[redacted]**D**[redacted]**GTTDYA**
A[redacted]**VKG**RFTI[redacted]RDDSKNTLYLQM[redacted]LNSEDTA[redacted]Y[redacted]CTT**VPLYRTGWDFDF**WGPGTLVTVSSGILGS
GGGGSGGGGSGGGGSNFMLTQPHSVSESPGKTVTISC**TRSSGSIAS**[redacted]**VQ**WYQQRPGSSPTTVIYE
[redacted]**NQRPS**GVPDRFSGSIDSSSNSASLTISGLKTEDEADYYCQSYDSSN**PYV**FGGGPRSPPIRNSRTKTY
F*

Y6 (x1)
QVQLVQSGAEVKKPGASVKVSCKASG[redacted]TFT**SYG**[redacted]SWVRQAPGQGLEW[redacted]**GW**I[redacted]**YNGNTNYA**[redacted]**K**
[redacted]**Q**GRVT[redacted]TTD[redacted]ST[redacted]TAYME[redacted]R[redacted]RSDDTAVY[redacted]CAR**DSHPMGIPFDH**WGQGTLVTVSSGILGSGGG
GSGGGGSGGGGLQEF*

Y7 (x2)
QVQLQQWGAGLLKPSETLSLTCAVYGGSF[redacted]**YYW**[redacted]WIRQPPGKGLEWIGE[redacted]**HSGSTNYNPSLKS**R
VTISVDTSKNQFSLKLSSVT[redacted]ADTAVYYCAR**DLTSSWFGFDY**WGHGTLVTVSSASTKGPSGILGSG

GGGSGGGGSGGGGFETTLTQSPAFMSATPGD[redacted]V[redacted]ISCKASQDIDDDMNWYQQKPGEAAIFIIQEAT
TLVPGIPPRFSGSGYGTDFTLTINN[redacted]E[redacted]EDAAYYFCLQHDNFPLTFGQGTKVEINPEF*

Y8 (x22)
QVQLVQS[redacted]AEV[redacted]KPGSSVKVSCKA[redacted]G[redacted]TFS[redacted]YA[redacted]SWVRQAPGQGLEWMGGIIPI[redacted]GT[redacted]YAQKFR
GRVTITAD[redacted]ST[redacted]TAYMELSSLRSEDTAVYYCARVGGGYNGRQGYYYYAMDVWGQGTTVTVSSGI
LGSGGGGSGGGGSGGGGSE[redacted]TLTQSPAFMSATPGDKV[redacted]ISCKASQD[redacted]DDMNWYQQKPG[redacted]A[redacted]IF
IIQEATTLVPGI[redacted]PRF[redacted]GSGYGTDFTLTINNIESEDAA[redacted]YFCLQHD[redacted]FPLTFGQGTKVEIKSGILEQKLI
SEEDL*

Y9 (x1)
QVQLWSLGEAWYSLGGP*

Figure 6.2: Amino acid sequences of scFv-yeast clones selected from rounds 3-5 yielded 9 different sequences. The occurrence of these clones is as follows: Y1:16, Y2:15, Y3:2, Y4:2, Y5:1, Y6:1, Y7:2, Y8:22, Y9:1. Unhighlighted regions are antibody framework and/or linkers. Yellow regions are CDRs of the antibody. Green amino acids are deviations from the best matching antibody from an NIH IgBlast. (Appendix 1)

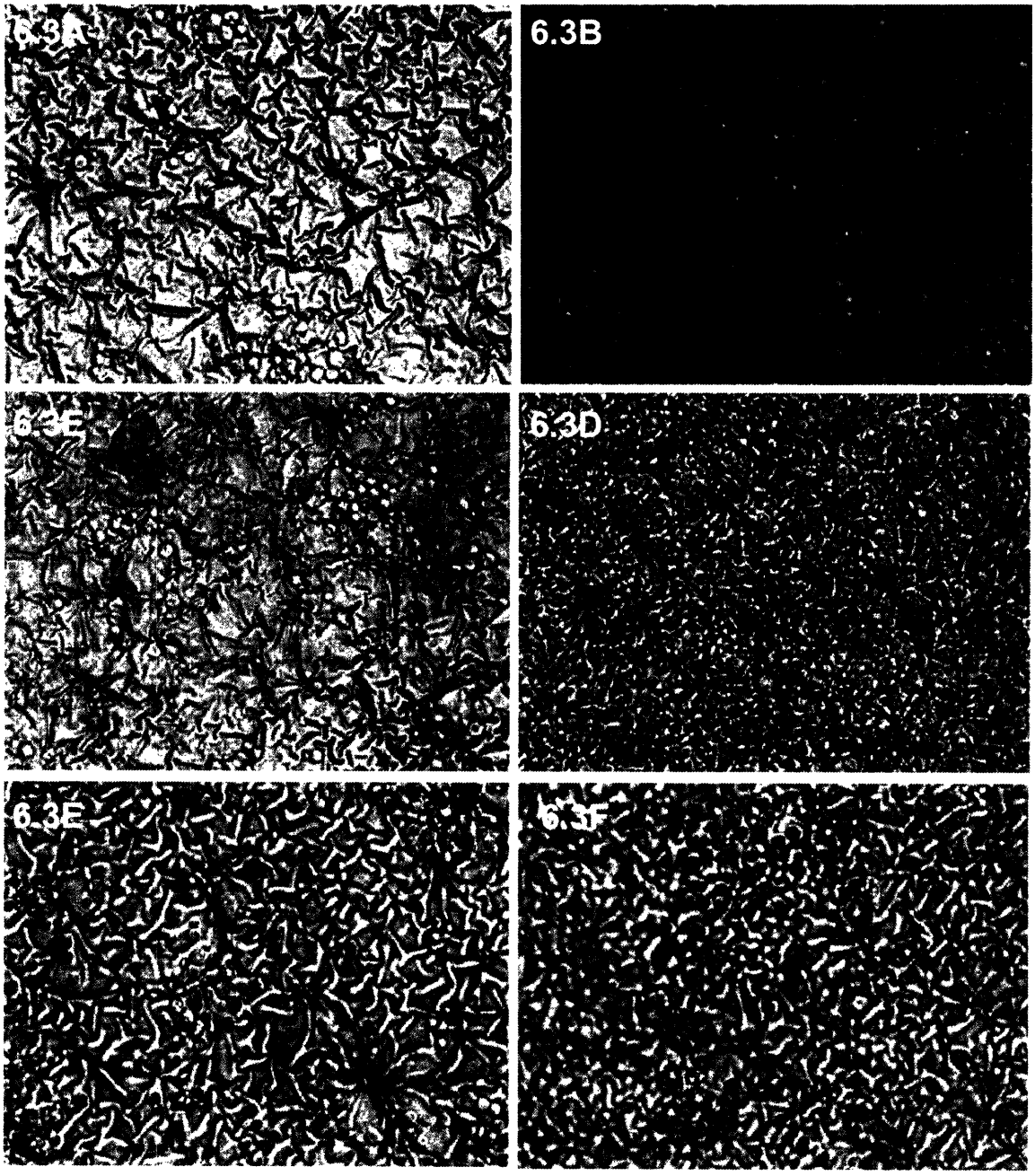
6.3A
6.3B
6.3E
6.3D
6.3E
6.3F

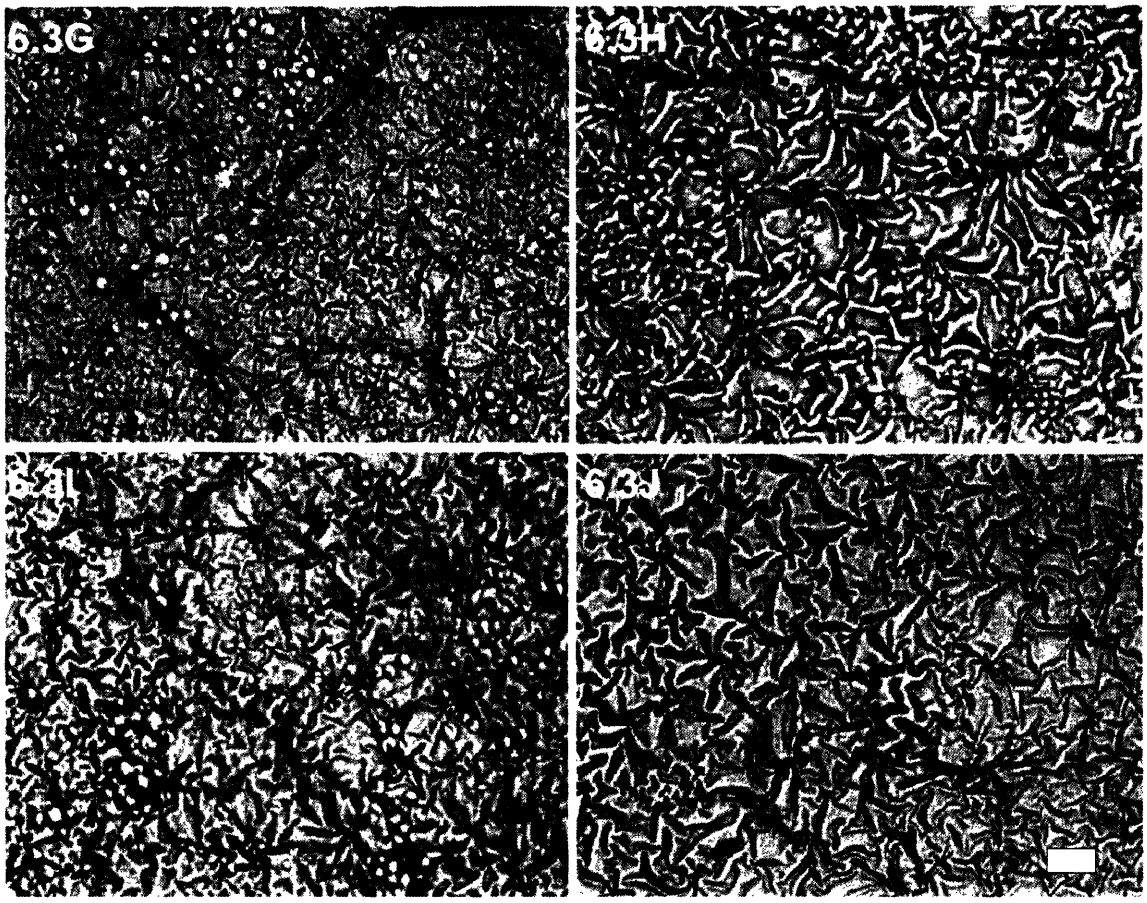

Figure 6.3: Optical micrographs of human derived scFv clones tethered to yeast and bound to the PPyCl substrate. 6.3A-I) Y1-Y9. 6.3J) PPyCl. Scale bar = 10 μm.

The micrographs from Figure 6.3 were taken on an Olympus IX51 inverted optical microscope equipped with an Olympus Qcolor digital CCD with images collected using SimplePCI version 5.2.0.2404 (Compix Inc.) and represent the SG-CAA interacted clones. As seen in the figure above yeast clones Y1, Y3, Y5-Y9 bind to PPyCl, but not nearly to the extent of clones Y2 and Y4. Figure 6.4A is the graphical representation of the growth after a period of 43 hrs of the clones interacted in SG-CAA media with PPyCl. Figure 6.4B represents the galactose to dextrose binding ratio of the clones when interacted in either media SG-CAA or SD-CAA, all clones were interacted in triplicate.

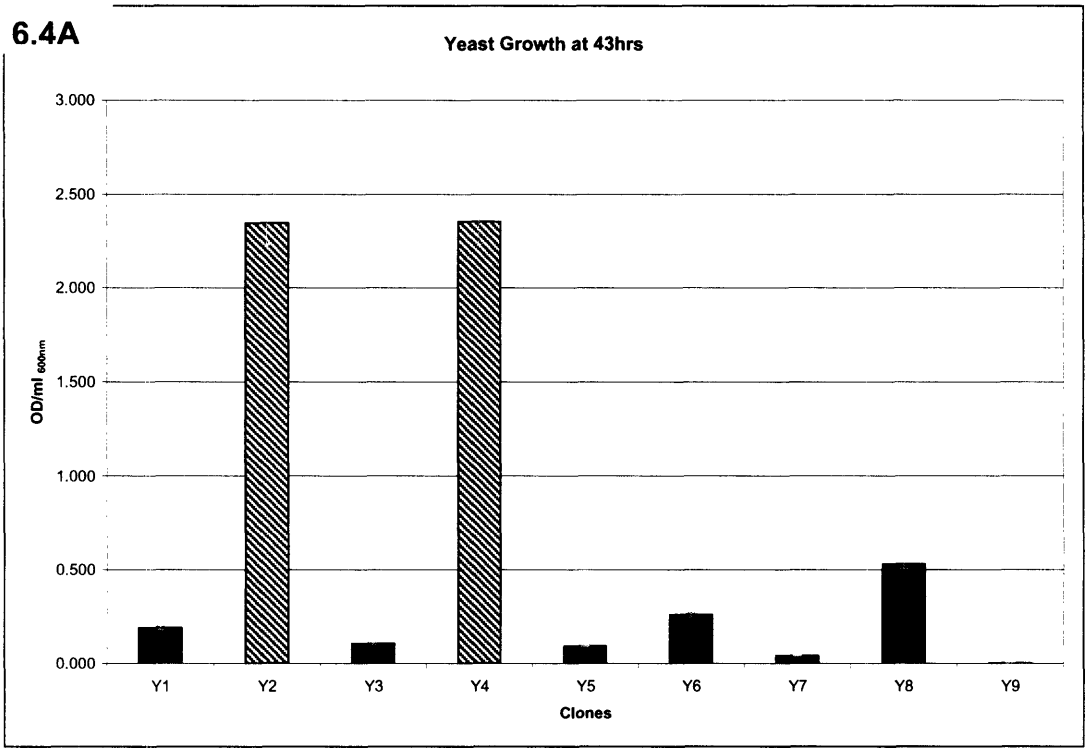

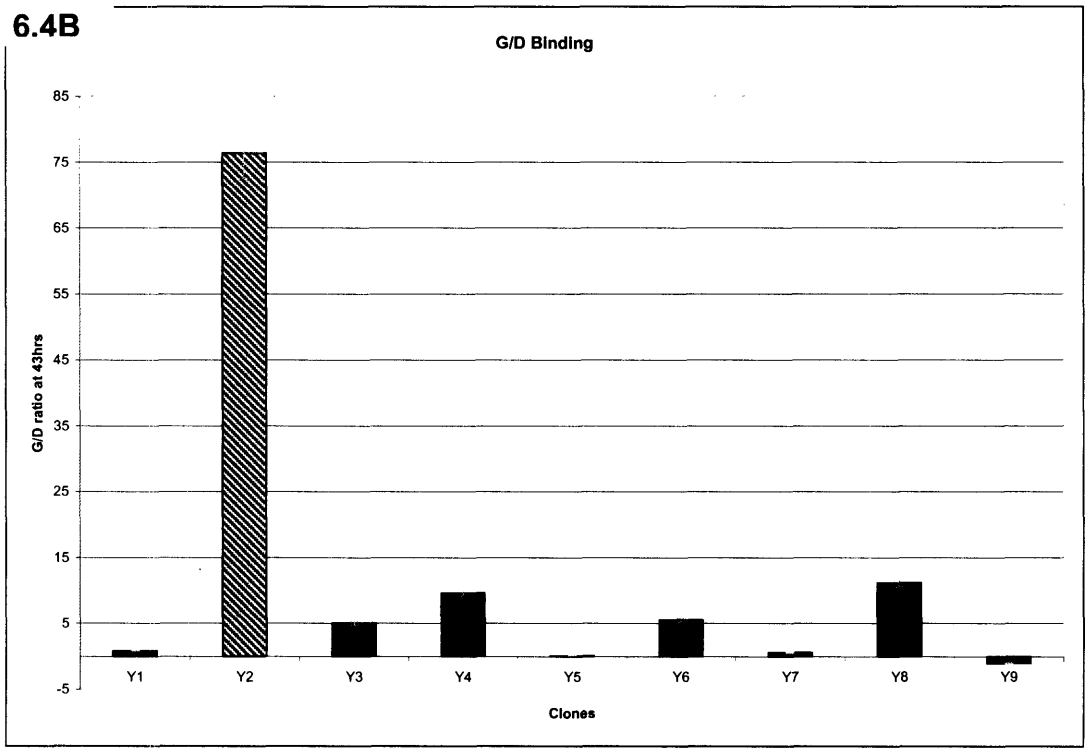

Figure 6.4: 6.4A) The yeast clones Y1-Y9 with OD_{600nm}/ml readings after 43 hrs of growth off of PPyCl. Highlighted by diagonal hatchings are significant binding clones Y2 and Y4, 6.4B.) Yeast clones Y1-Y9, with a significant G/D ratio from Y2. Error bars = ±1 SD.

From Figure 6.4A it is apparent after 43hrs of growth that the most abundant yeast samples are Y2 and Y4. Assuming that all clones enrich at the same rate, Y2 and Y4 clones had to have had initially more binding yeast on the surface of the PPyCl sample after washing and before enrichment began. Therefore of the nine yeast clones selected for PPyCl, Y2 and Y4 are the best binders in SG-CAA media.

The galactose/dextrose ratio of the yeast samples interacted with PPyCl, in Figure 6.4B, provides a better insight into what the binding of these clones is to PPyCl. As one can see the G/D ratio of Y4 is significantly lower than that of Y2, which may mean that cell wall proteins other than scFv are binding to the surface of PPyCl. The Y2 clone G/D ratio on the other hand is significantly larger than that of Y4. Because the ratio is much greater in favor of galactose containing media than dextrose containing media, one can deduce that the scFv of Y2 is responsible for the binding of the Y2 clone to the surface of PPyCl. Therefore, of the nine yeast clones selected for PPyCl Y2 and Y4 clones are the best binding, but Y2 possesses the best ability to turn on and off binding of the yeast clone to the surface of PPyCl.

After binding studies were performed the difference between Y2 and Y4 sequence composition came to our attention. Referring to Figure 6.1, the Y2 clone is comprised of a full scFv with minor amino acid substitutions in the CDR2 and CDR4 regions along with additional substitutions in the VL region of the scFv. This clone is closest in homology to VH6-1 (NIH Ig: AB019441), and O2 (NIH Ig: X59312) [57]. The Y4 clone is the result of a frame shift, and therefore no specific homology can be found. Initially, it was surprising that both types of clones, a full scFv and frame shift, could bind to PPyCl, but after individual binding studies were performed the full scFv (Y2) was evidently the

better binding of the two. This was determined by the G/D ratio of binding to PPyCl, thus revealing that Y4 is more likely a non-specific interaction because of its ability to bind to PPyCl in dextrose containing media. Additionally, the use of full-length scFv in Y2 would provide better water solubility for labeling and possible biomolecule conjugation to the PPyCl surface.

6.3 Conclusions

Screening human derived scFv through yeast surface display is an effective method for determining recognition events on PPyCl. These recognition events would not normally occur in nature, but through molecular interaction of scFv and polymeric materials scientist are able to control their interaction. The complete scFv Y2 was statistically the best binding clone out of nine different clones selected from 62 sequences. The next best binding clone was Y4, which is a frame shifted scFv, that is comparable in binding to Y2 in galactose containing media, but the ability to control the binding of the Y4 clone is insufficient in dextrose containing media implying that yeast cellular surface proteins other than that of Y4 are responsible for binding the PPyCl surface.

Chapter 7: Antibody Mediated Recognition of Chlorine-Doped Polypyrrole

7.1 Purpose

To make this technology applicable further down the biomedical device pipeline it is necessary to implement cellular recognition of the biomedical applicable polymer mediated by the antibody that specifically recognizes that polymer. From Chapter 6, yeast surface display of scFv antibodies has been shown to effectively find a specific recognition antibody to the surface of PPyCl. The Y2 antibody derived from this screening can possibly be used to integrate into cell types and mediate binding of these cells to PPyCl, where normally they would not. This integration, if successful, would show a proof of principle that the Y2 antibody could be used as a mediator for attachment of potential therapeutic cell lines within a nerve guidance channel system.

The vehicle needed for this integration needs to able to display the Y2 antibody on the exterior of mammalian cells. A fine candidate for this approach is that of the pDisplay™ vector (Invitrogen). pDisplay™ is a mammalian expression vector designed to tether recombinant proteins to the surface of mammalian cells. The antibody of interest is anchored to the cell surface by cloning the gene of interest in frame with the vectors unique N-terminal secretion signal and the C-terminal transmembrane anchoring domain of platelet-derived growth factor receptor (PDGFR). In contrast to phage display vectors which operate exclusively in prokaryotic cells, the pDisplay™ vector offers the advantage of having the displayed antibody processed in mammalian cells. Therefore, recombinant antibodies of eukaryotic origin, such as the scFv from humans, that are expressed from pDisplay™ more closely resemble their native form. In addition to the

N-terminal cell surface targeting signal and C-terminal transmembrane anchoring domain, the pDisplay™ vector contains the following key features: T7 promoter/priming site for sequencing of inserts, recombinant proteins expressed contain the hemagglutinin A and *myc* epitopes for detection by immunolabeling, neomycin resistance for selection in mammalian cells using Geneticin®, and an ampicillin resistant gene for selection in *E. coli.* Previous work has been conducted using a form of pDisplay to express *c-jun* on SK-BR-3 human breast carcinoma cells for the ultimate binding of these cells to phOx hapten [58]. Thus, this previous work proves that this technique is a useful tool for the display of recombinant proteins on the surface of mammalian cells. From the experimentation that is to be conducted it is within these same constraints, except for the fact that the antibody to be displayed on the surface of the mammalian PC12 cell will be binding to a therapeutically interesting polymer, PPyCl.

7.2 Experimental Methods and Results

For the implementation of using the Y2 antibody to mediate cellular recognition of PPyCl there are three stages of experimentation that were performed. The first stage consists of integrating the Y2 antibody coding region of DNA into the pDisplay plasmid that will be used for integration into PC12 cells. This stage uses standard molecular biological techniques such as polymerase chain reaction (PCR), enzyme digests, and ligation of both the Y2 insert with the vector pDisplay. Additional work complementing this stage was the use of spectrophotometric quantitation of DNA and sequencing to confirm the presence of the Y2 insert in frame with the vector pDisplay forming an Y2-pDisplay plasmid. The second stage after creating the Y2-pDisplay plasmid was the use of it into PC12 cells mediated by a lipid transfection technique. This stage of the

work required characterization of the Y2 antibody being expressed on the surface of PC12 cells which was done by immunological labeling of the hemagglutinin A portion of the Y2 antibody that is expressed extra-cellularly. The techniques used to analyze this stage of the work were fluorescence microscopy and flow cytometry. The third and final stage of this experimentation consisted of evaluating the binding capability of the Y2 expressing PC12 cell to the surface of PPyCl which is performed by interacting Y2-pDisplay transfected PC12 cells with a sample of PPyCl and evaluating the degree of binding by imaging using optical microscopy.

The initial construction of the plasmid that will represent the Y2 antibody that recognizes the surface of PPyCl starts with the yeast surface display plasmid DNA. This DNA is extracted with the RPM® Yeast Plasmid Isolation Kit (Qbiogene) and transfected into One Shot® Top10 *E. coli* (Invitrogen) for an increase in DNA concentration. A BioRad™ Micropulser was used to electroporate the yeast DNA into the bacterial cells, which was set to Ec2 with a time constant of 5.90 ms and an average voltage passed of 4.0 kV using a 2 cm electroporation cuvette (VWR). The electroprated bacteria were incubated for 1.5 hrs to allow recovery at 37°C and plated using spreading beads on LB plates supplemented with 100 μg/ml ampicillin and incubated overnight at 37°C. The resulting bacterial colonies were amplified in LB media supplemented with 100 μg/ml ampicillin overnight and spun down with the bacterial pellet collected for DNA extraction using QIAprep Spin Miniprep Kit (Qiagen). The resulting bacterial DNA was quantitated spectrophotometrically and confirmed by sequencing and used for subsequent plasmid construct experiments.

The portion of the bacterial DNA that codes for the Y2-antibody was isolated by using a forward and reverse primers with incorporated recognition sites for the restriction endonucleases Bgl II and Sal I, respectively labeled pD5'BglII and pD3'SalI in conjunction with the Expand High Fidelity PCR System (Roche). The PCR parameters deviated from the protocol because of the size of the Y2 insert and are represented in Table 7.1. A schematic of Y2 DNA used in PCR, double restriction endonuclease digest, and the ligation is represented in Figure.7.1.

	Temp (°C)	Time (s)	Cycle
Initial Denature	94	120	1x
Denature	94	35	20x
Anneal	60	30	20x
Elongate	72	60	20x
Final Elongation	72	420	1x
Cool	4	600	1x

Table 7.1: PCR parameters for the production of the Y2-insert with 5'BglII and 3'SalI sticky ends.

Label	5'	3'	Length (bps)
Y2-insert	GGTGGTGGTGGTTCTGGTGGTGGTGGTTCTGGTGGTGGTGGTTCTGCTAGCCAGG.....GGGACCAAGCTGGAGATCAAATCCGGAATTCTAGAACAAA		902
pD5'BglII	ATGATCAGATCTTCTGGTGGTGGTGGTTCTGGTGGTGGTGGTTCTGCTAGCCAGG		55
pD3'SalIrc	GGGACCAAGCTGGAGATCAAATCCGGAGTCGACGATCATA		40
PCR product	AGATCTTCTGGTGGTGGTGGTTCTGGTGGTGGTGGTTCTGCTAGCCAGG.....GGGACCAAGCTGGAGATCAAATCCGGAGTCGAC		875
Y2DD product	'GATCTTCTGGTGGTGGT.....AGATCAAATCCGGAG'		822
pDDD product	..CGGCCA' 'TCGACGAACAA. ...		5299
ligation product	CGGCCA'GATCTTCTGGTGGTGGT.....AGATCAAATCCGGAG'TCGACGAACAA.....		6168

Figure 7.1: Schematic resource of Y2 and pDisplay DNA used for PCR, double restriction endonuclease digest, and ligation. Black = Y2 DNA, Green = Bgl II recognition site, Red = Sal I recognition site, Magenta = pDisplay DNA.

The PCR product was run on a 1% TAE agarose gel set to a constant voltage of 125 V with standard controls of a 1 kilobase ladder (NEB), 5' and 3' primers, and neat Y2 *E. coli* DNA. The gel was rinsed after staining with ethidium bromide and imaged using a Biorad™ Gel Doc system as can be seen in Figure 7.2.

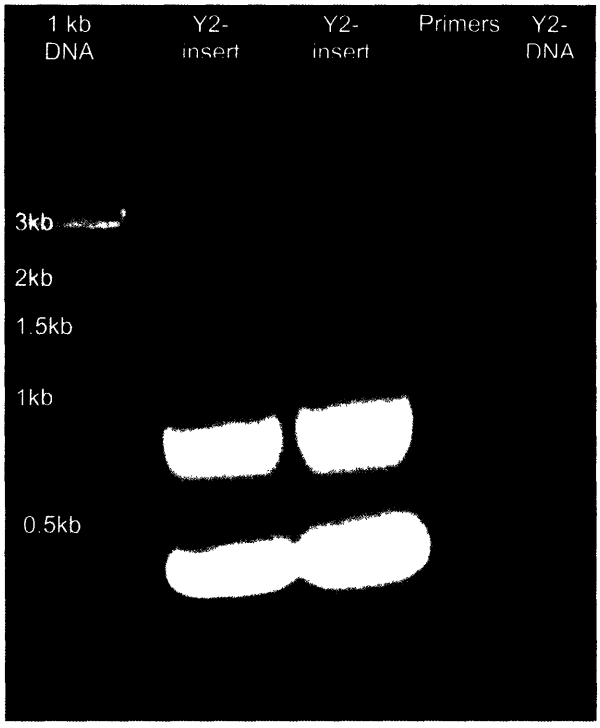

Figure 7.2: Fluorescent image of the PCR product from the use of a 5' and 3' primer to the Y2 E. coli plasmid creating an 902 bps Y2-antibody insert.

The resulting bands associated with the 902 bps PCR product which will express the Y2 antibody were extracted from the gel and purified using the QIAquick Gel Extraction Kit (Qiagen). The DNA was then quantitated spectrophotometrically to prepare for the double restriction endonuclease digest.

The double restriction endonuclease digest for both pDisplay and the Y2 PCR product called Bgl II-Y2-Sal I consisted of selecting a buffer that both enzymes, Bgl II and Sal I can function properly in, bovine serum albumin incorporation at a concentration of

100 mg/ml to stabilize the oligonucleotide components and obviously Bgl II and Sal I enzymes with both the vector pDisplay and insert Y2. The vector is super-coiled and was boiled at 100°C for 5 min to uncoil prior to the digest. The digest proceeded at 37°C for 1 hr and was run on a 1% TAE agarose gel set at a constant voltage of 125 V. Negative controls run on the gel consisted of enzymes with no insert or vector DNA and super-coiled pDisplay which can be seen in Figure 7.3.

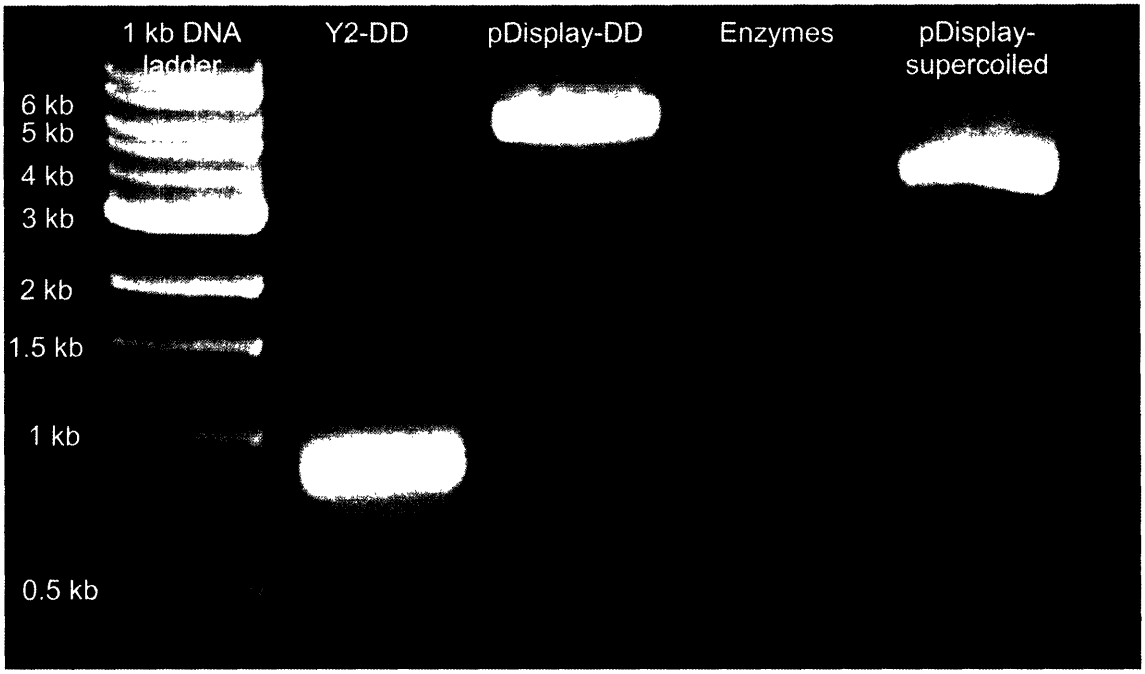

Figure 7.3: Fluorescent image of double restriction endonuclease digest for both Y2 and pDisplay.

As can be seen in Figure 7.3 there is a consistent separation of expected products of Y2-DD around 822 bps, pDisplay-DD around 5299 bps, no enzymes, and because the super-coiled pDisplay has a greater electrophoretic mobility, due to its reduced size compared to pDisplay-DD, it is lower on the gel. The Y2-DD and pDisplay-DD band were collected as before and their respective oligomers were extracted and quantitated as previously described.

Ligation of the Y2 insert into the linearized vector pDisplay creating the Y2-pDisplay plasmid was initially performed with T4 DNA ligase (NEB) and traditional ligase reaction buffer (50 mM Tris-HCl,10 mM $MgCl_2$, 1 mM ATP,10 mM dithiothreitol, 25 µg/ml BSA, pH 7.5 at 25°C) with no transfection of the plasmid into One Shot® TOP 10 *E. coli*. Because no transfection occurred an alternative ligase buffer, Quick Ligation Reaction Buffer (NEB), was used which decreased the time while increasing the efficiency of the ligation. This was evident by the transformation of 0, 3, 6, and 12 molar excess of insert to vector reaction mixtures ligated for 5 min at 25°C into electrically competent One Shot® Top10 *E. coli* (Invitrogen). The transfection was performed as previously described for electrically competent One Shot® Top10 *E. coli*. Transformation efficiencies were determined for a positive control, pUC19, and the 4 ligation reactions by counting the number viable bacterial colonies forming units (cfu) grown overnight at 37°C on LB plates supplemented with 100 µg/ml Ampicillin. The quantities were as follows: pUC19 = 204 cfu, 0x = 1 cfu, 3x = 2 cfu, 6x = 67 cfu, 12x = 252 cfu. The equation for the calculation of transformation efficiencies is represented in Equation 7.1 and the values in Table 7.2.

Equation 7.1: Transformation efficiency

$$\text{transformation efficiency (cfu/µg)} = \frac{\text{number of colonies (cfu)}}{\text{weight of DNA (ng)}} \times \frac{1\text{x}10^3\ \text{(ng)}}{1\ (\mu\text{g})} \times \frac{\text{total ligation volume (µl)}}{\text{plated volume (µl)}}$$

Sample ID	cfu	weight of DNA (ng)	total Rx volume (µl)	plated volume (µl)	transformation efficiency (cfu/µg DNA)
pUC19	204	0.01	302	10	6.16E+08
0x	1	5	302	100	6.04E+02
3x	2	5	302	100	1.21E+03
6x	67	5	302	100	4.05E+04
12x	252	5	302	100	1.52E+05

Table 7.2: Transformation efficiencies for the ligation reactions with a positive control of the plasmid pUC19.

The transformation efficiency for the positive control of pUC19 is as expected around $1\text{x}10^9$ cfu/µg DNA and it is apparent as there is an increase in transformation efficiency as the insert to vector ratio increases. This increase is observed by the span of the transformation efficiency by four orders of magnitude from 10^2 to 10^5. This is not necessarily essential to the process, but did show that, at least using pDisplay and the specified length of the Y2 insert, as the ratio of insert to vector is increased there is an increase in transformation efficiency. Colonies from these plates were collected and grown in LB media supplemented with 100 µg/ml ampicillin overnight at 37°C to collect the bacterial DNA, as previously described using the QIAprep Spin Miniprep Kit, for subsequent sequence confirmation of the Y2-pDisplay plasmid, quantitation, and transfection into PC12 cells. Sequencing of the grown colonies confirmed the presence of the Y2 insert in frame with the pDisplay vector as can be seen in Figure 7.4.

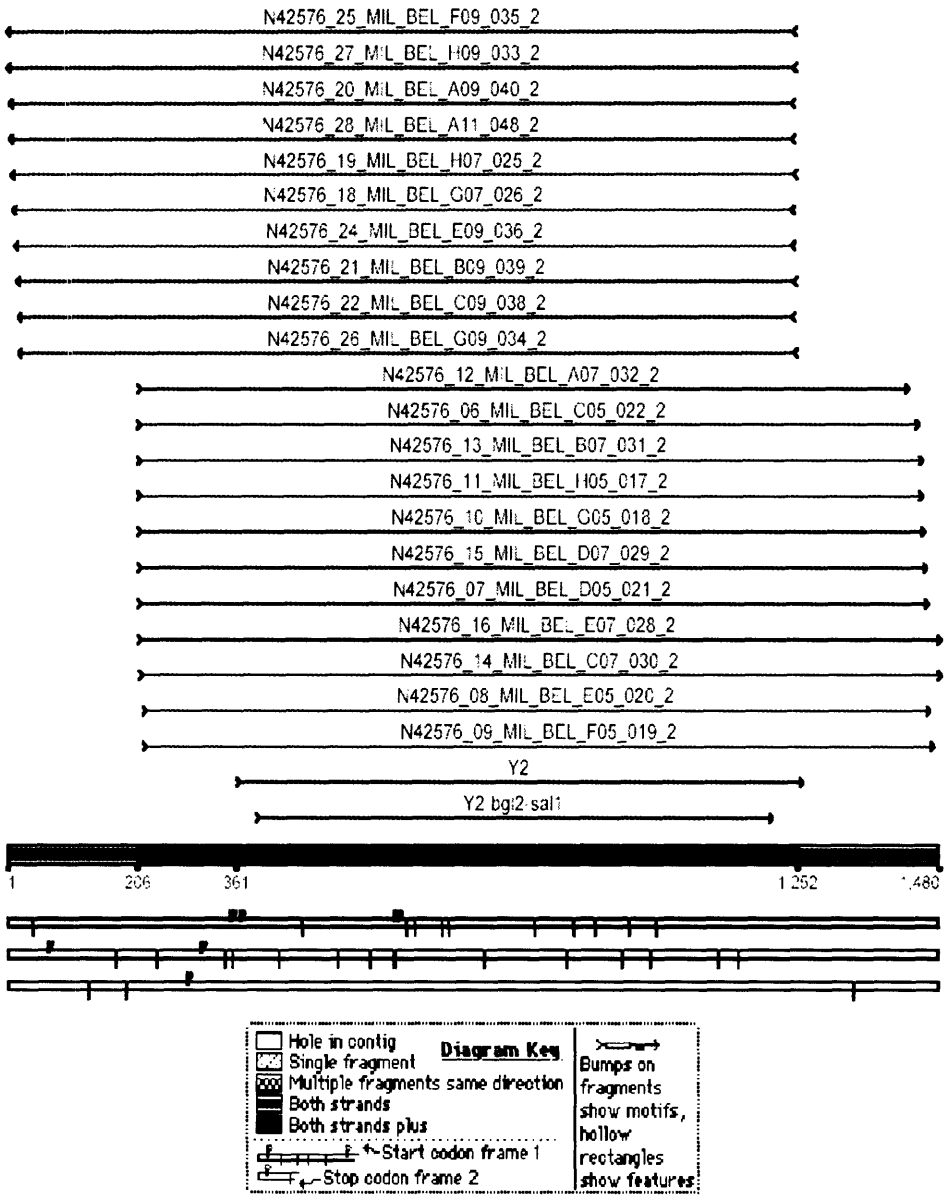

Figure 7.4: Y2-pDisplay sequences confirming Y2 insertion into pDisplay (Sequencher)

After the construction of the Y2-pDisplay plasmid the second phase of the experimentation commenced by transfecting the plasmid into PC12 cells. This was performed by using Lipofectamine 2000™ (Invitrogen) as the transfection vehicle. Specifically, the PC12 cells were plated in 0.5 ml of standard growth media without antibiotics onto collagen coated tissue culture polystyrene at 2.5 x 10^5 cells per well to

achieve 90% confluency the day of transfection. 2 µl of Lipofectamine 2000™ reagent was diluted with OPTI-mem® I Reduced Serum Medium (Invitrogen) and incubate for 5 min at 25°C. The Lipofectamine 2000™ dilution reagent was combined with a 50 µl dilution of the Y2-pDisplay DNA at a quantity of 0.8 µg in the same medium and DNA-Lipofectamine complexes were allowed to form for 20 min at 25°C. The complexes were then introduced into the PC12 wells for transfection for a period of 4 hrs at 37°C and 5% CO_2. After 4 hrs the cellular media was replaced with fresh media. The cells were then incubated for 24 hrs to allow the progression of the transfection to take place. After this period of time the cells were sub-cultured into flasks containing complete media supplemented with 200 µg/ml of Geneticin® to allow for specific growth of only sufficiently transfected cells. After a period of 1 week cells were collected from these cultures and were used to determine the presence of antibody expression on the surface of the PC12 cells, quantitate the number of antibodies on the surface of the PC12 cells, and test binding of the Y2-pDisplay transfected cell (Y2-cell) line to the surface of PPyCl.

Conveniently, the Y2-pDisplay cell line can be fluorescently labeled for analysis using both fluorescent microscopy and flow cytometry. The labeling was performed by removing the non-adherent cells from the collagen coated flasks using 1X trypsin-EDTA at approximate concentration of 10^5 cells per flask and centrifuging them for 30 sec at 3000 rpm. The cells were then washed twice with 700 µl of PBS supplemented with 1% (w/v) BSA. The primary antibody, anti-hemagglutinin A (clone 12CA5) (Roche), was then introduced at a volume of 100 µl and dilution of 1/1000 in PBS/1%BSA and incubated on ice for 30 min. The cell suspension was then washed twice with 700 µl of PBS/1%BSA and centrifuged to remove unbound primary antibody. The cells were then

resuspended in 100 µl of secondary antibody, goat-anti-mouse-FITC (Invitrogen), at a dilution of 1/1000 in PBS/1%BSA and were incubated on ice for 30 min. The cells were again washed twice with 700 µl of PBS1%BSA with centrifugation of the cells in between washes for 30 sec at 3000 rpm. The fluorescently labeled cells were then resuspended in 250 µl PBS/1%BSA. The controls for these experiments were untransfected PC12 cells unlabeled, interacted with primary and secondary antibodies, interacted with only secondary antibody, Y2-cells unlabeled, and interacted only with secondary antibody.

The confirmation of the presence of the Y2 fusion to the cellular membrane of the PC12 cell was initially confirmed by immunolabeling the hemagglutenin A portion of the protein. Fluorescent images of this experiment can be seen in Figure 7.5.

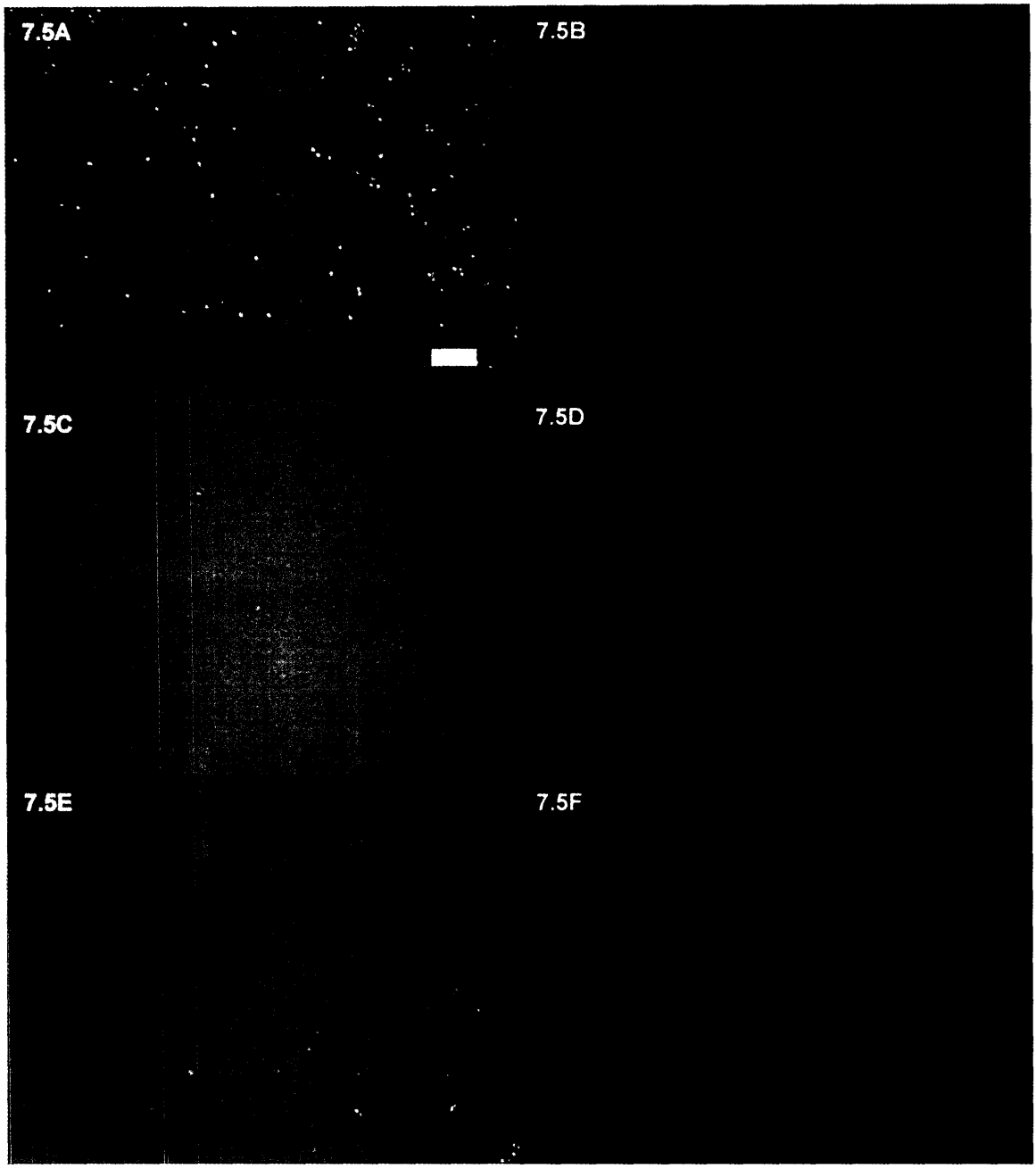
7.5A
7.5B
7.5C
7.5D
7.5E
7.5F

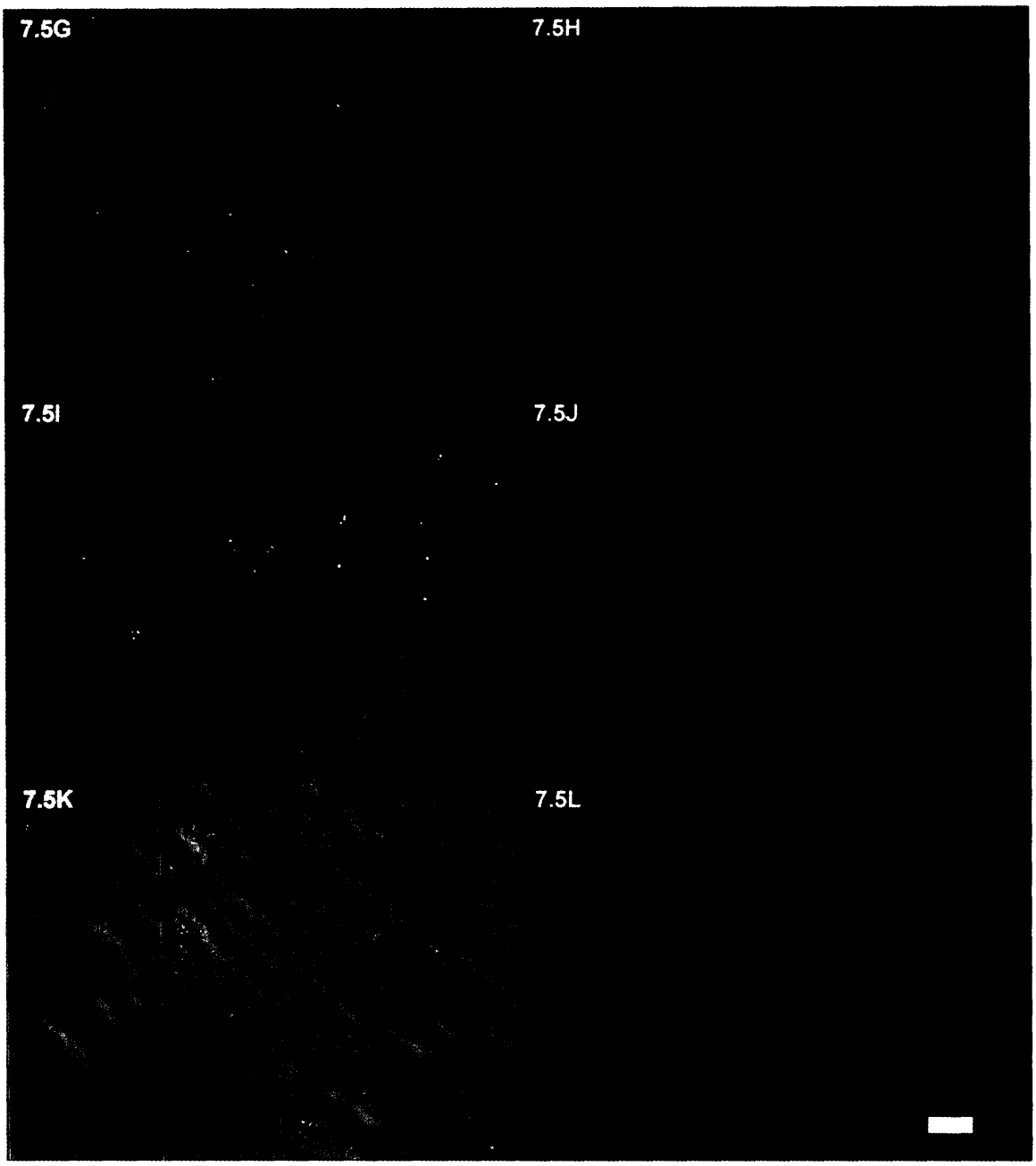

Figure 7.5: Bright field (bf) and fluorescent (fl) optical micrographs of immunolabeled PC12 and Y2-cells. 7.5A) PC12bf, 7.5B) PC12fl, 7.5C) PC12-2°bf, 7.5D) PC12-2°fl, 7.5E) PC12-1°-2°bf, 7.5F) PC12-1°-2°fl, 7.5G) Y2bf, 7.5H) Y2fl, 7.5I) Y2-2°bf, 7.5J) Y2-2°fl, 7.5K) Y2-1°-2°bf, 7.5L) Y2-1°-2°fl. 1° = primary antibody, 2° = secondary antibody, Scale bar = 20 μm.

As expected from the immunolabeling of the PC12 cells one is able to observe that there is little to no background fluorescence from PC12 cells TheY2-cells with no label

have little to no fluorescent signal and one is also able to observe that the secondary antibody does not non-specifically label the Y2-cells. The Y2-cells incubated with primary and secondary antibodies display a much larger fluorescent intensity than that of all the other control samples. Thus immunlogically confirming the presence of Y2 antibody being displayed on the surface of the PC12 cells.

The immunological labeling of the Y2 antibody fused to the cell membrane of the PC12 cell also lends itself to characterization by flow cytometry. What one hopes to obtain from this technique is the quantity, within an order of magnitude, of how many antibodies are being displayed on the surface of the cell. This quantity can initially be compared to that the expression level on the surface of *S. cerevisiae*, which is around 50,000 copies per cell [54] and eventually be used for cell seeding densities when modified cell lines are incorporated into the nerve guidance channel for *in vivo* applications. Immunolabeling was performed as described previously with the same controls. The quantity of antibodies on the surface of cells were back calculated from quantification with the Quantum™ MESF high level kit (Bangs Laboratories) and analyzed by QuickCal® version 2.3 (Bangs Laboratories). A Coulter Epic XL cytometer was used to analyze the cells with flow plots represented in Figure 7.6 and analysis of these plots in Figure 7.7.

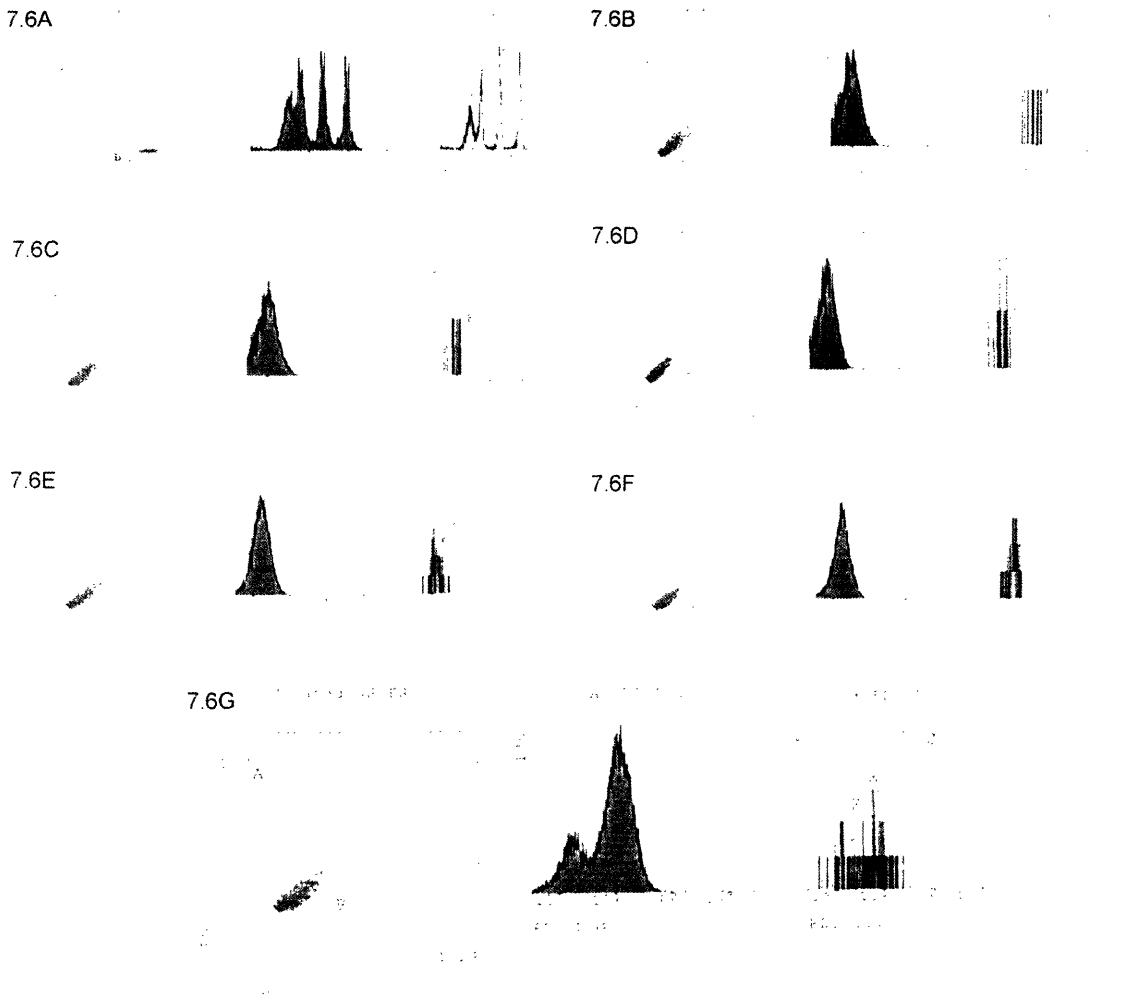

Figure 7.6: Flow plots of immunolabeled PC12 cells. 7.6A) Quantum MESF kit calibration, 7.6B) untransfected unlabeled cells, 7.6C) untransfected 2°, 7.6D) untransfected 1°2°, 7.6E) Y2-cells unlabeled, 7.6F) Y2-cells 2°, 7.6G) Y2-cells 1°2°.

When the flow plots are looked at as a whole, it is observed that there is a slight forward to side scatter difference between untransfected (7.6B-D) and Y2-cells (7.6E-G). This slight difference in scatter is most likely caused by the Y2 antibody being expressed on the surface of cell. What really stands out from this data is the two populations of the cells in 7.6G representing unlabeled and labeled cells as the log scale increases. This is important because one is able to analyze unlabeled and labeled Y2-cells with the calibration to determine the degree of labeling and thus an order of magnitude representation of Y2 antibodies on the surface of PC12 cells.

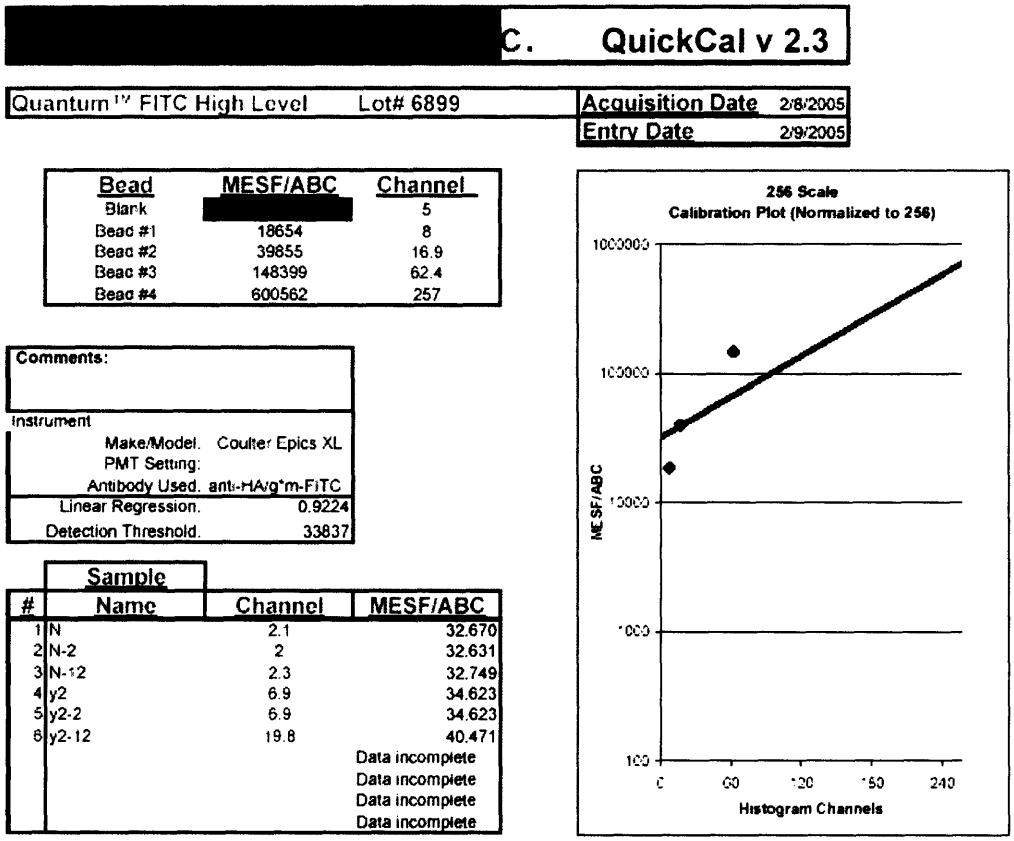

Figure 7.7: QuickCal® analysis of flow plots determining the degree of fluorescence from the plots.

If it is assumed that there is one secondary label per primary antibody and one primary antibody per Y2 antibody, then the molecular equivalent of soluble fluorophore (MESF) of the Y2-cells labeled with the primary and secondary antibody (y2-12) can be used to determine the relative quantity of the Y2 antibody on the surface of the PC12 cell. Other values needed for this calculation are protein concentration of the secondary antibody and the fluorophore quantity per protein molecule in the secondary antibody. These values were determined by diluting the secondary antibody 50 times in PBS/1%BSA and taking the absorbance at 280.0 nm, for amino acids, and 494.0 nm, fluorophore, and were as follows: 280.0 nm = 0.0709 au, 494.0 = 0.1345 au. The above

values were calculated according to Equation 7.2.

Equation 7.2:
A) Protein Concentration
B) Fluorophore/Protein Molecule

$$\text{A) protein concentration (M)} = \frac{(Abs_{280nm} - (Abs_{494nm} \times 0.30)) \times \text{dilution}}{203{,}000\ cm^{-1}\ M^{-1}}$$

$$\text{B) fluorophore/protein molecule} = \frac{Abs_{494nm} \times \text{dilution}}{68{,}000\ cm^{-1}\ M^{-1} \times \text{protein concentratiom (M)}}$$

From Equation 7.2A the 0.30 factor is from the absorbance of the protein at 494.0 nm and the molar absorbtivity is a typical value for this FITC conjugated secondary antibody and from Equation 7.2B the molar absorbtivity is a typical value for the FITC portion of the antibody. Using the equations from above and the absorbance values at 280.0 nm and 494.0 nm the protein concentration and fluorophore per protein molecule were calculated with the results being: protein concentration = 7.524 μM and approximately 13 fluorophore molecules per protein molecule. Thus when you take the MESF of the y2-12 cells (40,471) and divide it by the 13 fluorophore molecules per protein molecule and again take into account the assumptions of a single secondary antibody per primary antibody and a single primary antibody per Y2 antibody on the surface of the cell we arrive at a value of approximately 3,100 Y2 antibodies on the surface of the PC12 cell. As previously described the yeast cells that express the Y2 antibody on its surface have approximately 50,000 copies of the antibody. When these two values are compared there is only a single order of magnitude difference in the expression of the antibody on the surface of these cells, which without expression

optimization, is a sufficient amount to acknowledge a success of creating a neuronal cell line that could bind to PPyCl. Previous values given for the expression level of antibodies on the surface of mammalian cells range from approximately 100 to 5,000 depending on the method of quantization used [58, 59].

The final stage of incorporating an antibody displaying plasmid into a mammalian cell was used to test the hypothesis that one can utilize a non-biological binding entity across species with retention of binding capabilities. This was tested by using the Y2-cells and a sample of PPyCl allowing them to interact with one another and ultimately evaluate binding. The 0.5 cm^2 PPyCl samples were pre-sterilized with ethanol as before. The Y2-cells were collected from culture flasks and centrifuged for 30 sec at 3,000 rpm to pellet the cells. They were washed twice with PBS/1%BSA prior to interaction with the PPyCl sample. The interaction ensued for 1 hr in 500 µl PBS/1%BSA at 25°C with medium rocking with a cell density of $1x10^5$ cells/ml. The samples were then washed twice for 5 min with medium rocking to remove any unbound cells from the surface of PPyCl. 500 µl of PBS/1%BSA was finally added to image the cells in media therefore not imaging stagnant cells. To test the binding capability of ordinary cells, untransfected PC12 cells were used. To determine the specificity of the Y2 antibody on the PC12 cells surface an alternative expressing clone was used. This clone was derived from a cadmium sulfide specific antibody and selected in the same manner, through yeast surface display; this cell line is called D07-cells. To address the issue of a possible sticky end tethering from the cells due to the pDisplay vector expressing a portion of protein on the surface of the cell, pDisplay-cells were used. When the image analysis was conducted there were few cells found on the surface of the PPyCl samples. Initially this was troublesome and a

thorough evaluation of the binding assay needed to be performed to account for the lack of cells. When evaluating the binding conditions of the cells to the surface of PPyCl, it was obvious that the media was PBS/1%BSA, but this was not the binding media that the Y2 antibody was initially selected in, that being SG-CAA media. Obviously an additional binding assay was needed to analyze the binding of the Y2-cells in both medias. The same conditions were applied and the interaction conditions were altered to include a set of cells that were interacted and washed in SG-CAA media. Image analysis for this data is presented in Figure 7.8 with supporting optical micrographs in Figure 7.9.

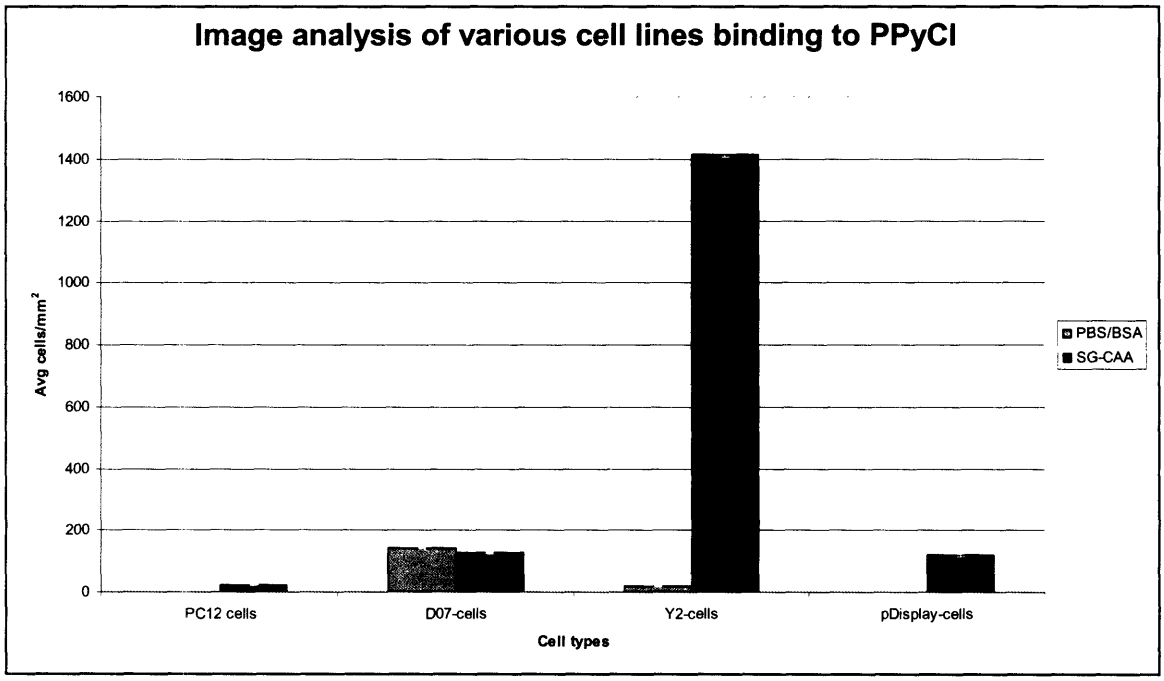

Figure 7.8: Image analysis of various cell lines binding to PPyCl in either PBS or SG-CAA. Error bars = ±1 SD.

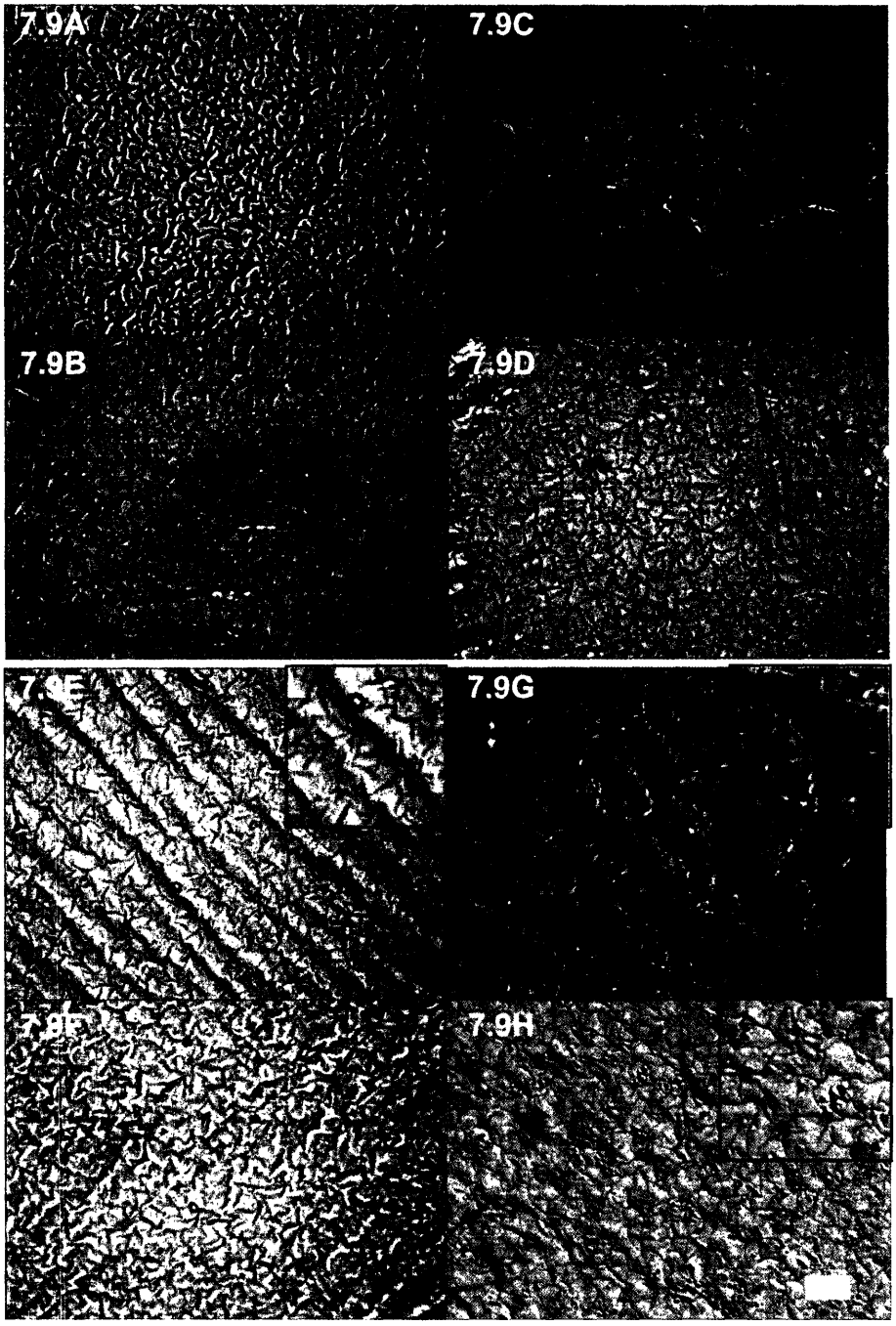

Figure 7.9: Optical micrographs of various PC12 cell lines bound to PPyCl. 7.9A) PBS-PC12, 7.9B) PBS-D07, 7.9C) PBS-pDisplay, 7.9D) PBS-Y2, 7.9E) SGCAA-PC12, 7.9F) SGCAA-D07, 7.9G) SGCAA-pDisplay. 7.9H) SGCAA-Y2, Scale bar = 20 μm.

From the image analysis data it was observed that there is a significant increase in binding capacity of the Y2-cells when interacted in SG-CAA media, 1414 cells/mm^2. As for the other cell lines in SG-CAA media; there is very little binding with less than 130 cells/mm^2. The binding of the varying cell lines in PBS/1%BSA as previously described is minimal with the highest being that of D07-cells at 143 cells/mm^2. Thus from this data the Y2-cells bind an order of magnitude better than the next best cell type in SG-CAA. Additionally, there is an unanswered question that needs to be addressed which is, why SG-CAA media facilitates binding and PBS/1%BSA does not? Could it be that there is a component within the SG-CAA media that facilitates binding or is it that SG-CAA is needed as a whole? If the later is the case, how much of a dilution of SG-CAA media is needed for binding of Y2-cells?

These questions can be addressed by conducting a binding study of an Y2 displaying system with the single components and varying dilutions of SG-CAA. The display system chosen for this technique was the yeast display system because of its ease in up and down regulating the expression the antibody in the presence of galactose. Single components for SG-CAA media consisted of galactose, bactocasoamino acids, yeast nitrogen base, disodium hydrogen phosphate, and sodium dihydrogen phosphate hydrate, and dilutions of complete SG-CAA were 0%, 25%, 50%, 75%, and 100%. The binding assay was performed as the previous yeast selection techniques were with expression of the Y2 antibody of the surface of the yeast cell at a concentration of $1x10^7$ cells/ml for 18 hrs in complete 100% SG-CAA at 30°C with agitation. After induced expression the concentration was determined by optical density at 600 nm and approximately $1x10^8$ cells/ml were dispensed into appropriate tubes. The yeast were then

centrifuged for 30 sec at 3,000 rpm to pellet and resuspended in either one of single components or a dilution of SG-CAA. The 0.5 cm^2 samples of PPyCl were sterilized as before and pre-blocked for 5 min with the appropriate media. The yeast and PPyCl samples were allowed to interact for 10 hrs at 25°C with medium rocking. The samples were rinsed twice 1 ml of appropriate buffer w/ 0.1% Tween and washed once with same media for 4 hrs at 25°C. The samples were then submerged in media and analyzed optically. The imaged samples were then incubated in dextrose containing media to facilitate grow off as previously described in Chapter 6. Figure 7.10 is the analysis of the grow off of the Y2 yeast cells bound in varying media and Figure 7.11 are optical micrographs supporting this data.

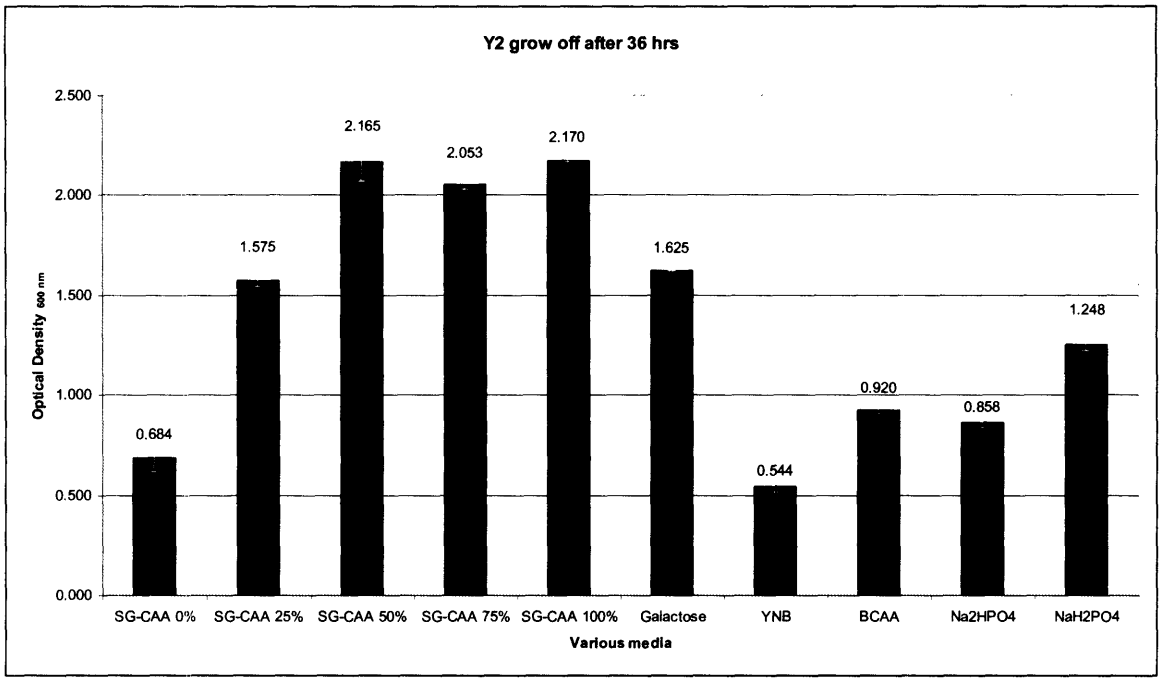

Figure 7.10: Y2 grow off in various media. Error bars = ±1 SD.

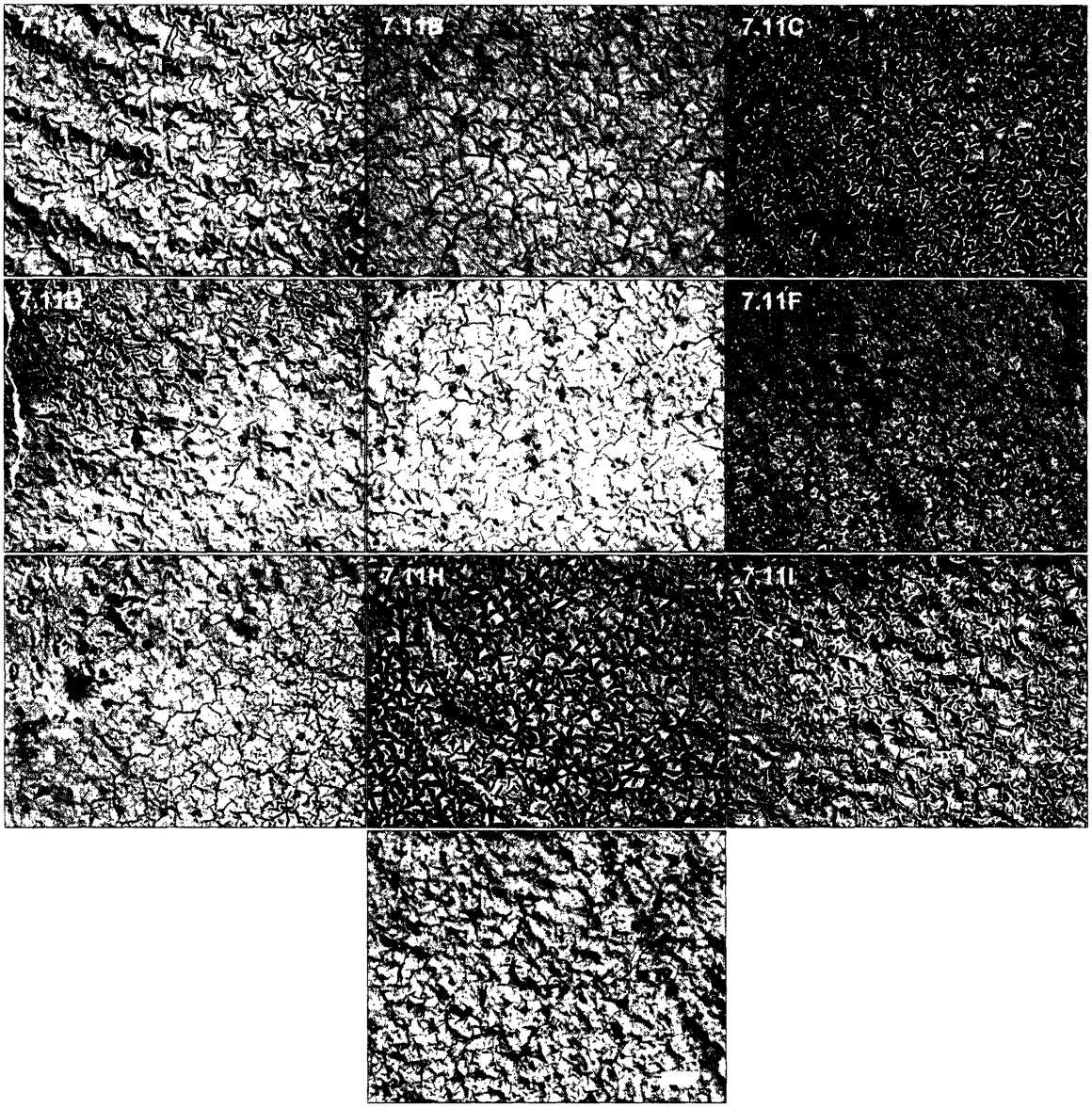

Figure 7.11: Y2 yeast clones bound to PPyCl in various media. 7.11A) 0% SGCAA, 7.11B) 25% SGCAA, 7.11C) 50% SGCAA, 7.11D)75% SGCAA, 7.11E) 100% SGCAA, 7.11F) Bactocasoamino acids, 7.11G) Galactose, 7.11H) Na2HPO4, 7.11I) NaH2PO4, 7.11J) Yeast Nitrogen Base. Scale bar = 20 μm.

It is shown from this data the 100% SG-CAA media initially had the most yeast bound on its surface, but very close to that amount are 75% and 50% SG-CAA. There is a large reduction of cells after these three dilutions with the next being that of the single component galactose and 25% SG-CAA. The rest of the varying media were significantly less than the above mentioned ones, with less than half the initial amount of cells on the

surface of PPyCl, except for the galactose media. What is interesting about the galactose media is that it bound Y2 displaying cells better than half of the dilutions and was the best of the single component analysis. Possible reasons for this increase in binding may be due to a region on the Y2 antibody that interacts with galactose thereby instigating a slight change in secondary structure of Y2 providing the necessary structure for binding to the surface of PPyCl. This change in structure is not initiated by any other media components to the extent that it occurs in galactose. Fortunately, for the *in vivo* scaffold work that could continue this work an introduction of galactose into media, to facilitate uncommon cell types binding to PPyCl once transfected with a vector containing the Y2 insert, would not be deleterious; where as the introduction of the complete mixture of SG-CAA could be. Thus galactose would be a cofactor in the binding of at least Y2-cells, with the possibility of extrapolating these two entities into other mammalian cellular systems.

As was performed for the tethering of PC12 cells to PPyCl through T59-GRGDS, a 5 min rotational agitation was performed to determine if the Y2-cells could be removed from the surface of PPyCl. Because the Y2-cells recognized PPyCl in SG-CAA serum-free media this was the only media type used in the experiment.

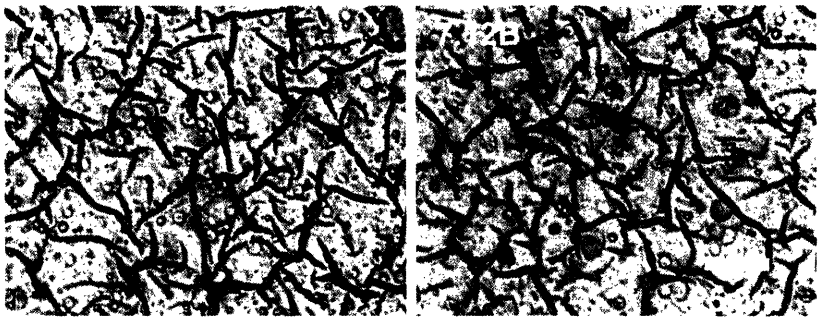

Figure 7.12) 7.12A) Y2-cells interacted in SG-CAA with PPyCl, 7.12B) Y2-cells interacted in SG-CAA with PPyCl after 5 min rotational agitation.

The data from the optical micrographs of the Y2-cells interacted in SG-CAA with PPyCl it is apparent that there is no significant lose of cells after 5 min physical disruption of binding of the Y2 antibody expressed on the surface of the PC12 cell, suggesting that the Y2-cell binding to PPyCl is at least as strong binder as the PC12 cells tethered to PPyCl through the T59-GRGDS peptide.

To initially analyze the idea above that the Y2-cells are at least as strong of a binder as the T59-GRGDS peptide tethered cells, a competitive study was performed. The experiment consisted of interacting $1x10^5$ Y2-cells with PPyCl in SG-CAA and washing any unbound cells. The same concentration of T59 peptide previously used (15 μm) in the saturation of PPyCl for cellular studies was used to try and compete off the Y2-cells from the surface of PPyCl. For the Y2-cells the SG-CAA media was removed and replaced with 15 μm T59 peptide in PBS and interacted for 1 hr at 25°C with medium agitation. Figure 7.13 represents this data.

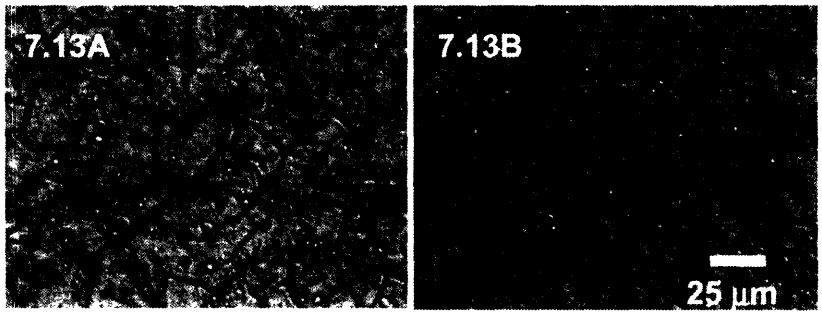

Figure 7.13) 7.13A) Y2-cells bound to PPyCl in SG-CAA, 7.13B) Y2-cells bound to PPyCl after interaction with 15 μm T59-GRGDS for 1 hr.

Figure 7.13 optical micrographs reveal that 15 μm of T59 peptide interacted with Y2-cells bound to PPyCl can not compete a significant amount of Y2-cells off the surface, as can be seen by the lack of difference in cells from Figure 7.13A and Figure 7.13B. This finding suggests that the Y2-cells at least bound as well as the T59 peptide.

7.3 Conclusions

The use of an antibody binding to an inanimate surface is a novel idea that can be used in many applications such as constructing biological tethers to the surface and attaching entities to the surface that would not normally do so. By selecting an antibody through yeast surface display that will attach to the surface of PPyCl, a biological entity has been found that will attach to an inanimate object. Furthermore, through standard molecular biology techniques the Y2 portion of DNA has been removed from the yeast system and incorporated it into a mammalian display vector. The plasmid, Y2-pDisplay, was inserted into the a mammalian cell line, PC12, via a lipid mediated transfection agent, Lipofectamine 2000™, in the presence of 200 μg/ml Geneticin® to create a new cell line, Y2-cells, which displays the Y2 antibody on the PC12 cell surface. Through immunological labeling of the cells the presence of the Y2 antibody on the surface was confirmed as well determining the amount of Y2 antibody on the surface of the PC12 cell. This was performed by flow cytometry using the Quantum™ MESF kit for fluorescence reference with the arrival at approximately 3,100 Y2 antibodies per PC12 cell.

To focus more on the applications of this work a binding assay was needed to evaluate the binding of the new created cell line, Y2-cells, to PPyCl. This was initially conducted in PC12 cell accommodating media, PBS, but with little binding occurring the media was altered to represent the media that the Y2 antibody was selected initially, SG-CAA. The result was an order of magnitude increase in binding of the Y2-cells compared to all other cell types, ordinary PC12 cells, D07-cells (a semiconductor derived antibody cell type), and pDisplay-cells (to evaluate the presence of the vector alone in

PC12 cells). The use of the SG-CAA instead of PBS media for cell binding is an interesting occurrence. Therefore, further analysis was performed to determine what if any of the single components or dilutions of SG-CAA facilitated binding of the Y2 antibody to PPyCl. It became apparent after growing the Y2 yeast cells off the surface of PPyCl that down to 25% SG-CAA was a sufficient concentration to bind cells to PPyCl, but when the conducting the single component analysis, galactose was a main factor in binding the cells to PPyCl. Thus, these experiments lead to the hypothesis that in the presence of galactose one could bind Y2 displaying cells for the construction of an *in vivo* scaffold for nerve regeneration. To determine if the Y2-cells could be removed from the PPyCl by physical disruption a rotational agitation was performed with no significant difference of the amount of cells on the surface after 5 min of agitation. As a capstone experiment the T59 peptide was used to try and compete off the Y2-cells from PPyCl. The result had it gone either way in favor of T59 or Y2-cells would have been quite informative. From the data it is apparent that T59 can not compete off the Y2-cells from the surface of PPyCl, suggesting that the binding of Y2 to PPyCl is at least as strong as the bound between T59 and PPyCl, resulting in the no change in the amount of Y2-cells on the surface of PPyCl.

Chapter 8: Conclusions

8.1 Conclusions for the molecular recognition of PPyCl

As initially stated the objective of this work was to functionalize an existing polymer such that it better mimics natural tissue for tissue growth and regeneration. Numerous other processes have tried and accomplished this with intrusion into the bulk properties of the polymer of interest, but the focus of this work is to modify the polymer's cell binding capability while not altering the bulk properties. Through the use of both phage display of peptide libraries and yeast surface display of scFv libraries the surface of PPyCl has been modified to facilitate binding of neuronal phenotype cells. The selection of both libraries was performed on PPyCl that does not deteriorate in the presence of either binding media of TBS, SG-CAA, or F12.

The phage display of peptides provided a novel technique for the screening of a biomedical interesting polymer. The selection of T59 from this screening was tested for amplification effects and it was found to amplify as well as a clone selected from earlier rounds and non-engineered wild type phage, suggesting that it was not selected as apposed to other clones because of T59's ability to amplify better in *E. coli*. Binding analysis confirmed that, through titer count, T59 bound an order of magnitude better than two other clones from the same selection and wild type to PPyCl in 0.1% TBS-T for 1 hr with release being initiated by a change in pH from 7.5 to 2.2. Fluorescent labeling of the T59 bound to PPyCl showed significant increases when compared to random phage and wild type.

To further understand the binding mechanism of T59 to the surface of PPyCl variants were created to compliment the T59 peptide. These peptide variants coupled with the fluorescamine protein assay provided a quality technique for evaluating the amount of peptide that was on the surface. The data from these studies revealed that the aspartic acid in the 8^{th} position on T59 could be responsible for binding to PPyCl. Since the variant studies revealed that the last six amino acids (N-terminus to C-terminus) contained the aspartic acid residue peptide variant were created to determine which of these six are necessary to bind to PPyCl. Variants were created maintaining the charge of the hexamer, the length, and alanine substitutions were made throughout the length of the variant to evaluate the accompanying amino acids, besides aspartic acid, necessary for T59 binding to PPyCl. From the back six variants binding assay it was determined that aspartic acid can be replaced with glutamic acid, but not with asparagine to maintain the same binding capability. Additionally, leucine and tyrosine are essential accompaniments to aspartic acid with the best binder of this variant study being that of LDYAAA. Other back six clones supported this conclusion with almost no binding capability when both leucine and tyrosine are excluded from the variant. An interesting clone is that of AADDAA, which showed to bind almost as good as the full back six.

The applicable use for the T59 peptide was to tether biological entities to the surface of PPyCl, since PPyCl does not support single cellular attachment. To evaluate the capabilities of T59 to do so it was modified on the C-terminus with a RGD, a cellular binding epitope, with a glycine linker between the modification and the 12^{th} position of T59. Cellular binding assays were performed and it was determined that the modified T59 peptide provided attachment to both PPyCl and PC12 cells, thereby tethering the

cells to the surface of PPyCl. Furthermore, the modified peptide provided single cellular attachment and with the introduction of β-NGF the cells differentiated while still bound to PPyCl, showing the capabilities of the T59 peptide to provide biologically active cellular attachment. The ability of serum containing media to attach PC12 cells to PPyCl was negated by a physical disruption showing that the T59-GRGDS tethered was able to withstand the same physical disruption resulting in the presence of cells bound to PPyCl through the T59-GRGDS peptide.

The yeast surface display library of scFv's was used as an alternative selection technique which provided several advantages over the phage display system. First, visually the yeast are 4-5 μm in diameter and can easily be seen with an optical microscope, compared to phage which are approximately 6 nm x 880 nm and require a secondary label for visualization. The second advantage is the high specificity of scFv's to antigens, compared to peptides used for the same purposes. The third advantage is the ability to control the expression of the scFv's on the surface of the yeast using either galactose or dextrose in the media to up-regulate or down-regulate, respectively. For application purposes the yeast surface display system was used as a reverse engineering approach. Instead of tethering PC12 cells to PPyCl via a peptide linker, the scFv selected from the yeast library was used to mediate binding of the cells to PPyCl. This was accomplished by integration and expression of the PPyCl specific scFv into PC12 cells for the cellular recognition of a biomedical applicable polymer.

The screening of the yeast surface display library resulted in obtaining nine unique clones. Through binding assays two clones, Y2 and Y4, provided the best binding capability to PPyCl. Of these two clones Y2 possessed the best ability to release from

PPyCl when down regulated in dextrose media, leading to the conclusion that the scFv on the surface of Y2 was conducting the binding to PPyCl, and not the cell wall proteins.

As described previously, the eventual use of the scFv was expression of it on the surface of PC12 cells to mediate binding of the cells to PPyCl. Therefore the Y2 scFv was first inserted into a mammalian expression vector, pDisplay™. This portion was confirmed by DNA sequencing and the new plasmid, Y2-pDisplay, was transfected into PC12 cells using Lipofectamine 2000™ as a transfection agent. The presence of the extra-cellular expression region of Y2-pDisplay was confirmed by fluorescence antibody labeling, creating a cell line named Y2-cells. The amount of the scFv on the surface of the PC12 cells was evaluated using the Quantum™ MESF high level kit (Bangs Labs) and the data obtained estimated approximately 3,100 copies of the scFv on the surface. The presence of the Y2 scFv on the surface of PC12 cells provides the opportunity to evaluate the mediating capability of the scFv between the PPyCl surface and PC12 cells. The initial binding assay of Y2-cells and PPyCl in PBS was disheartening with very few cells bound. A secondary assay was performed using both PBS and SG-CAA with Y2-cells binding to PPyCl an order of magnitude better in SG-CAA than in PBS. This incidental information led to the study of evaluating the necessary media components for the Y2 scFv to bind to PPyCl. Various dilutions and all single components of SG-CAA were evaluated for binding of Y2 to PPyCl, with the determination that galactose is necessary for satisfactory binding of Y2 to PPyCl. Additional studies analyzing the Y2-cells binding ability during physical agitation confirmed that the Y2 scFv binds the PC12 cells well. A competition of T59 and Y2-cells binding to PPyCl resulted in the Y2-cells still bound after interaction with the peptide, suggesting that the Y2 scFv binds at least as

good as T59 to the surface of PPyCl, assuming that all the binding sites on the surface of PPyCl were consumed by the Y2-cells.

8.2 Suggested Applications

The idea to attach neuronal cells to a biomedical applicable polymer is only one of many uses for this type of surface modification technique. For instance, previously Schmidt et al [3] described the use of nerve guidance conduit for nerve regeneration purposes. One area of improvement on this technology would be spatial control of the placement of biomolecules, currently biomolecules are non-specifically bound to the interior of the conduit and they state that a concentration gradient of varying biomolecules would greatly affect the regeneration capabilities of this type of system. If one were able to mask the surface of this conduit and supply multiple types of biomolecules necessary when initiating nerve regeneration, then one would be able to provide a concentration gradient of varying types of biomolecules and or cells, such as nerve growth factor and Schwann cells. Furthermore, the ability of PPyCl to conduct current in conjunction with the concentration gradient of varying biological entities could greatly increase the effectiveness of the nerve guidance conduit compared to the nerve autograft [60]. Additional work conducted by Cosnier et al [61, 62] suggests the use of PPyCl for biosensors by attaching enzymes to the surface and monitoring the change in current as the enzymes are utilized, ultimately diminishing the amount of enzymes on the surface to an undetectable amount. A reusable surface would provide a large advantage over the current process, by being able to use the sensor in the same capacity multiple times. The incorporation of peptide linker would provide a major advantage over the

current setup. First, by tethering such a small peptide, like T59, to the surface linked to an enzyme there would be little decrease in current difference had it been just the enzyme linked to PPyCl. Second, the ability to replenish the biosensor for multiple uses would greatly increase the longevity of the sensor.

The same techniques could apply for scFv as provided for the peptide. But the scFv has an additional use in the biomedical field. Using the scFv within the biomedical field would provide a great asset by attaching native cells to polymer scaffolds for seeding of those scaffolds. The use of scFv would proceed as follows: select scFv for scaffold polymer, incorporate scFv into mammalian expression vector, culture native cells from a damaged region for grafting, express the scFv on the surface the native cells, seed the native cells expressing the scFv on to the polymer to facilitate adhesion of the cells to the surface of the polymer, creating a cell supporting polymer scaffold, implant the scaffold back into the damaged site for tissue repair. What is really beautiful about this type of integration is the scFv libraries ability to select for nearly any polymer scaffold, regardless of bulk properties. But as can be seen using PPyCl in nerve regeneration the bulk properties of the polymer become an advantage rather than a disadvantage in tissue regeneration.

Appendix 1: Yeast Clone Homology

Y1: VH1-18 (NIH Ig: AB019441).
Y2: VH6-1 (NIH Ig: AB019441), and O2 (NIH Ig: X59312).
Y3: VH6-1 (NIH Ig: AB019441).
Y4: Not Applicable.
Y5: VH3-5 (NIH Ig: AB019440), V1-22 (NIH Ig: D86996).
Y6: VH-18 (NIH Ig: AB019440).
Y7: VH4-34 (NIH Ig: AB019439), B2 (NIH Ig: x02485).
Y8: VH1-69 (NIH Ig: AB019437), B2 (NIH Ig: x02485).
Y9: Not Applicable.

References:

1. Millesi, H., Progress in peripheral nerve reconstruction. *World J Surg.*, 1990. 14: pp. 733—47.
2. Kotwal, A. and C.E. Schmidt, Electrical stimulation alters protein adsorption and nerve cell interactions with electrically conducting biomaterials. *Biomaterials*, 2001. 22(10): pp. 1055-1064.
3. Schmidt, C.E., V.R. Shastri, J.P. Vacanti, and R. Langer, Stimulation of neurite outgrowth using an electrically conducting polymer. *Proc. Nat. Acad. Sci. USA*, 1997. 94(17): pp. 8948-53.
4. Schmidt, C.E. and J.M. Baier, Acellular vascular tissues: natural biomaterials for tissue repair and tissue engineering. *Biomaterials*, 2000. 21(22): pp. 2215-2231.
5. Shastri, V.R., C.E. Schmidt, T.H. Kim, J.P. Vacanti, and R. Langer, Polypyrrole - a potential candidate for stimulated nerve regeneration. *Mater. Res. Soc. Symp. Proc.*, 1996. 414(Thin Films and Surfaces for Bioactivity and Biomedical Applications): pp. 113-118.
6. Fodor, S.P., J.L. Read, M.C. Pirrung, L. Stryer, A.T. Lu, and D. Solas, Light-directed, spatially addressable parallel chemical synthesis. *Science*, 1991. 251(4995): pp. 767-73.
7. Schultz, J.S., Biosensors. *Scientific Am.*, 1991. 265(2): pp. 64-9.
8. Aaron, R.K. and D.M. Ciombor, Therapeutic effects of electromagnetic fields in the stimulation of connective tissue repair. *J. Cell. Biochem.*, 1993. 52(1): pp. 42-6.
9. Ciombor, D.M. and R.K. Aaron, Influence of electromagnetic fields on endochondral bone formation. *J. Cell. Biochem.*, 1993. 52(1): pp. 37-41.
10. Politis, M.J. and M.F. Zanakis, The short-term effects of delayed application of electric fields in the damaged rodent spinal cord. *Neursurg.*, 1989. 25(1): pp. 71-5.
11. Zanakis, M.F., Differential effects of various electrical parameters on peripheral and central nerve regeneration. *Acupuncture and Electro-Theraputics Res.*, 1990. 15(3-4): pp. 185-91.
12. Goldman, R. and S. Pollack, Electric fields and proliferation in a chronic wound model. *Bioelectromag.*, 1996. 17(6): pp. 450-7.
13. Zhang, S. and M. Altman, Peptide self-assembly in functional polymer science and engineering. *Reac. & Func. Polym.*, 1999. 41: pp. 91-102.
14. Quirk, R., W. Chan, M. Davies, S. Tendler, and K. Shakesheff, Poly(L-lysine)-GRGDS as a biomimetic surface modifier for poly(lactic acid). *Biomater.*, 2001. 22: pp. 865-872.
15. Dee, K.C., D.C. Rueger, T.T. Andersen, and R. Bizios, Conditions which promote mineralization at the bone-implant interface: a model in vitro study. *Biomaterials*, 1996. 17(2): pp. 209-15.
16. Sperinde, J.J. and L.G. Griffith, Synthesis and Characterization of Enzymically-Crosslinked Poly(ethylene glycol) Hydrogels. *Macromolecules*, 1997. 30(18): pp. 5255-5264.

17. Park, A., B. Wu, and L.G. Griffith, Integration of surface modification and 3D fabrication techniques to prepare patterned poly(L-lactide) substrates allowing regionally selective cell adhesion. *J. Biomat. Sci, Polymer Ed.*, 1998. 9(2): pp. 89-110.
18. Koegler, W.S. and L.G. Griffith, Osteoblast response to PLGA tissue engineering scaffolds with PEO modified surface chemistries and demonstration of patterned cell response. *Biomaterials*, 2004. 25(14): pp. 2819-2830.
19. Hrkach, J., J. Ou., N. Lotan., and R. Langer, Poly (L-lactic acid-co-amino acid) graft copolymers. *J. Mater. Sci. Res.*, 1999. 78: pp. 92-102.
20. Xiao, S.J., M. Textor, and N. Spencer, Covalent attachment of cell-adhesive, (Arg-Gly-Asp)-containing peptides to titanium surfaces. *Langmuir*, 2000. 14(19): pp. 5507-5516.
21. Puleo, D.A., Biochemical surface modification of Co-Cr-Mo. *Biomaterials*, 1996. 17(2): pp. 217-22.
22. Healy, K., Molecular engineering of materials for bioreactivity. *Curr. Opn. Sol. Sta. & Mater. Sci.*, 1999. 4: pp. 381-387.
23. Tong, Y.W. and M.S. Shoichet, Peptide surface modification of poly(tetrafluoroethylene-co-hexafluoropropylene) enhances its interaction with central nervous system neurons. *J. Biomed. Mat. Res.*, 1998. 42(1): pp. 85-95.
24. Hern, D.L. and J.A. Hubbell, Incorporation of adhesion peptides into nonadhesive hydrogels useful for tissue resurfacing. *J. Biomed. Mat. Res.*, 1998. 39(2): pp. 266-76.
25. Diaz, A.F., J.I. Castillo, J.A. Logan, and W. Lee, Electrochemistry of conducting polypyrrole films. *J. Electroanal. Chem.*, 1981. 129: pp. 115-132.
26. Aebischer, P., R.F. Valentini, P. Dario, and C. Domenici, Piezoelectric guidance channels enhance regeneration in the mouse sciatic nerve after axotomy. *Brain Res*, 1987. 436: pp. 165-168.
27. Cairns, D.B., S.P. Armes, M.M. Chehimi, C. Perruchot, and M. Delamer, X-ray photoelectron specstroscopy characterization of submicrometer-sized polypyrrole-polystyrene composites. *Langmuir*, 1999. 15: pp. 8059-66.
28. Pfluger, P., M. Krounbi, G.B. Street, and G. Weiser, The chemical and physical properties of pyrrole-based conducting polymers: the oxidation of neutral polypyrrole. *J. Chem. Physics*, 1983. 78(6 Pt. 1): pp. 3212-18.
29. Scott, J.K., R. Hoess, S. Jackson, and W. Degrado, Bioactive peptides identification by panning against immobilized purified receptors. *Proc. Natl. Acad. Sci.*, 1992. 89: pp. 5398-5402.
30. Devlin, J.J., L.C. Panganiban, and P.E. Devlin, Random peptide libraries: a source of specific protein binding molecules. *Science*, 1990. 249(4967): pp. 404-6.
31. Doorbar, J. and G. Winter, Isolation of a peptide antagonist to the thrombin receptor using phage display. *J. Mol. Biol.*, 1994. 244(4): pp. 361-9.
32. Barry, M.A., W.J. Dower, and S.A. Johnston, Toward cell-targeting gene therapy vectors: selection of cell-binding peptides from random peptide-presenting phage libraries. *Nature Medicine*, 1996. 2(3): pp. 299-305.
33. Smith, M.M., L. Shi, and M. Navre, Rapid identification of highly active and selective substrates for stromelysin and matrilysin using bacteriophage peptide display libraries. *J. Biol. Chem.*, 1995. 270(12): pp. 6440-9.

34. Parmley, S.F. and G.P. Smith, Antibody-selectable filamentous fd phage vectors: affinity purification of target genes. *Gene*, 1988. 73(2): pp. 305-18.
35. Reiss, B.D., C. Mao, D.J. Solis, K.S. Ryan, T. Thomson, and A.M. Belcher, Biological Routes to Metal Alloy Ferromagnetic Nanostructures. *Nano Lett.*, 2004. 4(6): pp. 1127 - 1132.
36. Whaley, S.R., D.S. English, E.L. Hu, P.F. Barbara, and A.M. Belcher, Selection of peptides with semiconductor binding specificity for directed nanocrystal assembly. *Nature*, 2000. 405(6787): pp. 665-8.
37. Mao, C., D.J. Solis, B.D. Reiss, S.T. Kottmann, R.Y. Sweeney, A. Hayhurst, G. Georgiou, B. Iverson, and A.M. Belcher, Virus-Based Toolkit for the Directed Synthesis of Magnetic and Semiconducting Nanowires. *Science*, 2004. 303(5655): pp. 213-217.
38. Lee, S.-W., C. Mao, C.E. Flynn, and A.M. Belcher, Ordering of Quantum Dots Using Genetically Engineered Viruses. *Science*, 2002. 296(5569): pp. 892-895.
39. Flynn, C.E., C. Mao, A. Hayhurst, J.L. Williams, G. Georgiou, B. Iverson, and A.M. Belcher, Synthesis and organization of nanoscale II–VI semiconductor materials using evolved peptide specificity and viral capsid assembly. *J. Mater. Chem.*, 2003. 13(10): pp. 2414 - 2421.
40. Flynn, C.E., S.-W. Lee, B.R. Peelle, and A.M. Belcher, Viruses as vehicles for growth, organization and assembly of materials. *Acta Materialia*, 2003. 51(19): pp. 5867-5880.
41. Wanner, I.B. and P.M. Wood, N-Cadherin Mediates Axon-Aligned Process Growth and Cell-Cell Interaction in Rat Schwann Cells. *J. Neurosci.*, 2002. 22(10): pp. 4066-4079.
42. Foehr, E.D., X. Lin, A. O'Mahony, R. Geleziunas, R.A. Bradshaw, and W.C. Greene, NF-kappa B Signaling Promotes Both Cell Survival and Neurite Process Formation in Nerve Growth Factor-Stimulated PC12 Cells. *J. Neurosci.*, 2000. 20(20): pp. 7556-7563.
43. Udenfriend, S., S. Stein, P. Bohlen, W. Dairman, W. Leimgruber, and M. Weigele, Fluorescamine: a reagent for assay of amino acids, peptides, proteins, and primary amines in the picomole range. *Science*, 1972. 178: pp. 871-872.
44. Lorenzen, A. and S. Kennedy, A fluorescence-based protein assay for use with a microplate reader. *Anal Biochem*, 1993. 214: pp. 346-348.
45. Funk, G., C. Hunt, D. Epps, and P. Brown, Use of a rapid and highly sensitive fluorescamine-based procedure for the assay of plasma lipoproteins. *J Lipid Res*, 1986. 27: pp. 792-795.
46. Chung, L., A fluorescamine assay for membrane protein and peptide samples with non-amino-containing lipids. *Anal Biochem*, 1997. 248: pp. 195-201.
47. Bridges, M., K. McErlane, E. Kwong, S. Katz, and D. Applegarth, Fluorometric determination of nanogram quantities of protein in small samples: application to calcium-transport adenosine triphosphatase. *Clin Chim Acta*, 1986. 157: pp. 73-79.
48. Martell, A.E. and R.M. Smith, *Critical Stability Constants*. Vol. 1. 1974, New York: Plenum Press.

49. Shusta, E.V., R.T. Raines, A. Pluckthun, and K.D. Wittrup, Increasing the secretory capacity of Saccharomyces cerevisiae for production of single-chain antibody fragments. *Nat. Biotechnol.*, 1998. 8: pp. 773-7.
50. Kieke, M.C., E. Sundberg, E.V. Shusta, R.A. Mariuzza, K.D. Wittrup, and D.M. Kranz, High affinity T cell receptors from yeast display libraries block T cell activation by superantigens. *J. Molec. Bio.*, 2001. 307(5): pp. 1305-1315.
51. Kieke, M.C., B.K. Cho, E.T. Boder, D.M. Kranz, and K.D. Wittrup, Isolation of anti-T cell receptor scFv mutants by yeast surface display. *Protein Eng.*, 1997. 10(11): pp. 1303-1310.
52. Mao, C., C.E. Flynn, A. Hayhurst, R. Sweeney, J. Qi, G. Georgiou, B. Iverson, and A.M. Belcher, Viral assembly of oriented quantum dot nanowires. *PNAS*, 2003. 100(12): pp. 6946-6951.
53. Paoli, G.C., C.-Y. Chen, and J.D. Brewster, Single-chain Fv antibody with specificity for Listeria monocytogenes. *Journal of Immunological Methods*, 2004. 289(1-2): pp. 147-155.
54. Boder, E.T., K.S. Midelfort, and K.D. Wittrup, Directed evolution of antibody fragments with monovalent femtomolar antigen-binding affinity. *PNAS*, 2000. 97(20): pp. 10701-10705.
55. Boder, E.T. and K.D. Wittrup, Yeast surface display for screening combinatorial polypeptide libraries. *Nat. Biotechnol.*, 1997. 15(6): pp. 553-7.
56. Boder, E.T. and K.D. Wittrup, Optimal Screening of surface-displayed polypeptide libraries. *Biotechnol. Prog.*, 1998. 14: pp. 55.
57. Altschul, S.F., T.L. Madden, A.A. Schäffer, J. Zhang, Z. Zhang, W. Miller, and D.J. Lipman, Gapped BLAST and PSI-BLAST: a new generation of protein database search programs. *Nucleic Acids Res.*, 1997. 25: pp. 3389-3402.
58. Chesnut, J.D., A.R. Baytan, M. Russell, M.-P. Chang, A. Bernard, I.H. Maxwell, and J.P. Hoeffler, Selective isolation of transiently transfected cells from a mammalian cell population with vectors expressing a membrane anchored single-chain antibody. *Journal of Immunological Methods*, 1996. 193(1): pp. 17-27.
59. Suzuki, M., M. Shinkai, H. Honda, M. Kamihira, S. Iijima, and T. Kobayashi, Construction of tumor-specific cells expressing a membrane-anchored single-chain Fv of anti-ErbB-2 antibody. *Biochimica et Biophysica Acta*, 2001. 1525: pp. 191-196.
60. Hudson, T.W., G.R. Evans, and C.E. Schmidt, Engineering strategies for peripheral nerve repair. *ORTHOPEDIC CLINICS OF NORTH AMERICA*, 2000. 31(3): pp. 485-98.
61. Cosnier, S. and C. Gondran, Fabrication of biosensors by attachment of biological macromolecules to electropolymerized conducting films. *Analysis*, 1999. 27(7): pp. 558-564.
62. Cosnier, S., B. Galland, C. Gondran, and A. Le Pellec, Electrogeneration of biotinylated functionalized polypyrroles for the simple immobilization of enzymes. *Electroanalysis*, 1998. 10(12): pp. 808-813.

Vita

Kiley Preston-Halfmann Miller was born in Midland, Texas on March 23, 1977, the son of Peggie Ann Stacy and Max Arnold Miller. He graduated from Midland High School and attended Schreiner University in 1995. He received his Bachelor's of Science in Chemistry on May 5, 2000. On September 2, 2000 he joined the lab of Angela M. Belcher at the University of Texas at Austin. He joined the Belcher lab migration up north to the Massachusetts Institute of Technology on June 3, 2003. He will be working at Colgate-Palmolive in April 2005.

Permanent address: 158 Runyon Ave., Somerset, New Jersey, 08873

This dissertation was typed by the author.